UNC CHARLOTTE

Electrical and Computer Engineering

Wide Band Gap III-Nitride Compound Semiconductor Devices: The Universal Solution for Energy Applications

Ian Ferguson
University of North Carolina at Charlotte
Department of Electrical and Computer Engineering
Charlotte, NC 28223
Email: ianf@uncc.edu

α

ECE and
Energy Production Infrastructure Center

UNC CHARLOTTE
Electrical and Computer Engineering

EPIC and CRI

Typical EPIC floor plan

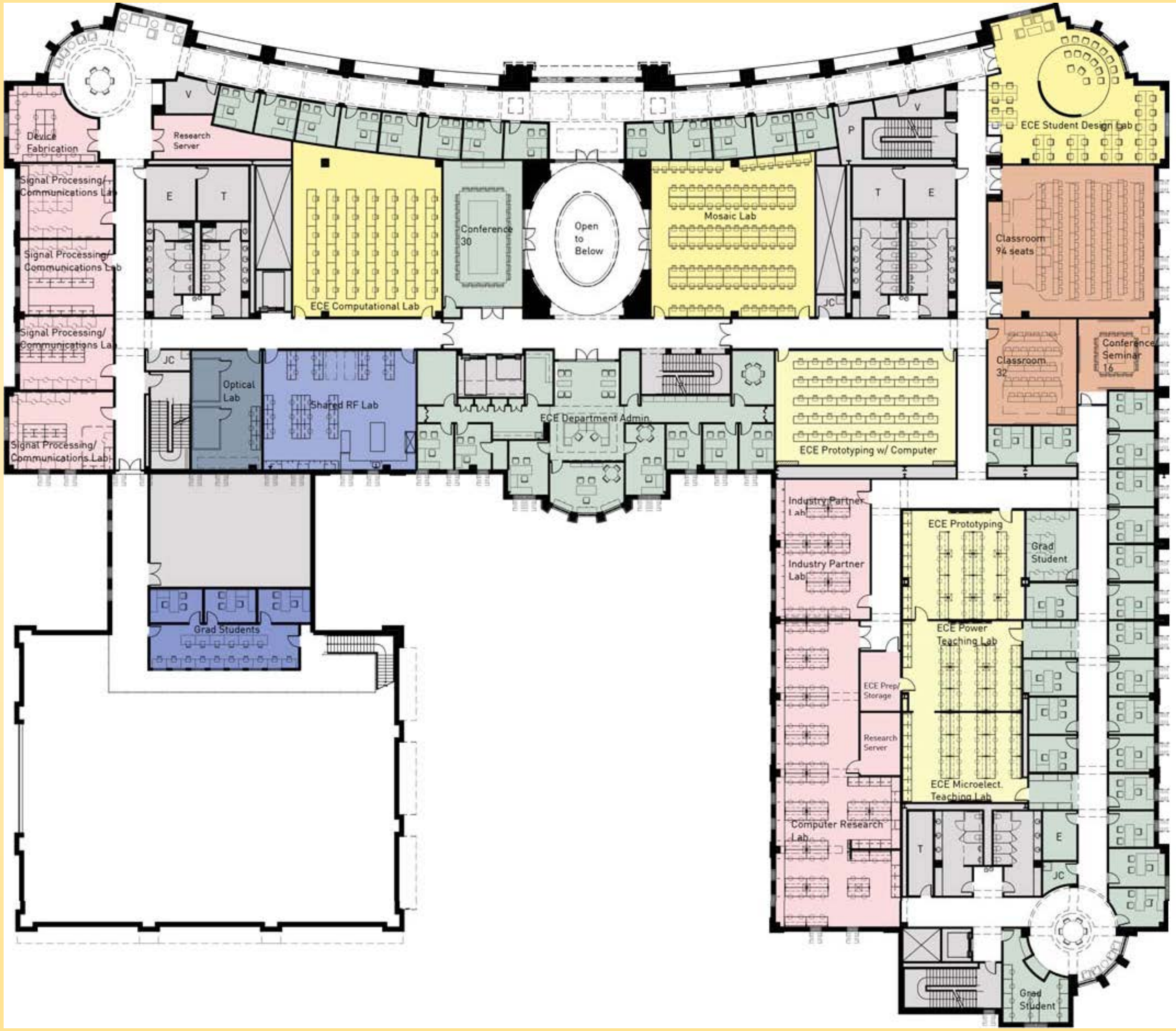

Solar Decathlon House UNCC

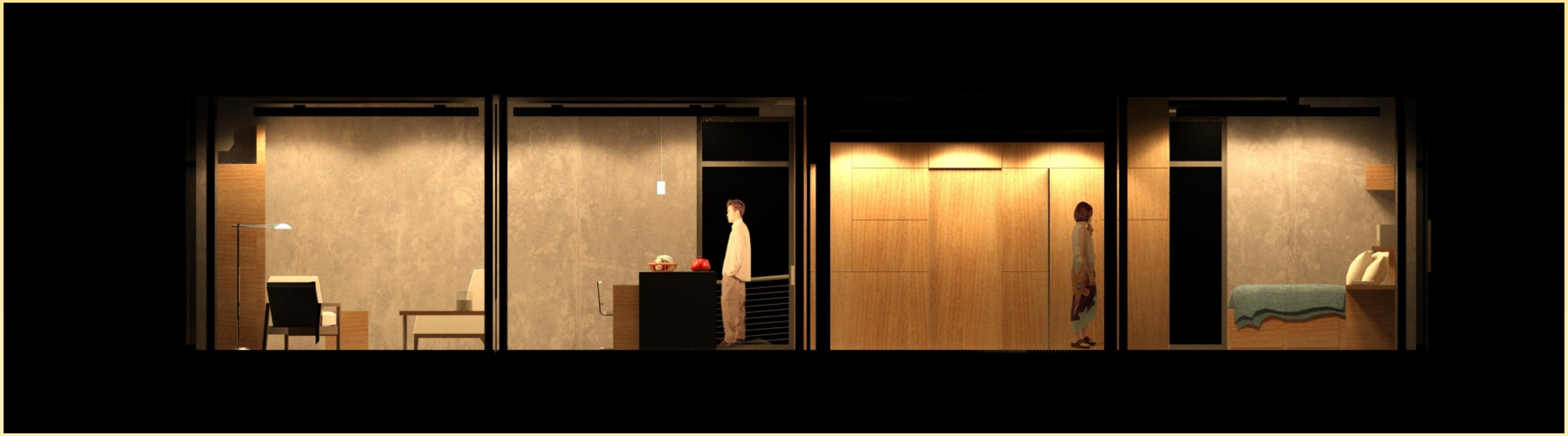

http://www.youtube.com/watch?v=j1H6ojXcitY

Solar Decathlon House GaTech

EPIC Education Focus

- Undergraduate Education
  - Energy Concentrations within ME, ECE, CE and ET
  - “Introduction to Energy” for all Engineering students
  - Expand Co-op and Internship program
  - Undergraduate Research Assistance
  - Student participation in Leadership Academy
  - Senior Design Project – Energy related
- Graduate Education in Development
  - MBA with Energy concentration
  - Energy certifications in all disciplines – retraining
  - Certifications – Energy Efficiency, Nuclear, Smart Grid, etc.
  - Energy Certification for Non-engineers
  - Graduate Research Assistance
  - Accredited short courses – PE through MS
- Coordination with Regional Universities
  - Concentrations and MS programs

EPIC Applied Research Clusters (1)

- *Power Systems Modernization*
  - Duke Energy Smart Grid Laboratory with RTDS and system analysis – NSF MRI
  - Distribution Automation and Micro-grids
  - Electric Vehicle and Energy Storage Integration
- *Large Energy Component Design and Manufacturing*
  - Siemens Large-scale Manufacturing Laboratory
  - Materials Characterization Laboratory (MCL)
  - Robotics and Welding Technologies
- *Power Infrastructure & Environmental Development*
  - Large-structures laboratory and T&D designs
  - Utilization and recycling of spent fuels and emission controls
- *Renewables and Energy Efficiency*
  - Clean-room with PV cell and LED research
  - Off-shore wind, biomass and small-scale hydro technologies
  - Integration of renewables and energy efficiency measures
- *Energy Markets and Systems Engineering*
  - Quality Assurance, Nuclear Safety, Regulatory and Standards
  - Distributed energy markets
  - Improved supply chain utilization

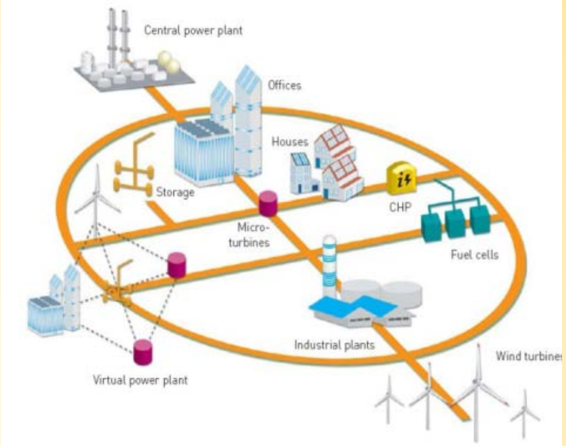

EPIC Applied Research Clusters (2)

- The Infrastructure, Design, Environment and Sustainability Center (*IDEAS)* *ideas.uncc.edu*
  - Development and utilization of biofuels
  - Natural and Built Site Design and Analysis (Green Buildings)
  - Materials Characterization Laboratory (MCL)
  - Environmental impact analysis
  - Environmental Assistance Office for Small Business (EAO)

IDEAS Center
Infrastructure, Design
Environment & Sustainability

- *Sustainable Integrated Buildings and Sites (SIBS)*
  - I/UCRC NSF Center with industry related research
  - PV integration in dense urban settings with limited roof space poor orientation, insurance issues, etc.
  - Optical collectors to guide light into PV building
  - Energy modeling for DSM, energy storage, and renewables
  - Thermal-energy storage for peak-shaving
  - Thermal storage technologies

SIBS
Sustainably Integrated Buildings and Sites Center

Founding Industrial Partners in EPIC

Board Members from Representative Organizations:

- Duke Energy
- Siemens
- Westinghouse
- AREVA
- URS Corp
- Shaw Group
- Electric Power Research Institute (EPRI)
- Tessera
- Steag Energy Services

Aba Ebong - EPIC Professor
Photovoltaic Research Laboratory (PVRL)

Vision Statement

Establish a world class research and education program at UNC Charlotte to attract young and talented minds in Science and Engineering to give USA a competitive advantage in the field of Photovoltaic Science, Engineering and Technology

Milestones:

- Conduct high quality research in Renewable Energy to foster fundamental understanding of the science and technology of photovoltaic cells, modules, systems , integration and distribution .
- Train undergraduate and graduate students
- Establish collaborative research with the industry to develop new materials for photovoltaic devices and serve as an R&D arm of the Photovoltaic industry
- Establish collaborative research with other universities within NC, USA and internationally.
- Establish certificate courses in Renewable Energy to position UNC Charlotte at the fore front in the field.
- Serve as a training center to provide experience for engineers and scientists.

Area of expertise:

- Silicon solar cell – Design, modeling, analysis, fabrication and characterization.
- III-V Light Emitting Diodes – Design, modeling, fabrication and characterization

Research Highlight:

- Cost effective and high efficiency solar cells through advanced structures, processes, understanding and reducing the parasitic losses.
- Understanding and improving every layer of a solar cell through optical, electrical, thermal and mechanical characterization of a solar cell
- Development of new and low-cost dielectrics for effective passivation of solar cells
- Development of novel contacting schemes including ink jet printing and light induced plating of Ni/Cu and Ag dip for crystalline silicon solar cell
- Development and optimization of inline process for <50 µm thick silicon application
- Investigate the microstructures of Ag and Al metal pastes and the liquid phase sintering thereof
- New module concepts and materials thereof
- Systems integration and connectors

Previous industry collaboration and funding:

Company name	Period	Amount
Heraeus Inc.	2006-2009	$609,000
Dupont Electronics	2010-2011	$200,000
Dow Advanced Electronics	2008-2009	$125,000
Konca Solar	2010-2011	$100,000
Despatch Solar	2009-2011	$200,000
TP Solar	2009-2011	$60,000
Wuxi Calex	2010-2011	$180,000
BASF	2006-2011	$510,000
Air Product	2009-2011	$180,000
Five Star Technologies	2008-2010	$260,000
Varian Semiconductors	2009-2010	$100,000

Number of graduate students envisaged: 10

Number of postdocs: 4

Expected Funds: Industry to start and then DOE and NSF

<u>Associated Publication s</u>

A. Ebong et. al "On the ink jetting of full front Ag gridlines for cost effective metallization of Si Solar Cells," IEEE Electron Device Letters, vol. 33, no. 5, 637-639, 2012.

A. Ebong et al "Capitalizing on the glass etching effect of silver plating chemistry to contact silicon solar cells with homogeneous 100-110 ohm/sq emitters" IEEE Electron Device Letters, vol. 32, no. 6, 779-781, 2011.

A. Ebong et al "Overcoming the technological challenges of contacting homogeneous high sheet resistance emitters (HHSE)" Proceedings 26th European PVSEC, Hamburg-Germany, September 5th-9th 2011.

A. Ebong et al ""Impact of surface cleaning on random texturing of crystalline silicon wafers" Proceedings 26th European PVSEC, Hamburg-Germany, September 5th-9th 2011.

A. Ebong et al ""Implementing narrow front silver gridlines through ink jet machine for high quality contacts to silicon solar cells" Proceedings 37th IEEE PVSC, Seattle, June 2011.

Aba Ebong - EPIC Professor
Photovoltaic Research Laboratory (PVRL)

Laboratory space required

4100 ft^2

Equipment needed


Wet bench for wafer clean & texturing


Inline Diffusion furnace for B & P diffusion


Tube Diffusion & PECVD furnace for p-n junction formation & AR coating


Inline Oxidation furnace for passivating oxide growth


Inkjet printer for Ag front contacts


Screen-printer for Ag front contacts


Belt line contact firing for contacts sintering


Plating station for Ni/Cu & Ag LIP

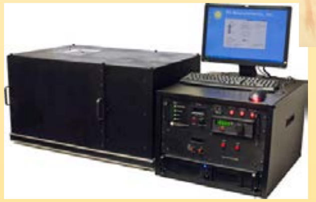
Solar cell simulator for measuring solar cell efficiency

Expected funding per year: $200K (Estimate)

Funding source: Industry, DOE and NSF

Equipment in storage awaiting installation

Start up funds: $400K from EPIC

Donation through equipment: $1,050K for equipment received in storage.

Equipment donation pending: $600K

Installation cost: $400K (Estimate)

Annual running cost: $50K (funds from sponsored projects)

Anything you can do GaN can do better…

Lattice Constant vs Bandgap

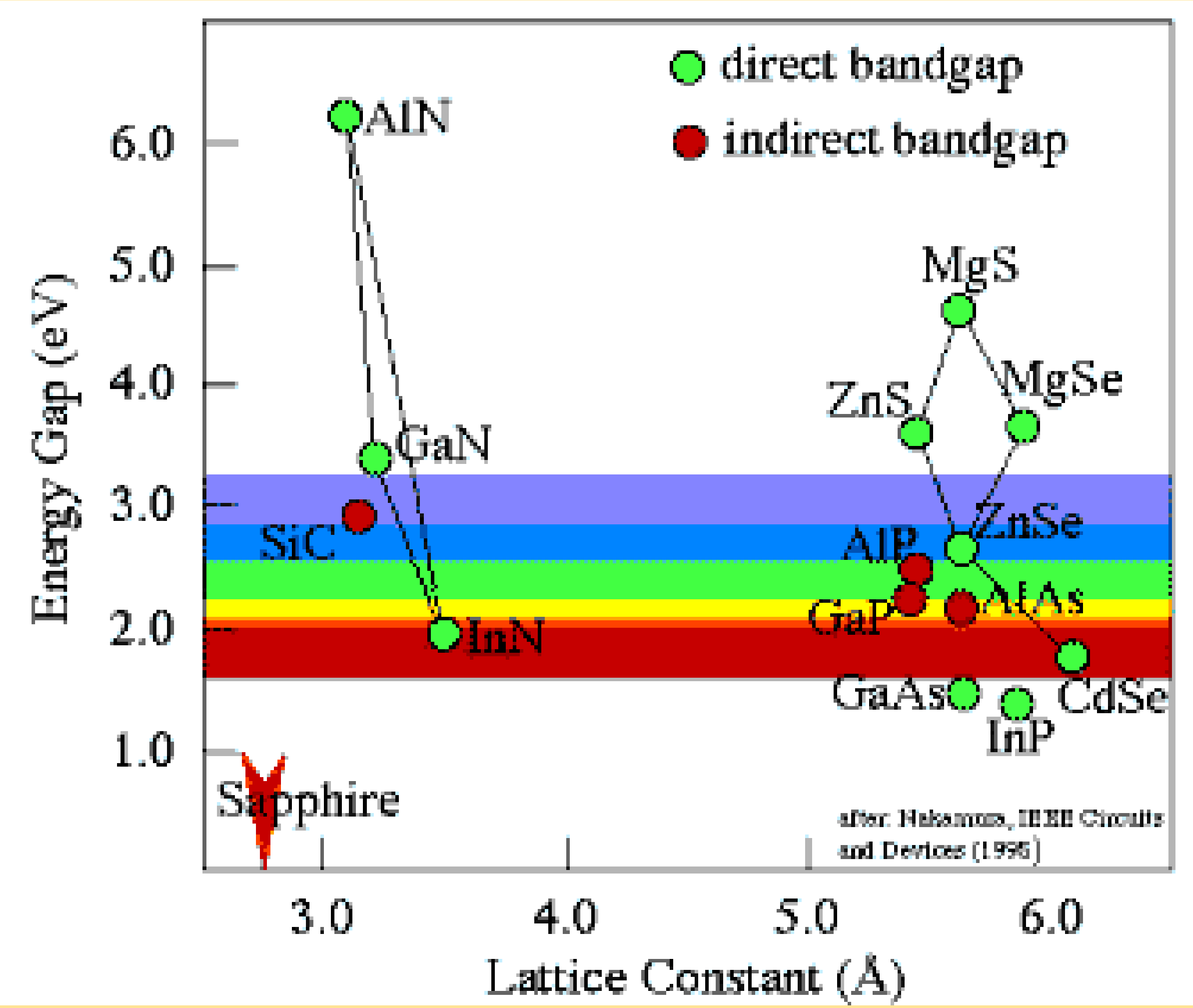

after Nakamura, IEEE Circuits and Devices (1995)

New Approaches to Solid State Lighting: A Diurnal Light Source

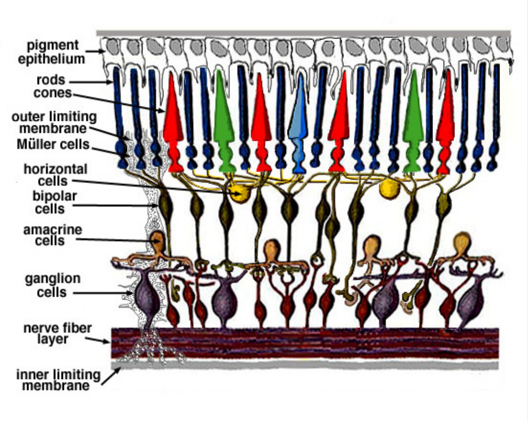

Melatonin response peaks around 464 nm →

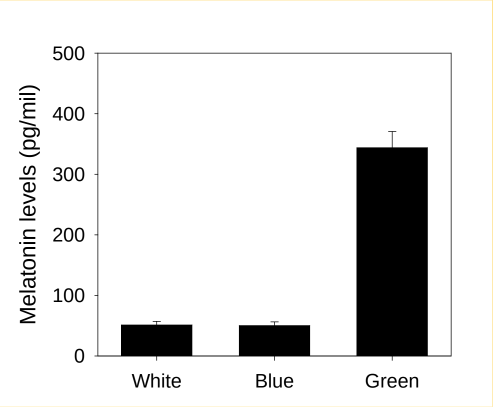

Visual Acuity → Psychological → Physiological

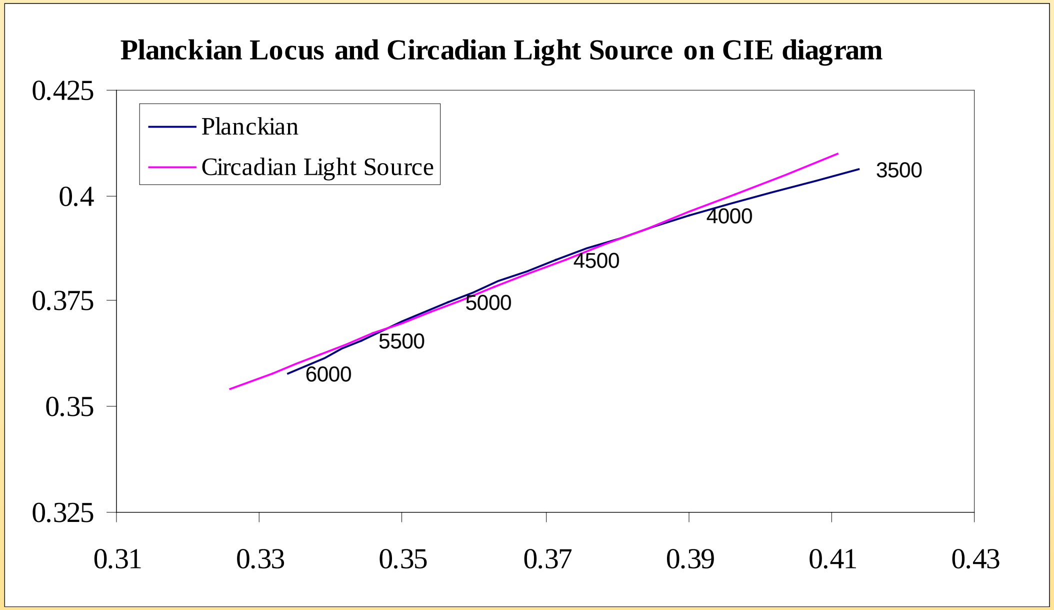

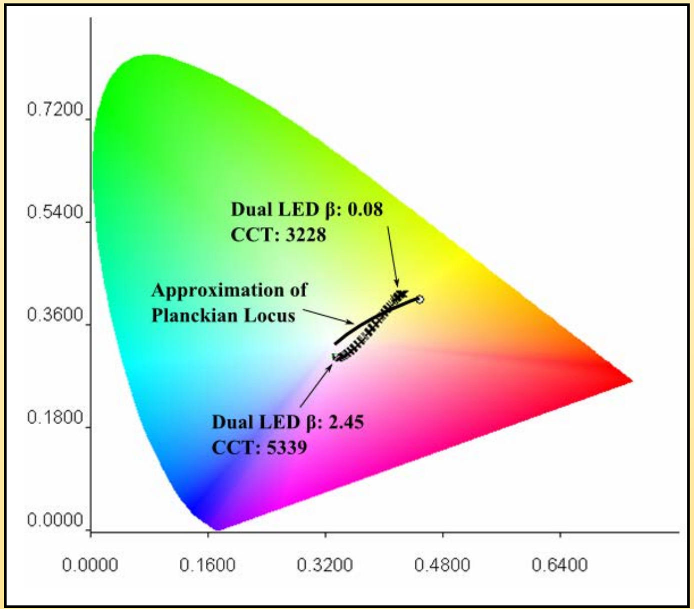

Dual LED β: 0.08
CCT: 3228

Approximation of Planckian Locus

Dual LED β: 2.45
CCT: 5339

Optimizing the dual emitter

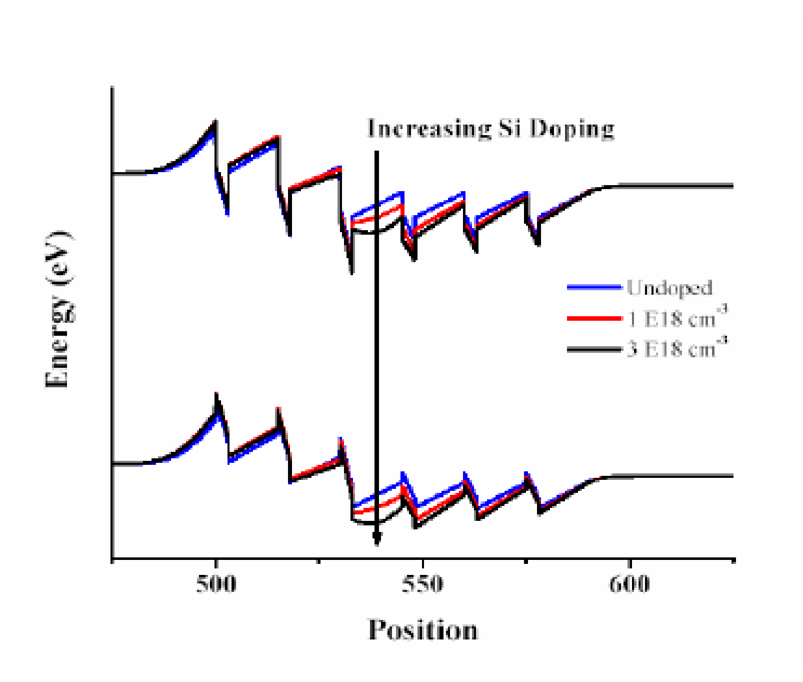

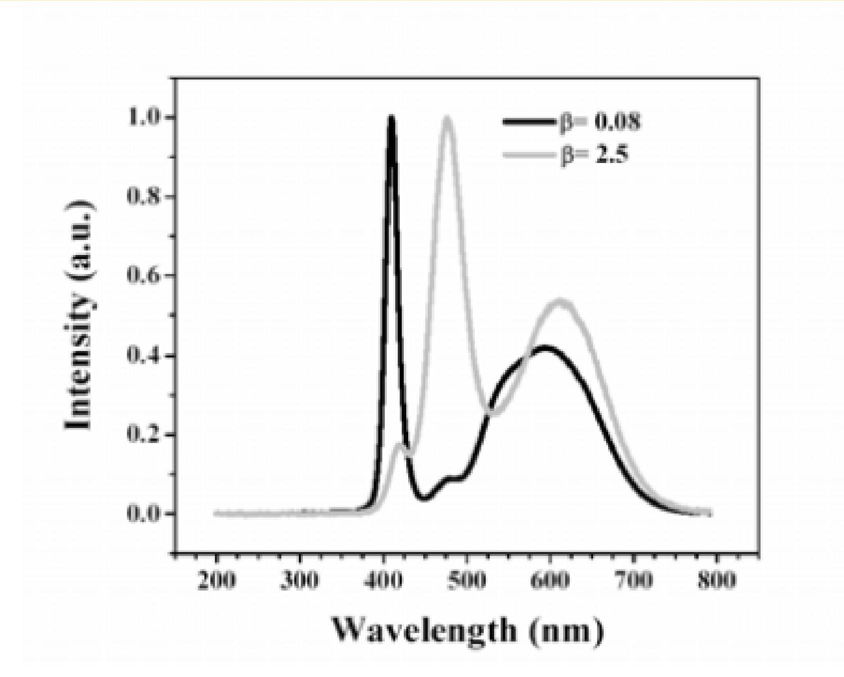

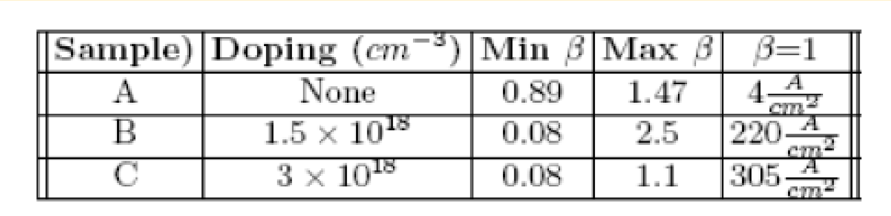

Sample)	Doping (cm^{-3})	Min β	Max β	β=1
A	None	0.89	1.47	$4\frac{A}{cm^2}$
B	1.5×10^{18}	0.08	2.5	$220\frac{A}{cm^2}$
C	3×10^{18}	0.08	1.1	$305\frac{A}{cm^2}$

New materials for semiconductor spintronics

Semiconductor

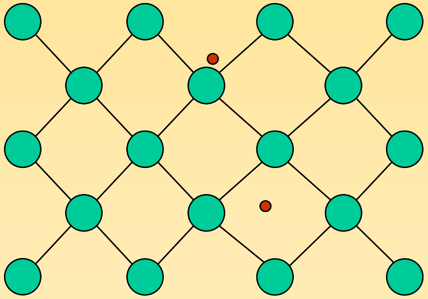

Ferromagnet

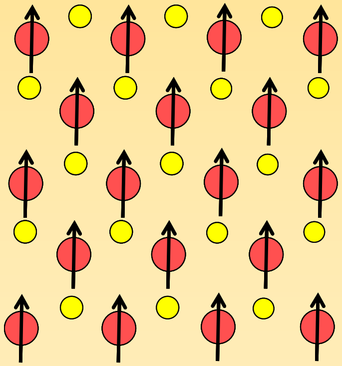

Dilute Magnetic Semiconductors

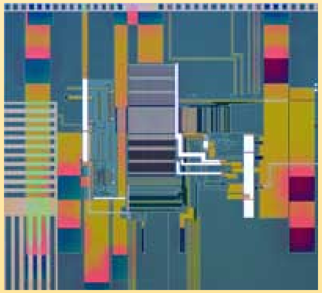

Nonvolatile memory

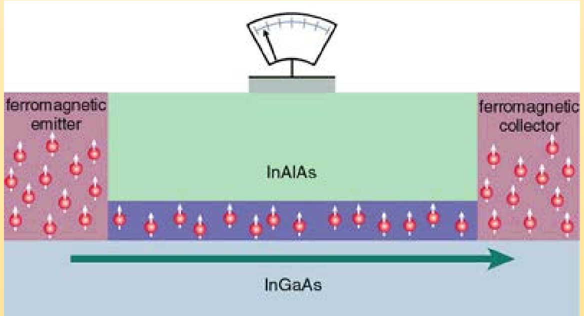

Spin-based logic and computation

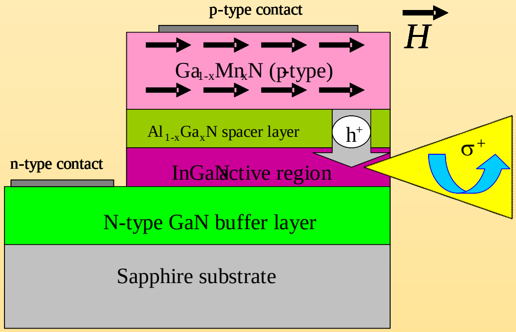

Spin emitters

Effect of doping on $Ga_{1-x}Gd_xN$

p-Unactivated

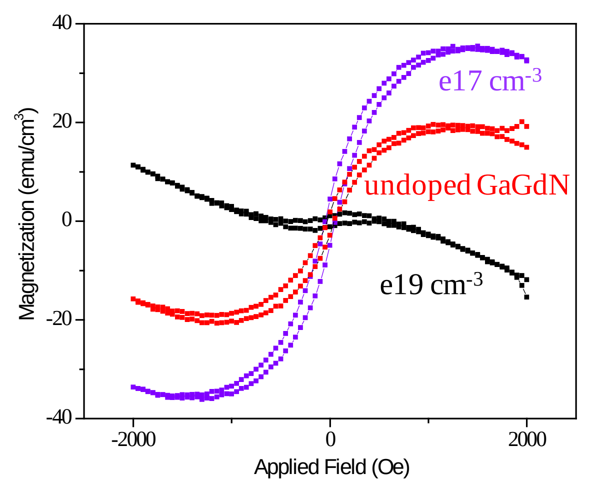

p-activated

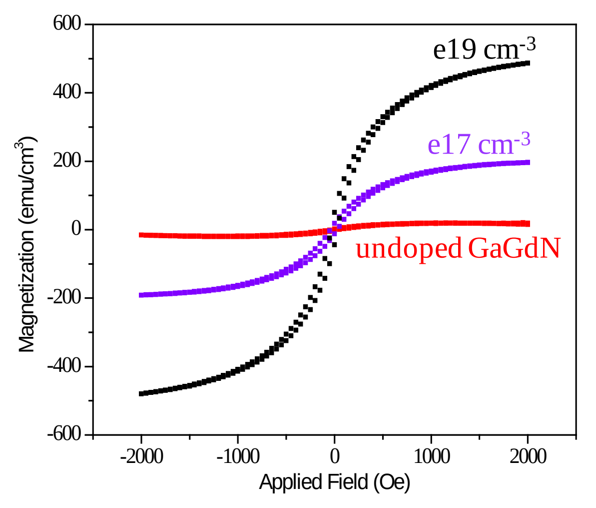

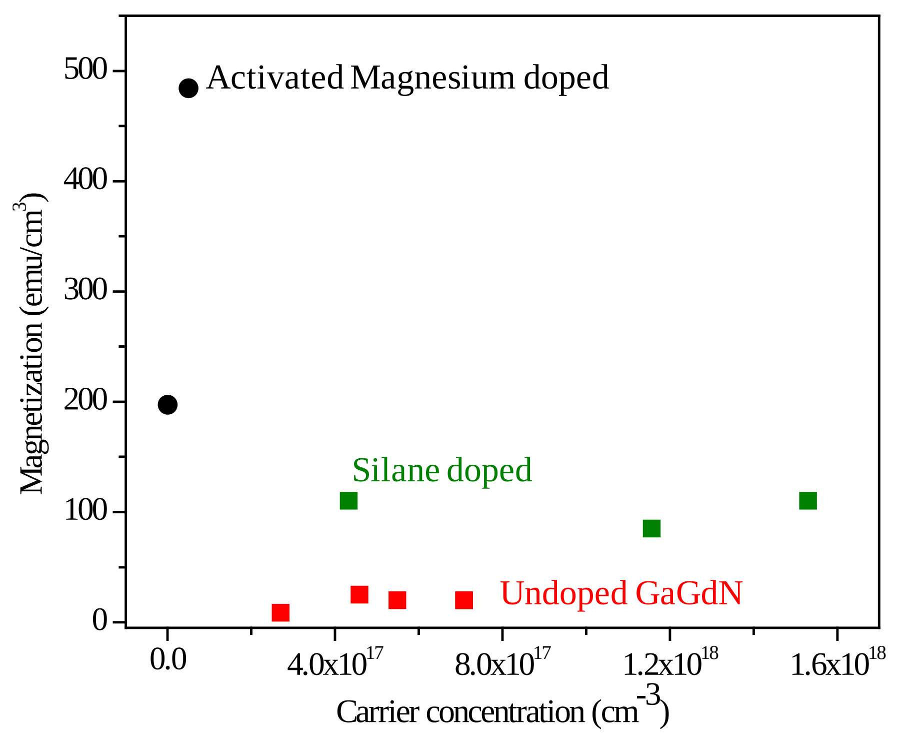

Activated p-doped $Ga_{1-x}Gd_xN$ results in a large magnetic moment

Spin-polarized LED emission

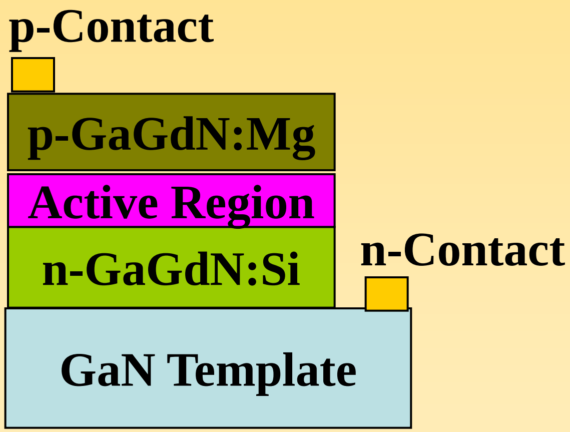

Spin LED Structure

- First MOCVD Gd doped GaN thin film report
- Increase conductivity with Gd doping
- Both n- and p-type films grown on GaN template
- p-n diode and LED structures with Gd doped GaN
- Spin-polarized LED fabricated – Under test

$P = (\sigma^- - \sigma^+) / (\sigma^- - \sigma^+) = 0.34$ (0G)
$= 0.22$(4kG)

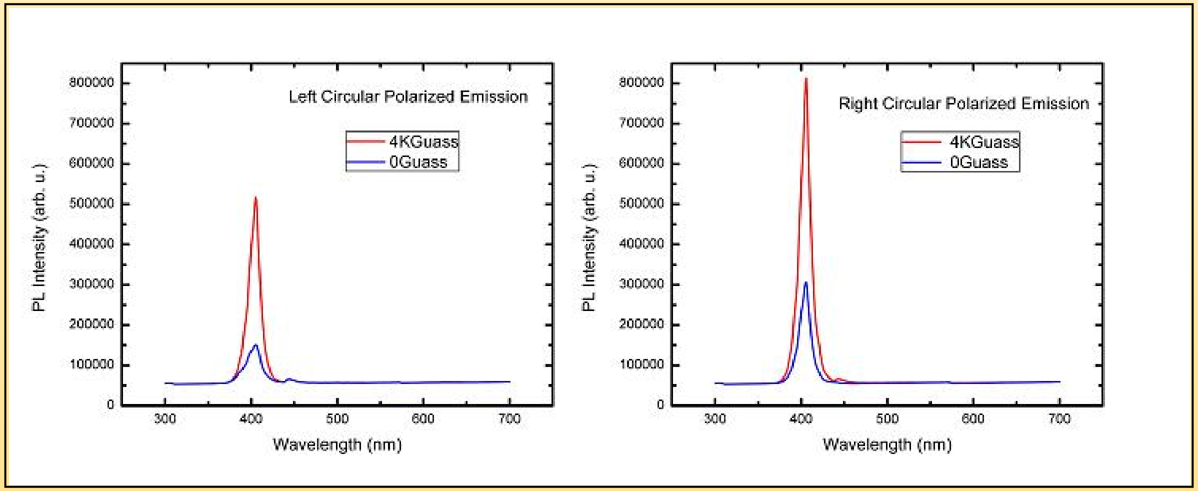

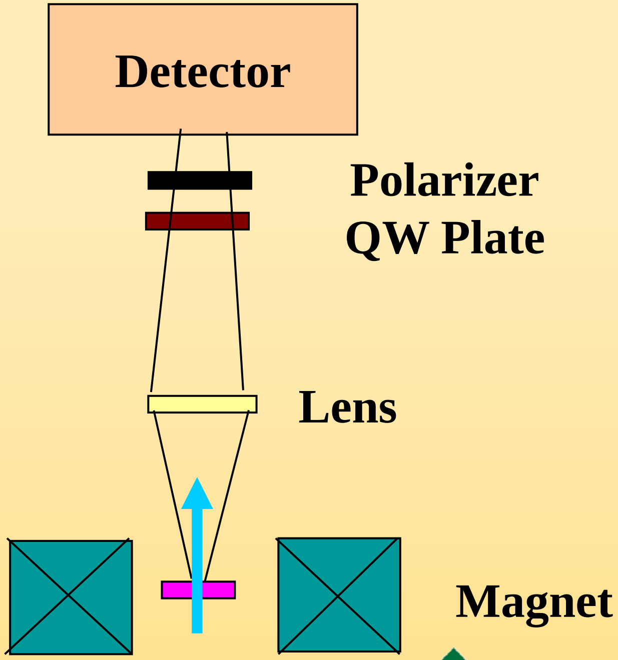

III-Nitrides for Neutron Detection

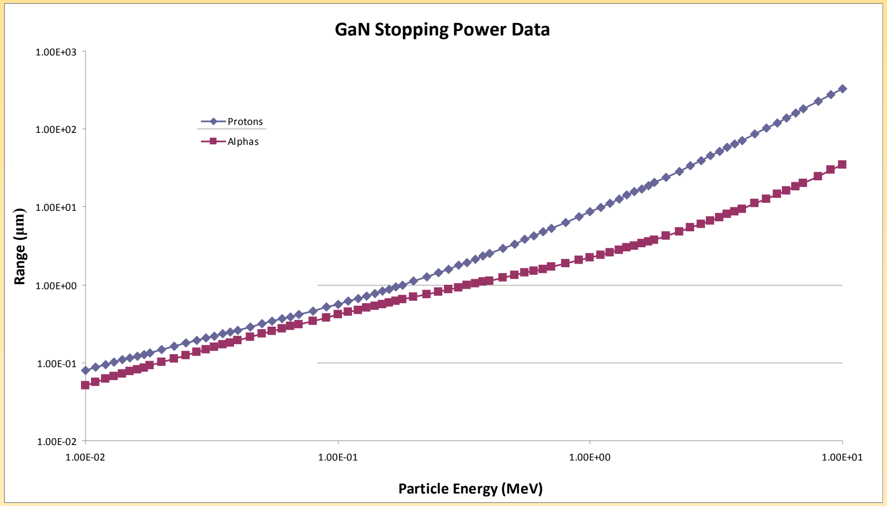

Reaction	Deposited Energy (MeV)	Range of Proton (µm)	Range of Alpha (µm)
10B@ 5MeV	2.8	-	13.6
14N@ 2.65	2.626	36.1	-

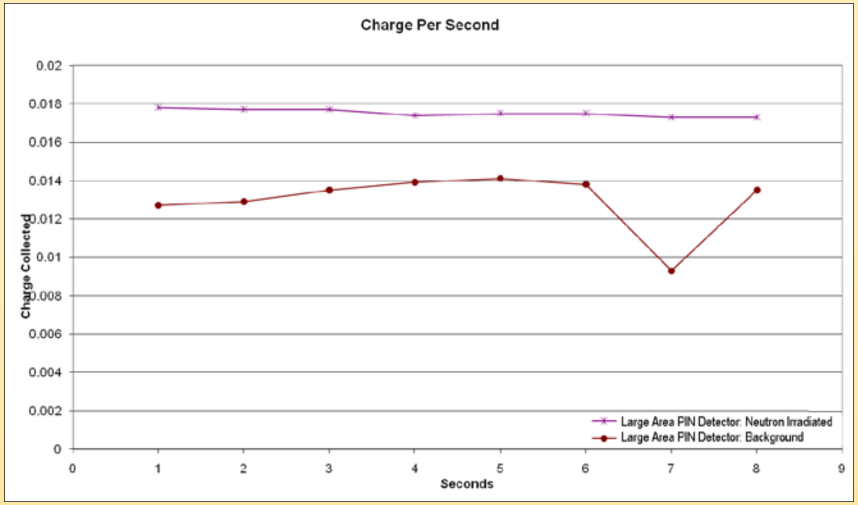

Clear trend in increased collected charge is indicator of (n,p) events

Neutron-Induced Scintillation

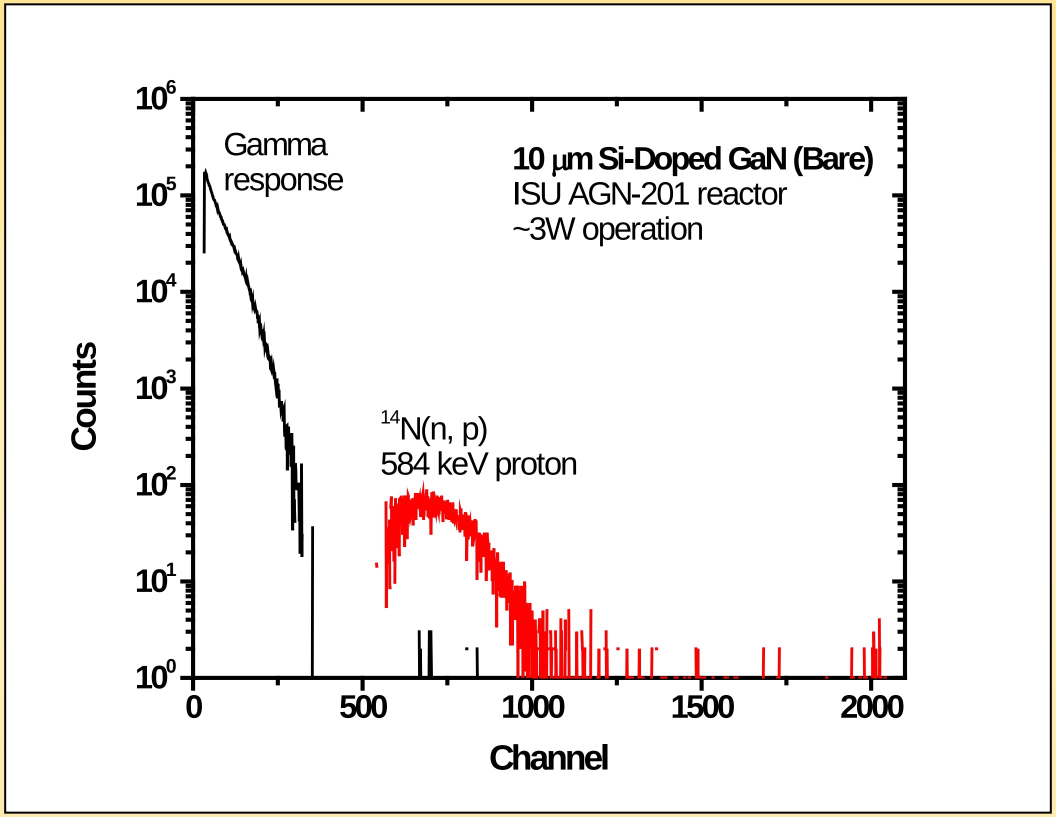

Excellent gamma discrimination observed

Future Direction: Multifunctional EMO devices

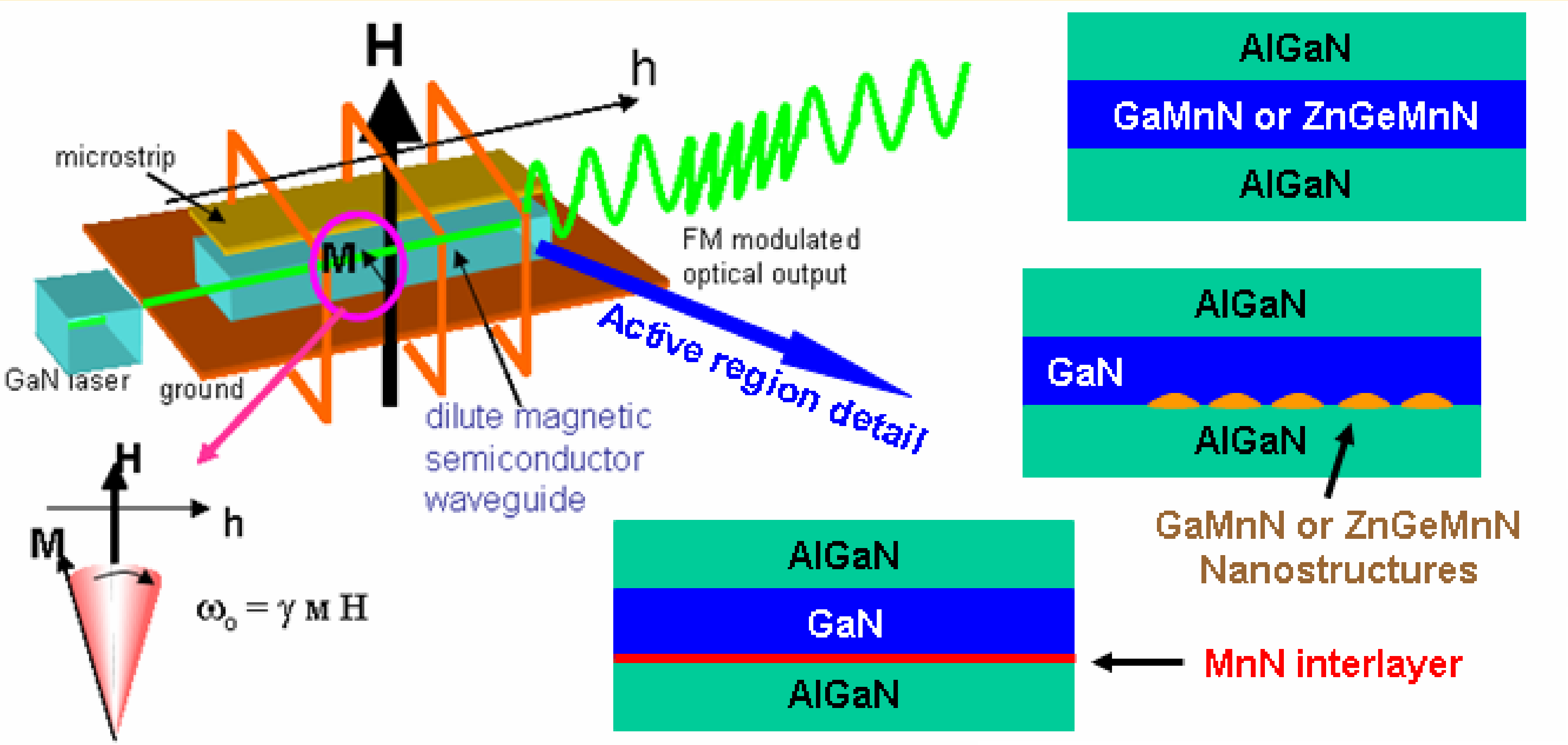

Devices where the Electrical, Magnetic and Optical (EMO) can interact.

III-Nitrides for Solid State Lighting

Historical Development of Lighting and LEDs

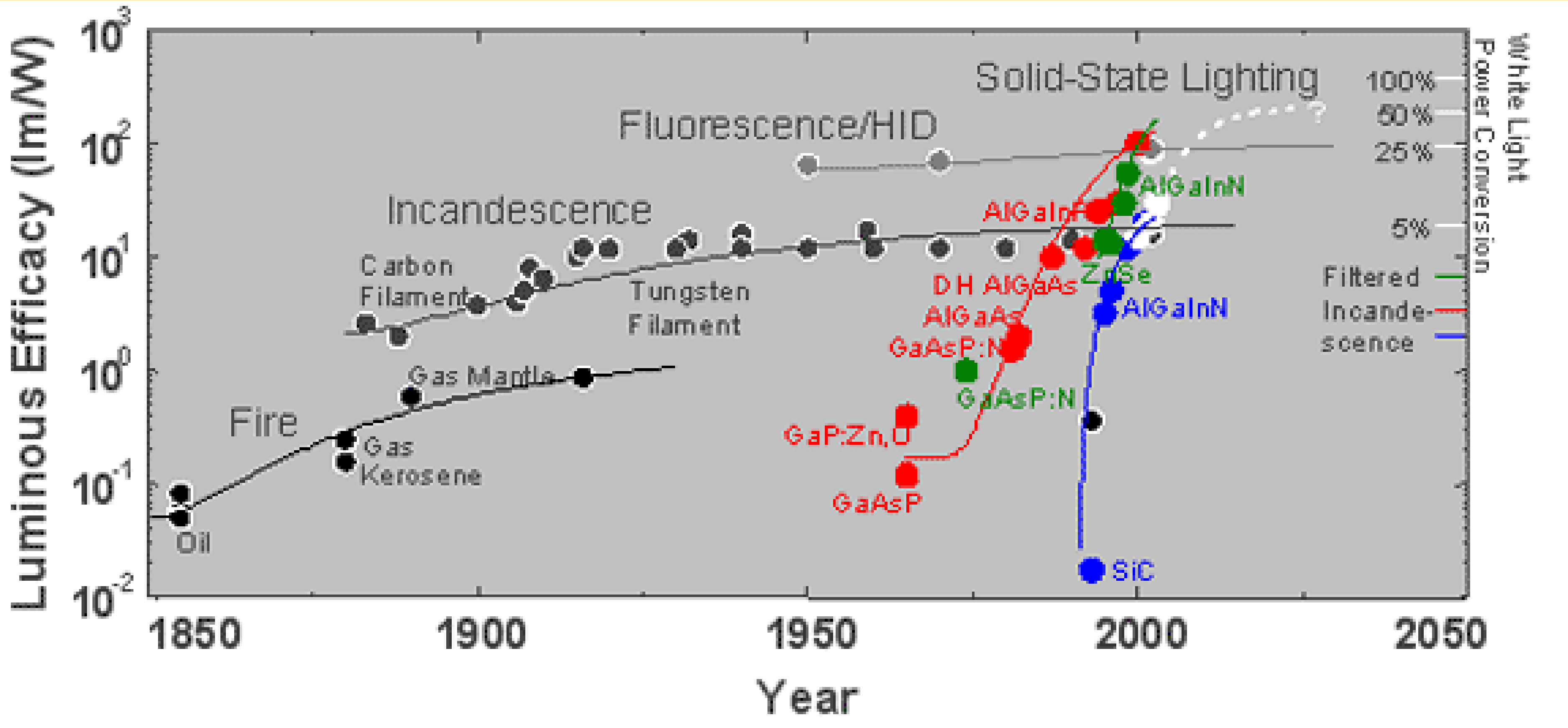

Ian Ferguson
(ianf@uncc.edu)

UNC CHARLOTTE
Electrical and Computer Engineering

Combined Blue LED and YAG:Ce,Pr Spectra=White

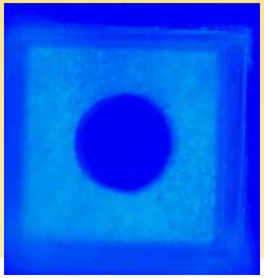

+

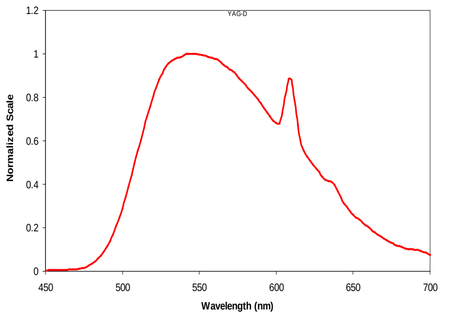

+

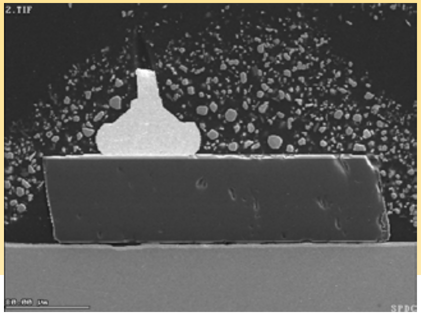

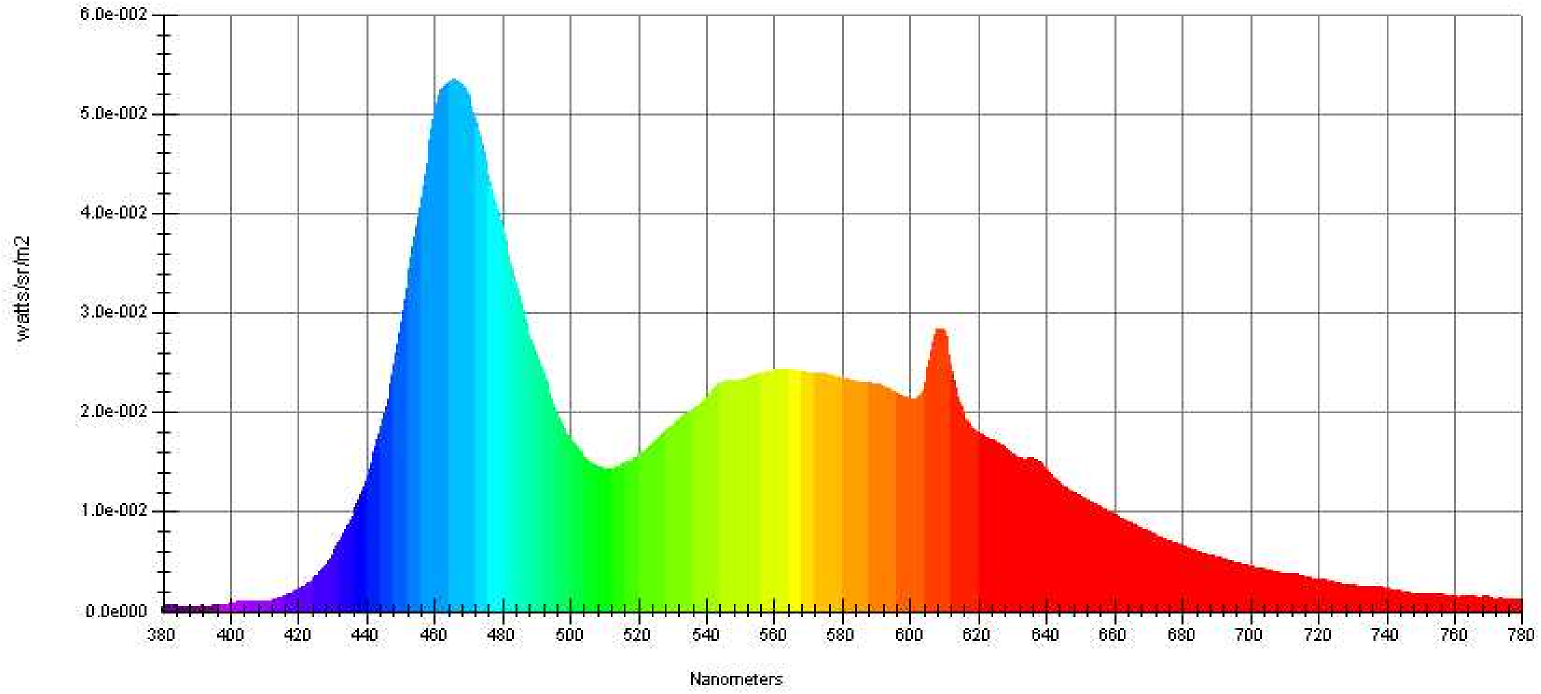

(Mueller et al., IDW 2000, Lumileds)

Solid State Lighting

- 100 years after the discovery of electroluminescence in a semiconductor, solid state illumination is enabled by advances in high power LED technology during the past 10 years
- Early history of the visible LED
- Development of high-power LEDs at Philips Lumileds
  - Light extraction
  - Packaging
  - Materials technology
- Emerging applications and new figures of merit

Clyde Bridge, Glasgow

Palace in Nancy, France

Street Lighting

- Ann Arbor
  - Replacing 1,500 streetlights
  - Payback 4 years
  - Using $100K less energy/yr
- Welland, Ontario
  - Retrofitted streetlights
- Tianjin, China
  - 1,500 streetlights
  - Energy savings and economic driver

Lighting in Egypt…

Al_2O_3 Transition layer-Schematic illustration

Atomic layer deposition (ALD) is used to provide a transition layer of Al_2O_3 on Si/ZnO substrates before nitride growth by MOCVD.

Al_2O_3 was grown at 100ºC for 5nm and 20nm, then annealed in a furnace at 1100ºC followed by AlN/GaN in MOCVD

GaN (2000nm)

AlN Buffer (50nm)

ALD Al_2O_3 5 nm

Si

MOCVD Growth of GaN on Si-Approaches

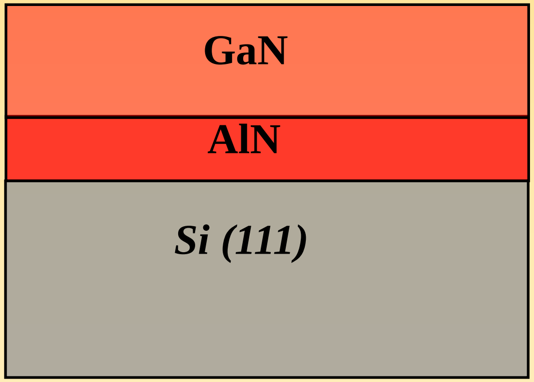

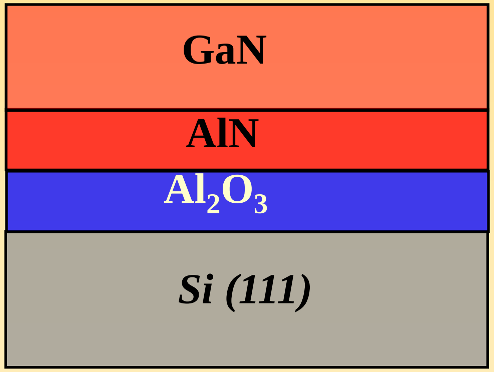

Develop MOCVD process for GaN on Si
Transfer the process to Al_2O_3/Si
Determine and compare the characteristics
Grow LED device structures and remove substrate

Structural Properties of GaN on Bare Si

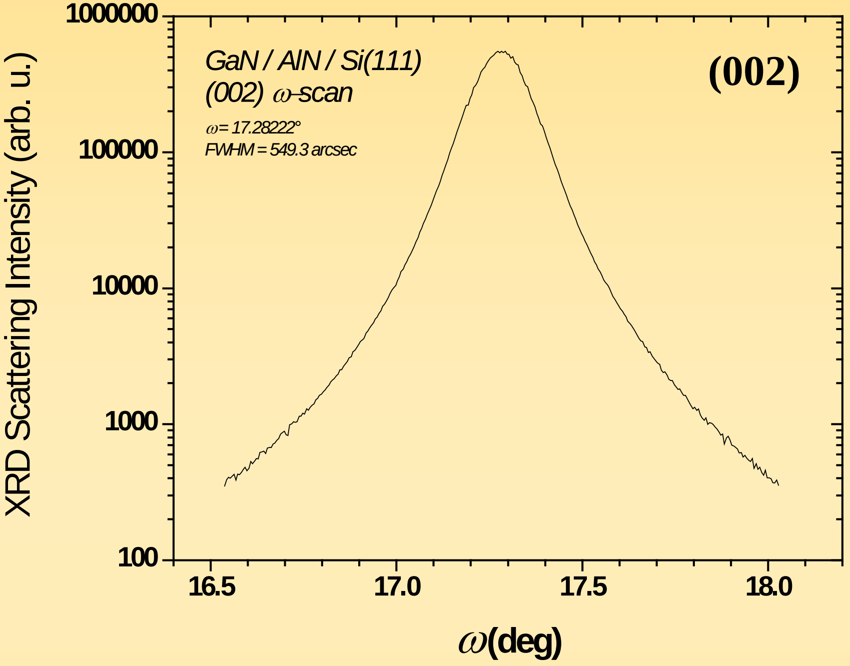

FWHM = 549.3 arcsec

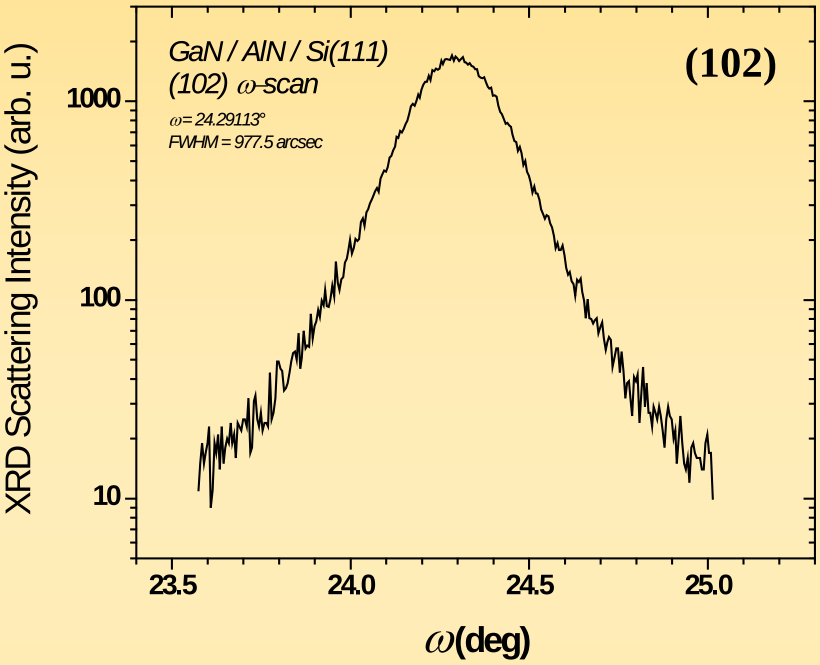

FWHM = 977.5 arcsec

- XRD shows good quality GaN (1.5 µm) material on Si

GaN on Bare Si - Summary

	XRD		PL		AFM
	(002) FWHM (arcsec)	(102) FHWM (arcsec)	FWHM (meV)	BL/YL	RMS roughness (Å)
HT-AlN buffer	**549.3**	**977.5**	**49.3**	**5.396**	**5.67**
LT-AlN interlayers	**436.8**	**1041.9**	**46.9**	**5.521**	**3.99**

MOCVD process developed for growth of high quality GaN on Si(111)

GaN on ALD/Si Substrate

Bare Si

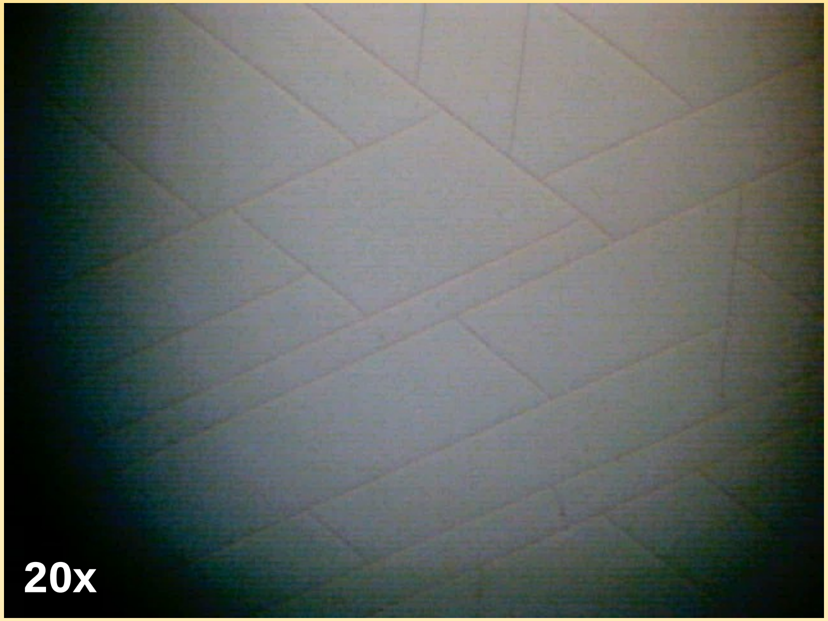

1.5um GaN on bare Si

10nm ALD-Al_2O_3/Si

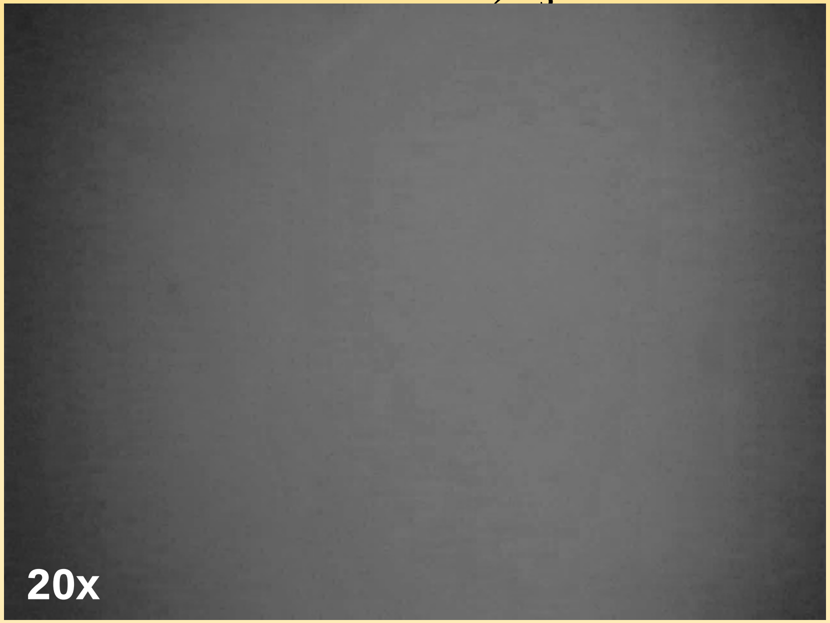

1.5um GaN on 10nm ALD-Al_2O_3/Si

The cracking issue has been resolved

Strain and Defect Density

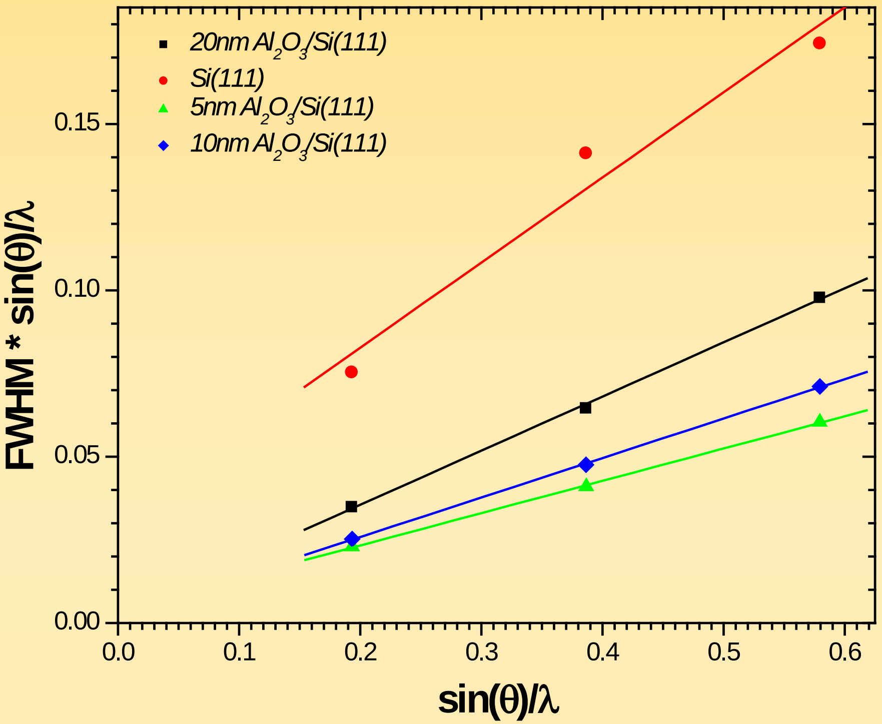

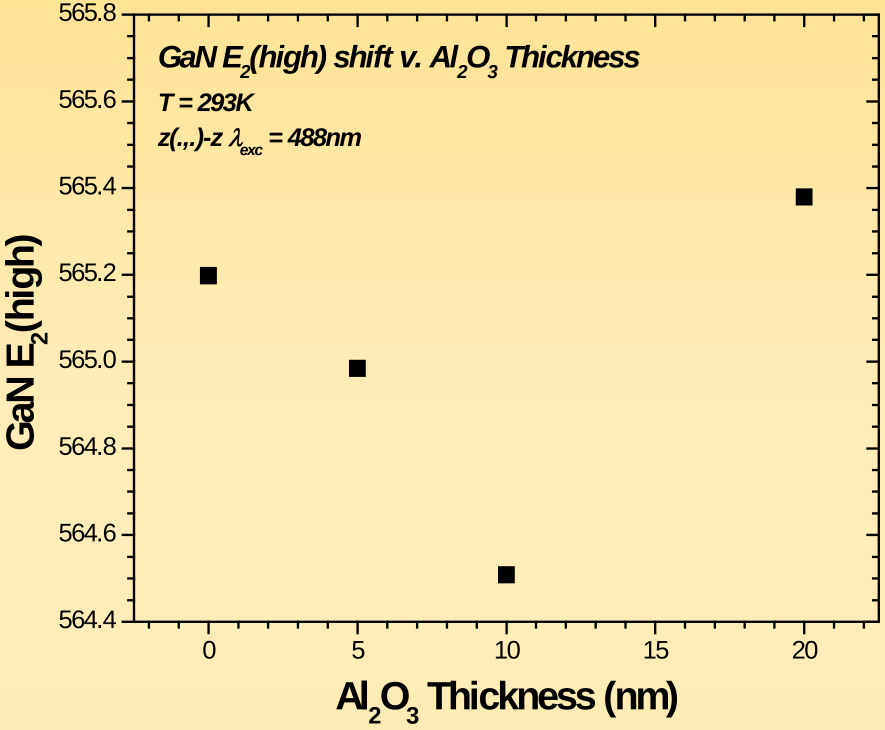

- Al_2O_3 layer reduces strain in GaN layer
- Decrease in tilt angle (α_{tilt})
- Decrease in dislocation density using ALD-Al_2O_3 layer

Process Summary - Comparison

	XRD		PL		AFM
	(002) FWHM (arcsec)	(102) FHWM (arcsec)	FWHM (meV)	BL/YL	RMS roughness (Å)
HT-AlN buffer	549.3	977.5	49.3	5.396	5.67
LT-AlN interlayers	436.8	1041.9	46.9	5.521	3.99
5nm Al_2O_3/Si	378.6	849.5	46.5	7.395	3.93
10nm Al_2O_3/Si	433.9	1344.6	47.7	4.497	5.65
20nm Al_2O_3/Si	416.6	740.1	43.4	28.223	3.70

Increased structural, optical, and surface quality compared to layers on bare Si

XRD linewidth approaching typical values for GaN on sapphire

Electrical Properties of GaN LEDs on Si and Sapphire

GaN-based LEDs were grown on ALD- Al_2O_3/Si and sapphire

Device structures consisted 1.0 µm n-GaN, 3-periods InGaN/GaN (3 nm/12 nm) MQWs and 150 nm p-GaN

Fabrication was performed to the device sizes of 350 × 350 μm^2

Similar turn-on voltage but higher series resistance for LED on ALD/Si than on sapphire.

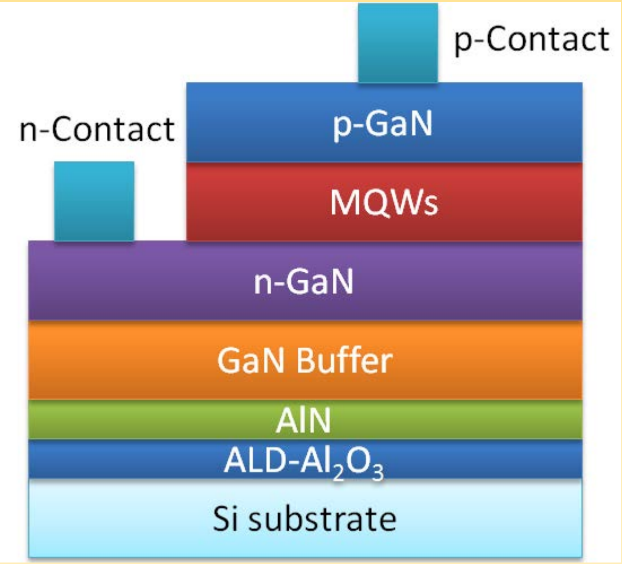

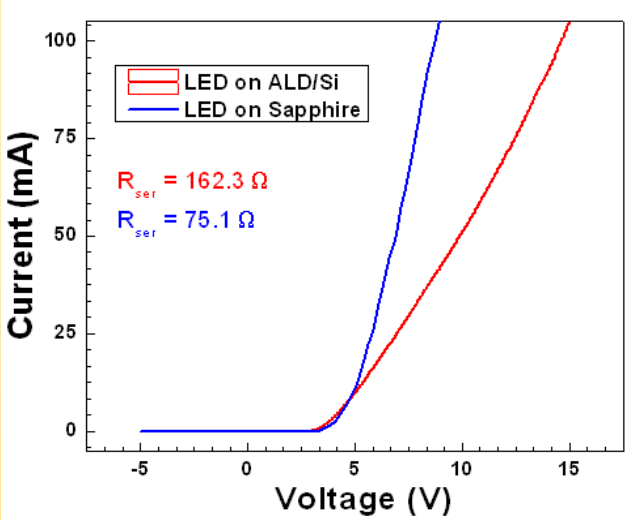

Crack-free LEDs on Si

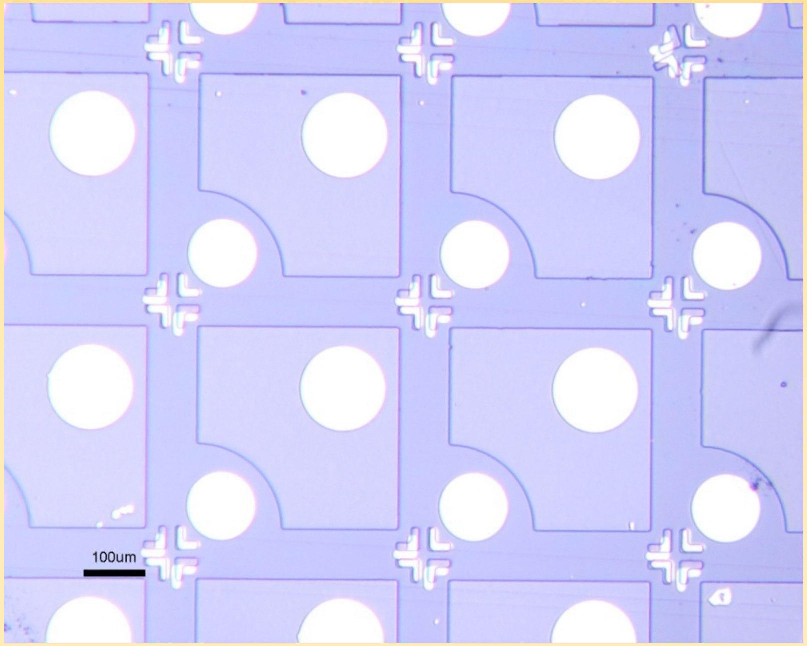

LEDs on ALD-Al_2O_3/Si

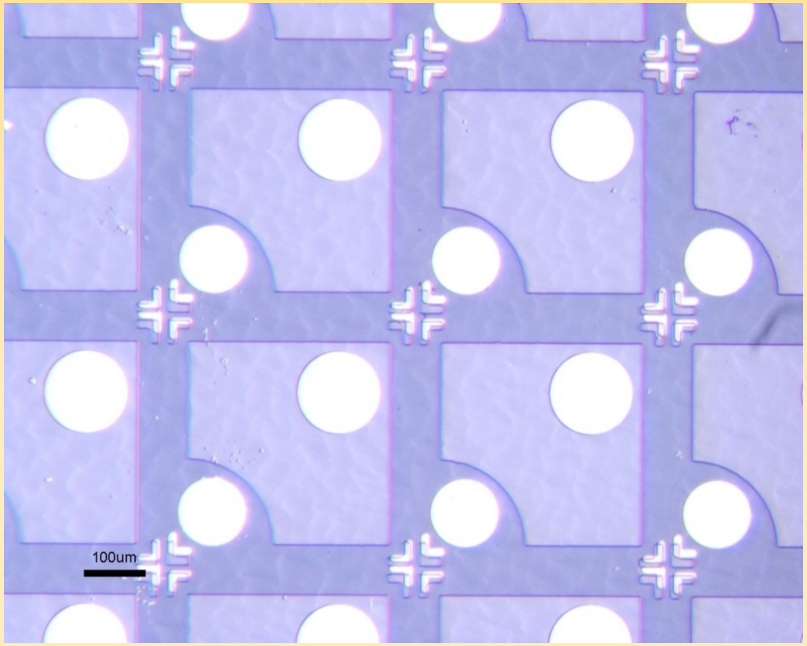

LEDs on GaN/sapphire

Crack-free GaN LEDs on ALD-Al_2O_3/Si substrates

Internal Quantum Efficiency (IQE)

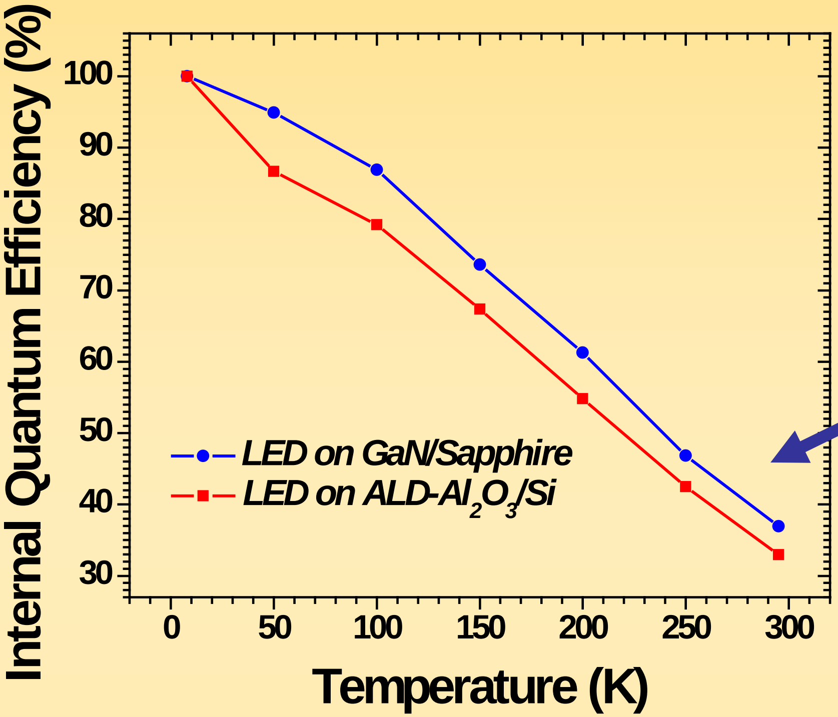

LEDs on sapphire and Al_2O_3/Si shows similar IQE values

Substrate	IQE
Sapphire	37%
Al_2O_3/Si	32%
Bare Si	~4%

Al_2O_3 /Si shows significant improvement in IQE over bare Si

Electroluminescence

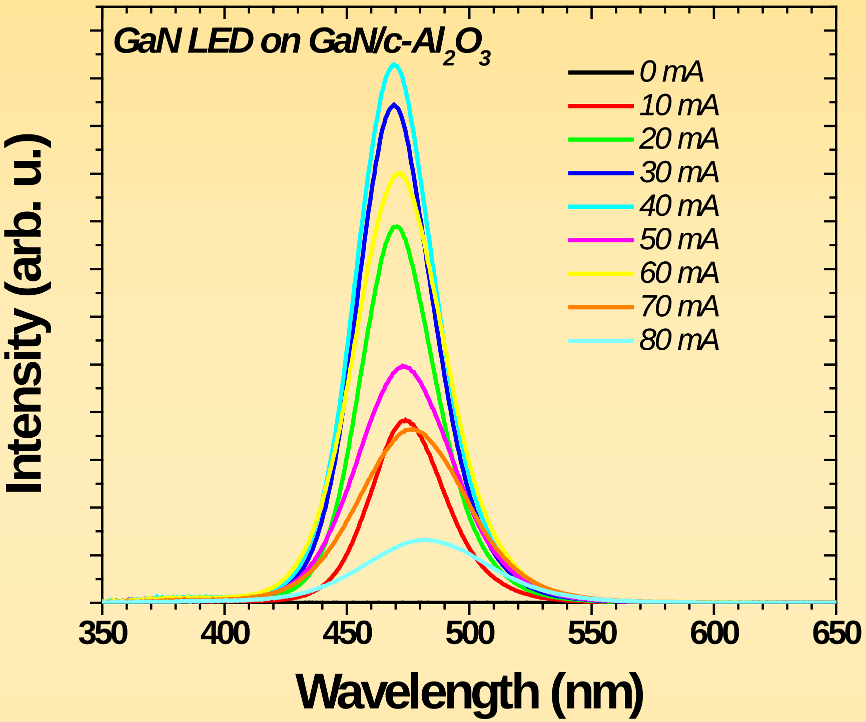

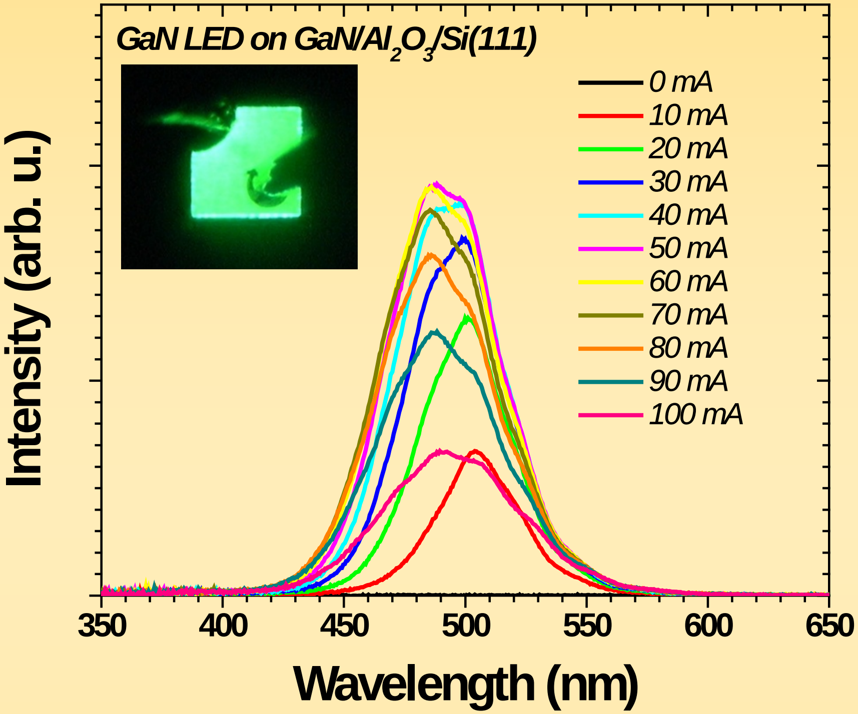

LEDs on ALD-Al_2O_3/Si substrates shifted to longer wavelengths

L-I curves

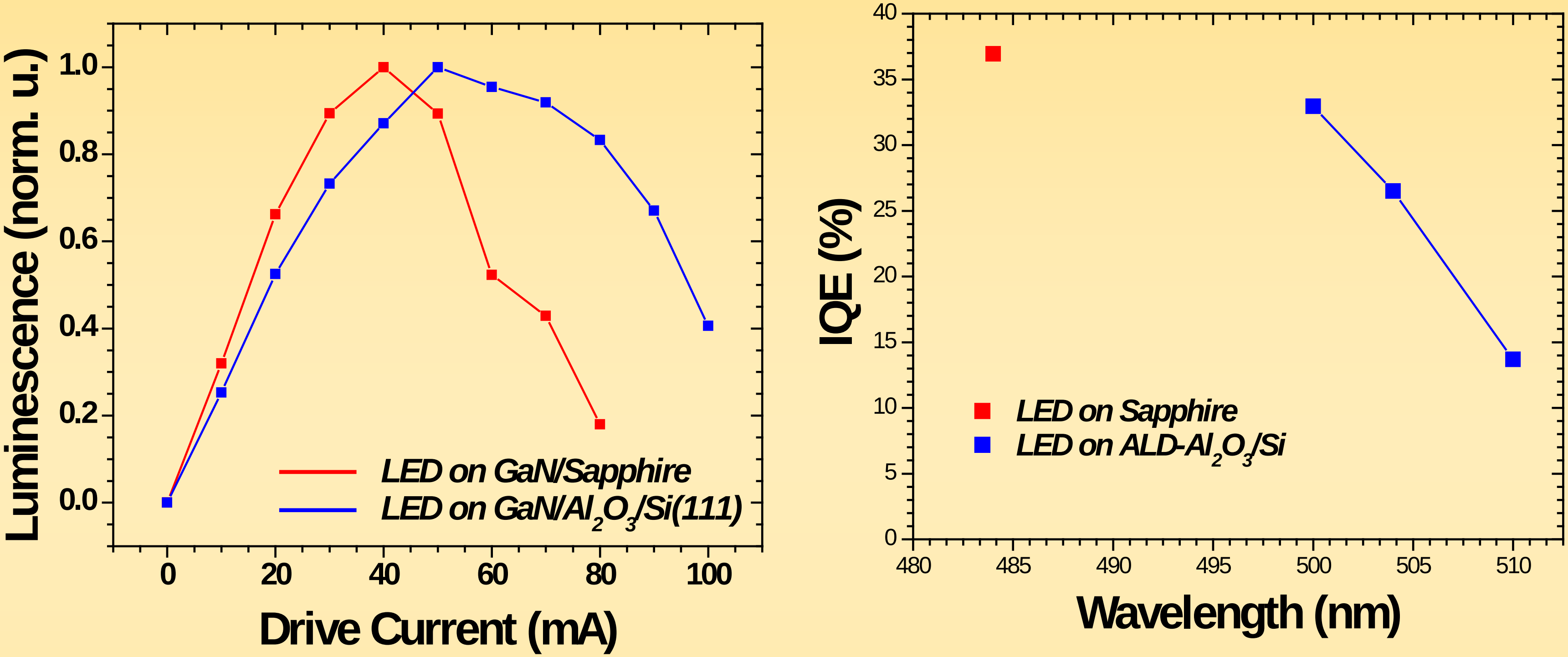

Higher efficiency at high drive currents for LEDs on ALD-Al_2O_3/Si
Drop in IQE with the shift toward longer wavelengths

Si Substrate Removal Process

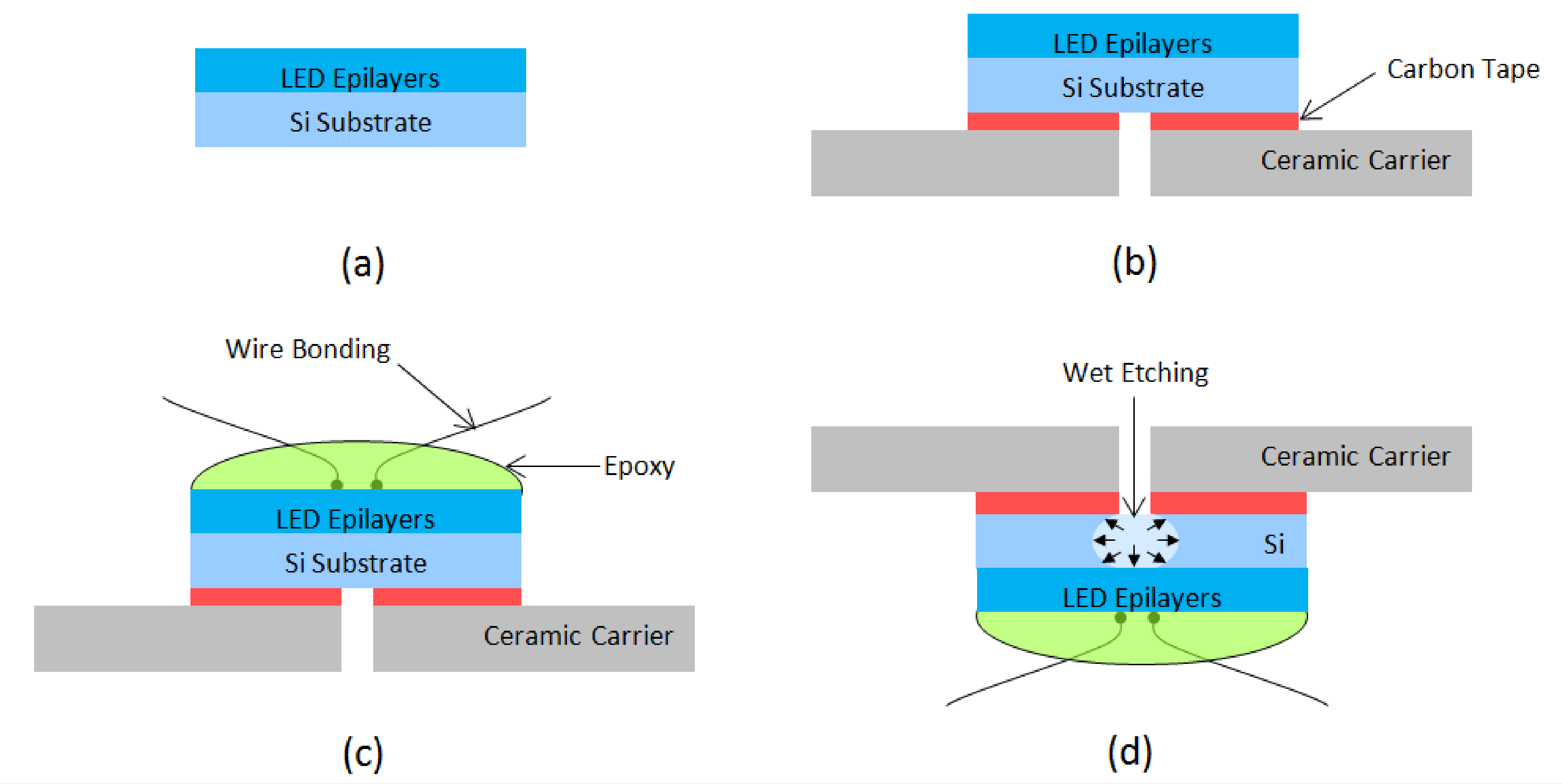

Selective wet etching process flow

(HNO3:HF:CH3COOH = 3:1:1)

Images of Substrate Removal Process Flow

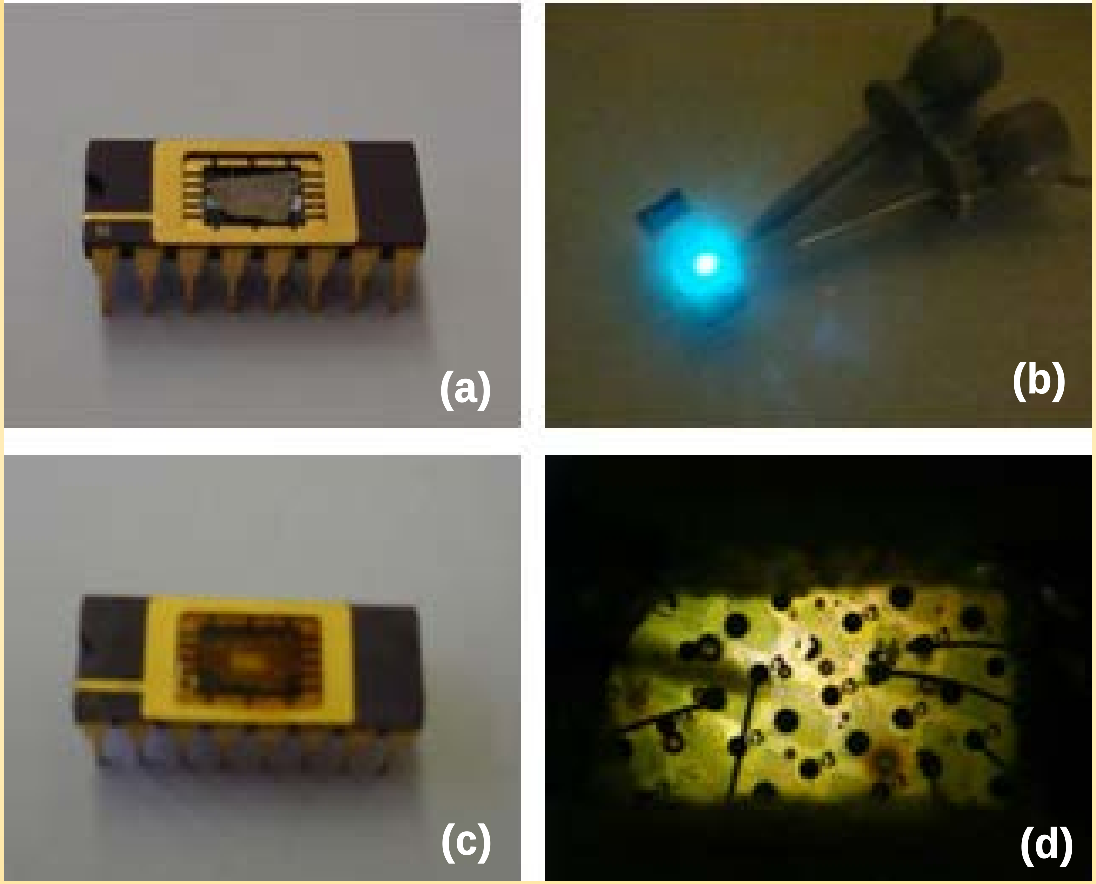

(a) GaN LEDs mounted on ceramic DIP holder by wire bonding
(b) LED lit up under forward driving current
(c) Si substrate selectively removed by wet etching
(d) Free-standing transparent GaN LED devices seen from back side.

Optical Properties Before and After Wet Etching

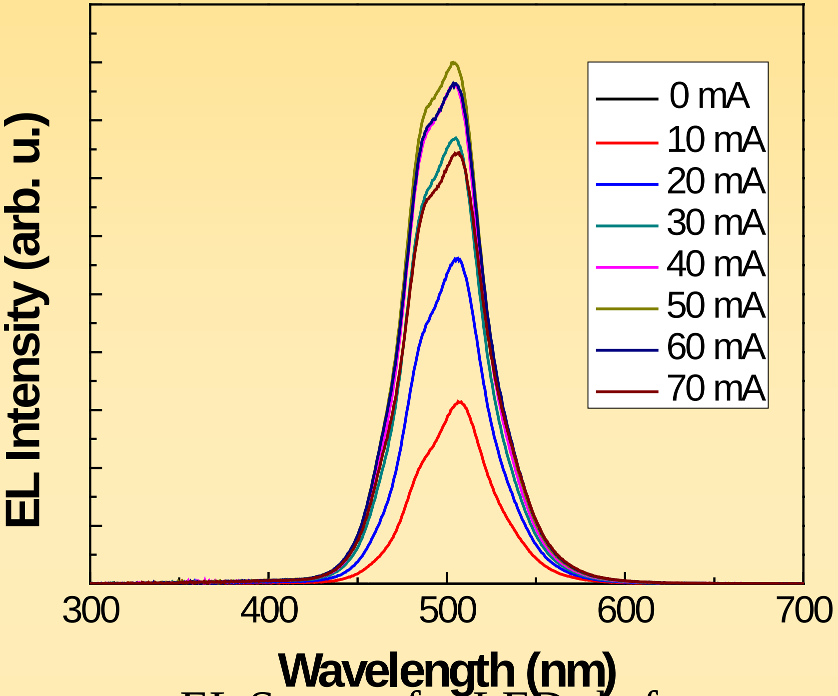

EL Spectra for LEDs before wet etching

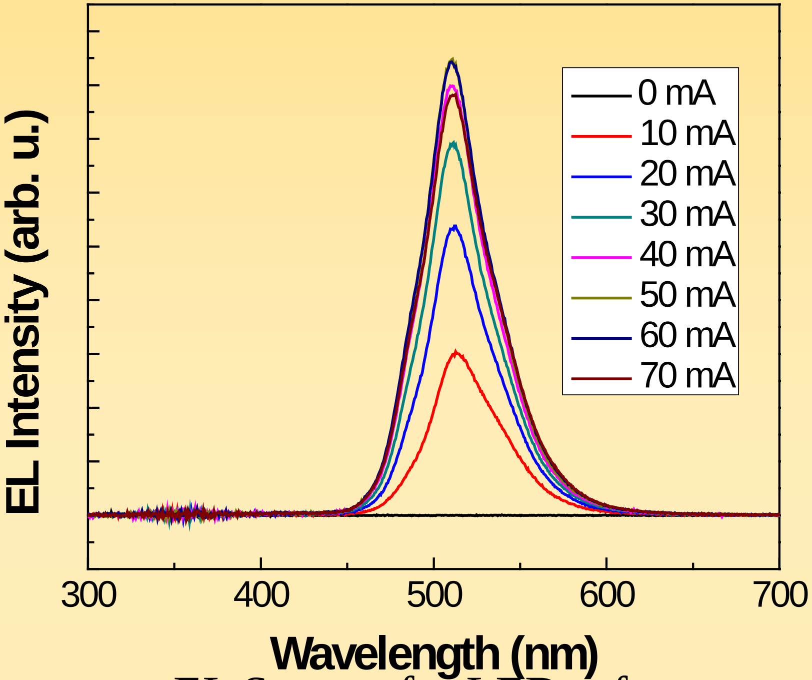

EL Spectra for LEDs after wet etching

No significant change in peak emission wavelength and EL intensity Vs drive current.

Wet etching process was effective to protect the devices from being damaged by acid etchant.

Electrical and Optical Properties

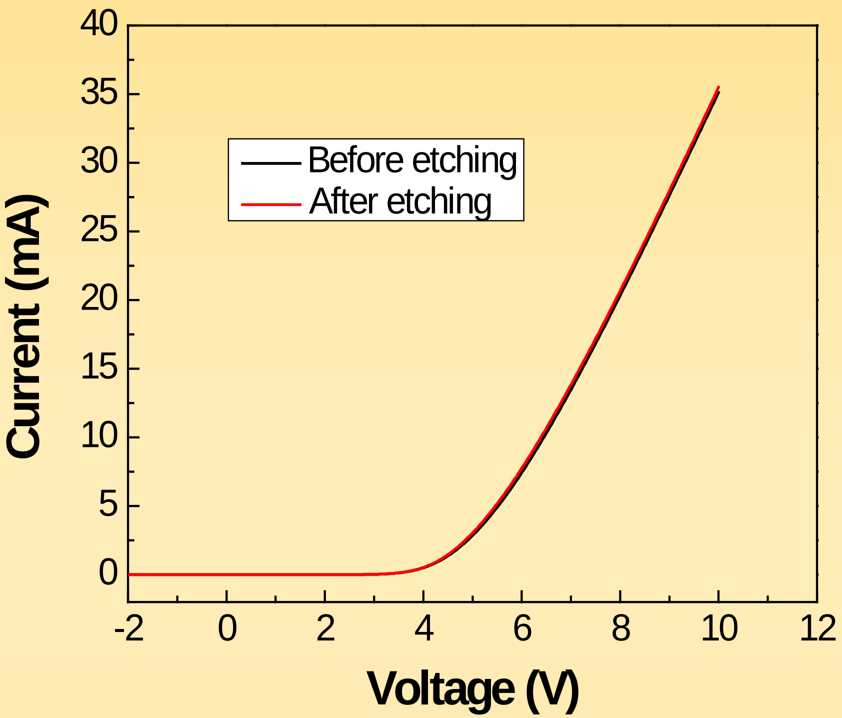

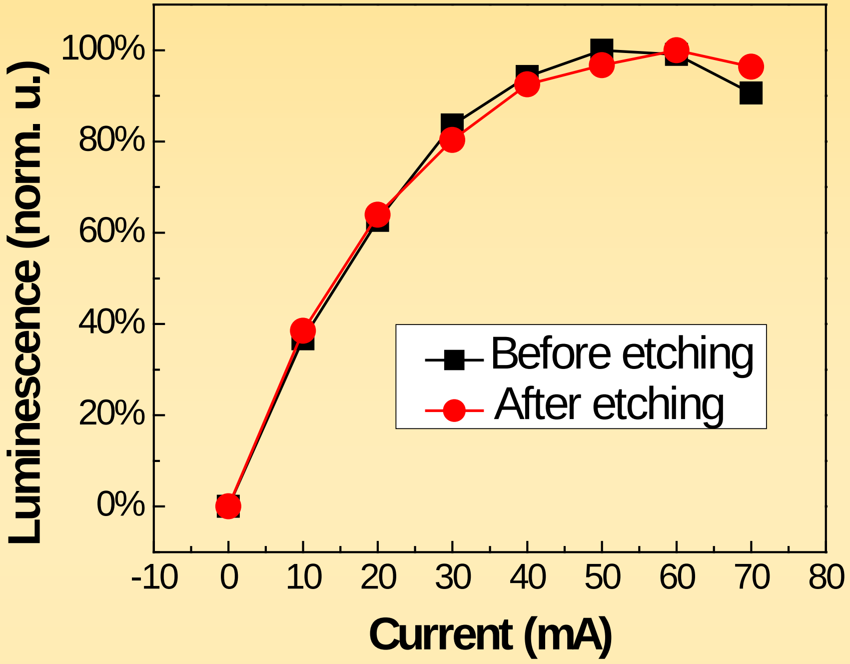

No degradation observed for electrical properties after the substrate removal process.

Efficiency of devices drop at higher drive current due to inefficient heat dissipation

III-Nitrides for Solar Cells

Motivation for PV: Energy demand

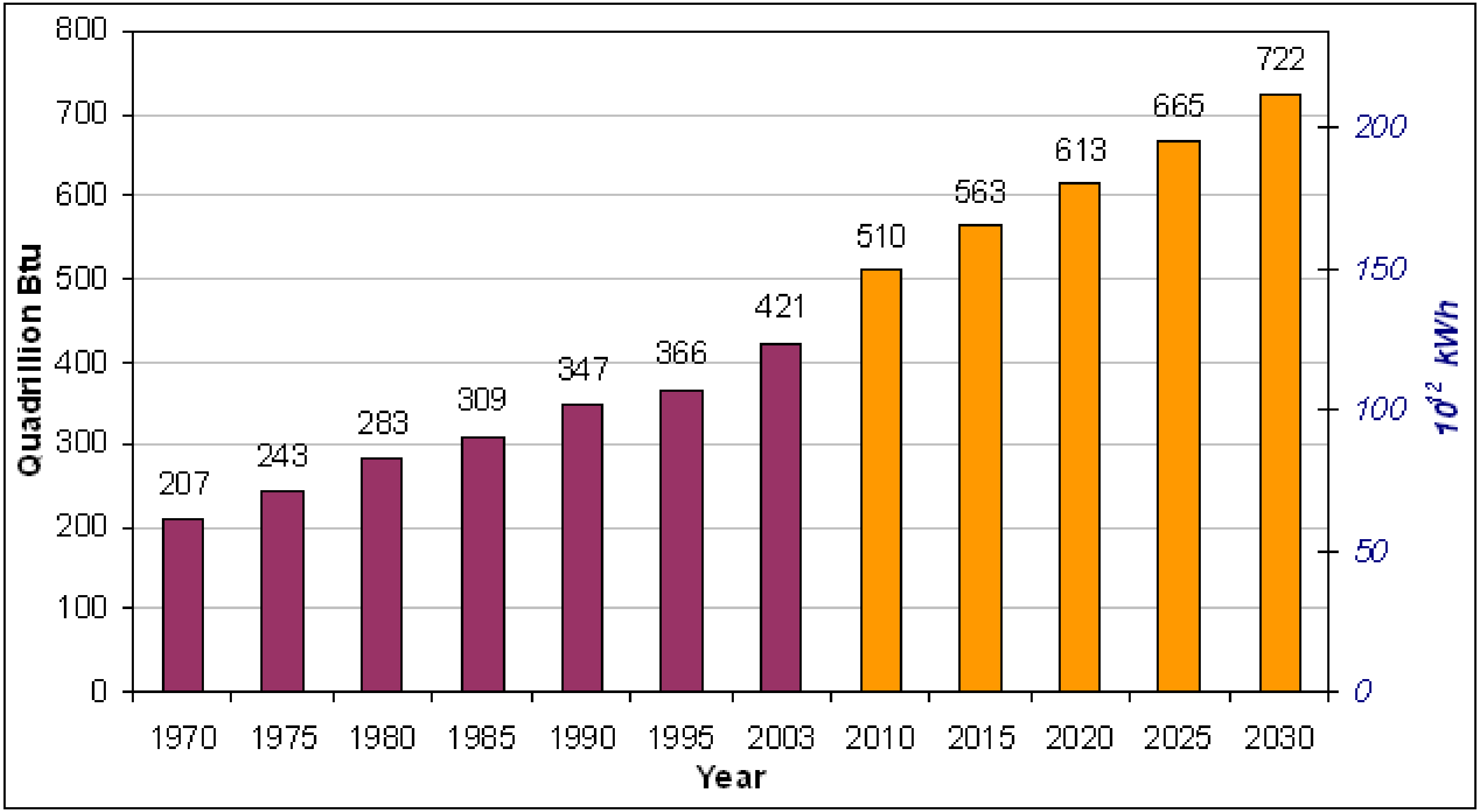

World marketed energy consumption, 1970 - 2030.

Source: DOE/EIA, Annual Energy Review, 2004.

High efficiency approach

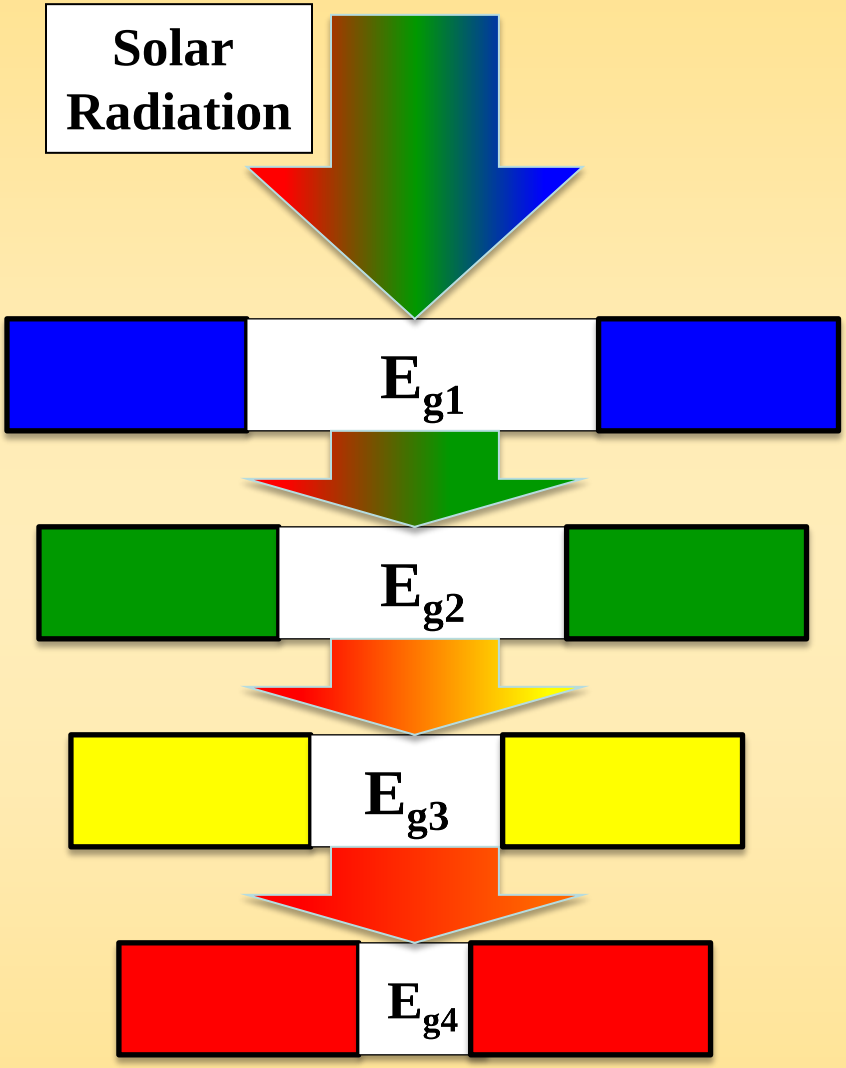

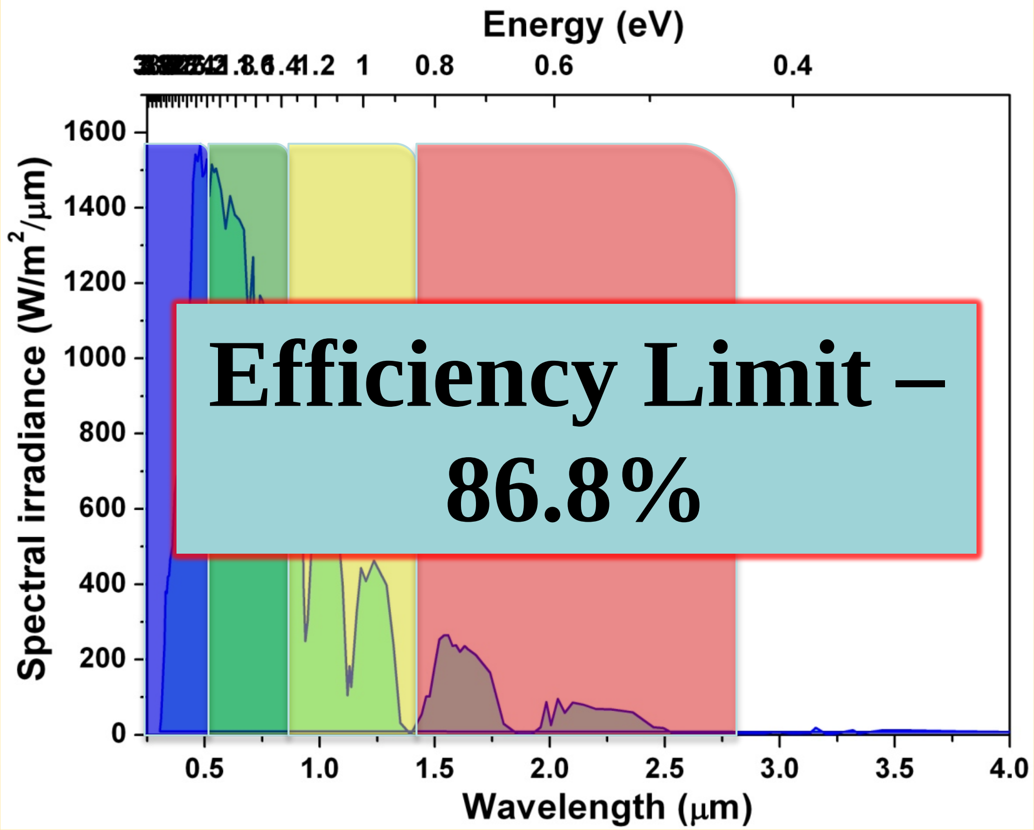

Efficiency Limit – 86.8%

Optical absorption edge ➔ Sharp
(No absorption below band gap)

Band Gap $E_{g1} > E_{g2} > E_{g3} > E_{g4}$

Ian Ferguson
(ianf@uncc.edu)

Towards achieving efficiency > 50%

Detailed Balance Calculations for 6000K Black Body Radiation, 500X.

n	Values of Band Gap								η (%)	0.8 · η (%)
3	0.7	1.37	2						*56*	*44.8*
4	0.6	1.11	1.69	2.48					*62*	*49.6*
5	0.53	0.95	1.4	1.93	2.68				*65*	*52*
6	0.47	0.84	1.24	1.66	2.18	2.93			*67.3*	*53.84*
7	0.47	0.82	1.191	1.56	2	2.5	3.21		*68.9*	*55.12*
8	0.44	0.78	1.09	1.4	1.74	2.14	2.65	3.35	*70.2*	*56.16*

Source: A. De Vos, "Detailed balance limit of the efficiency of tandem solar cells", Journal of Physics D (Applied Physics) 1980, 839-46

5 or more effective band gaps → 50% η

50% η → Band gap > 2.4 *eV*

III-Nitride material system

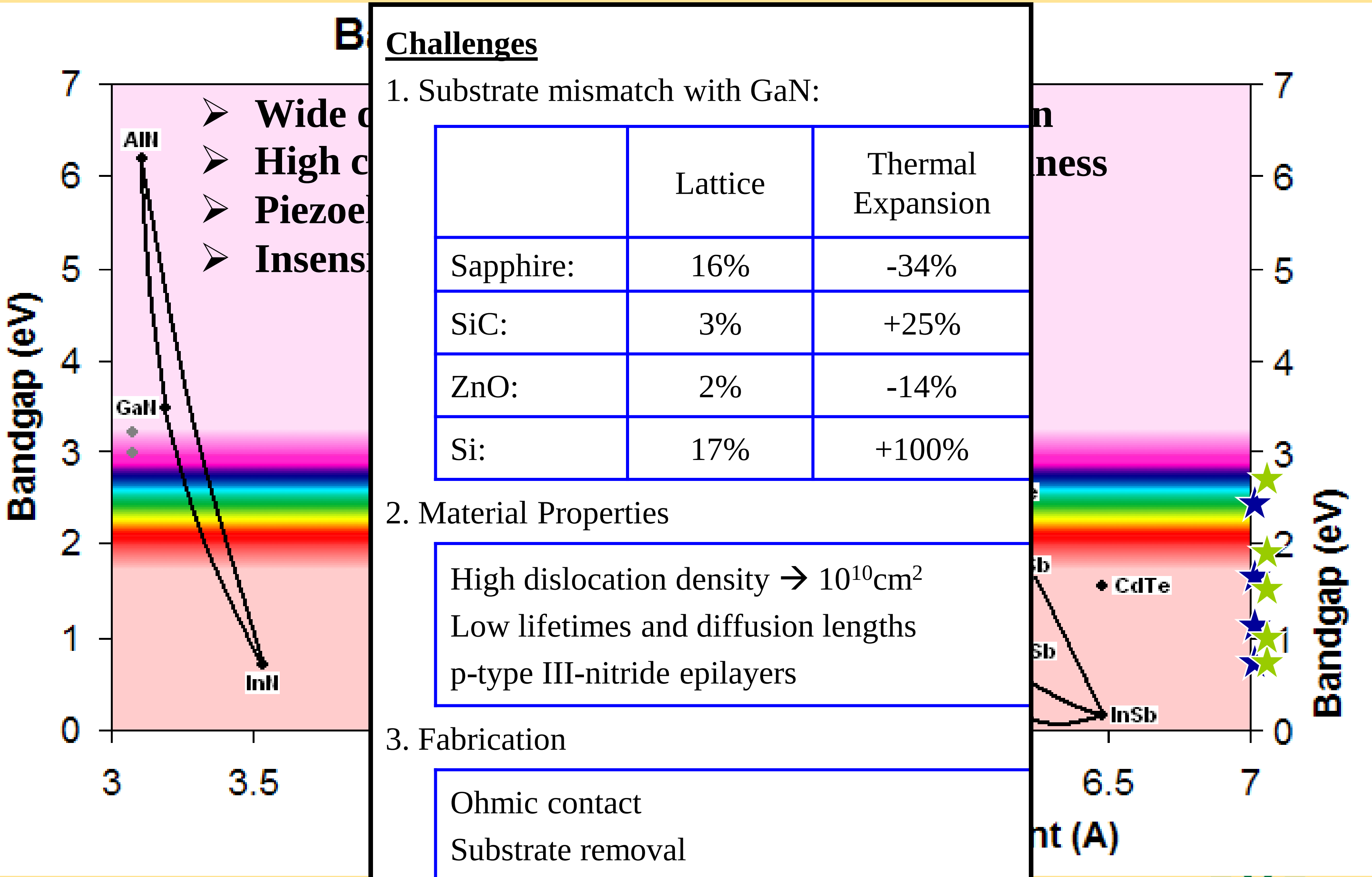

Challenges

1. Substrate mismatch with GaN:

	Lattice	Thermal Expansion
Sapphire:	16%	-34%
SiC:	3%	+25%
ZnO:	2%	-14%
Si:	17%	+100%

2. Material Properties

High dislocation density → 10^{10}cm^{2}
Low lifetimes and diffusion lengths
p-type III-nitride epilayers

3. Fabrication

Ohmic contact
Substrate removal

Very High Efficiency Solar Cells

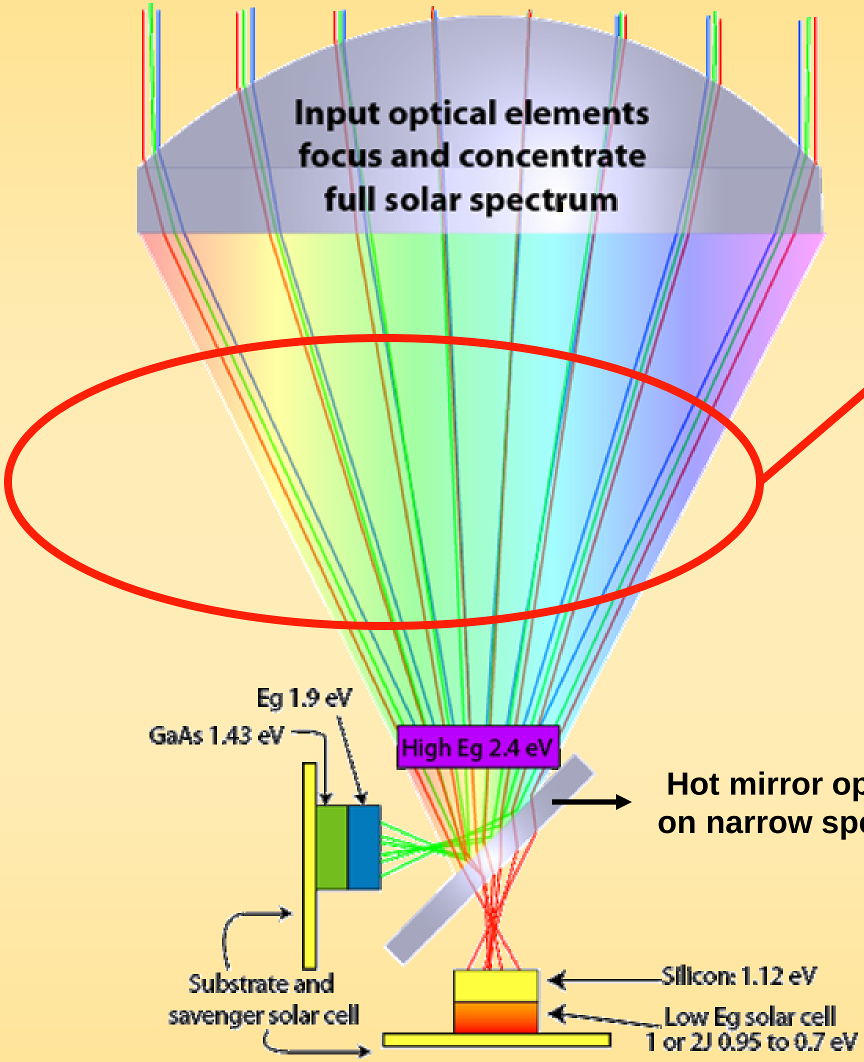

Hot mirror operates on narrow spectrum.

Operation of VHESC.

InGaN solar cells

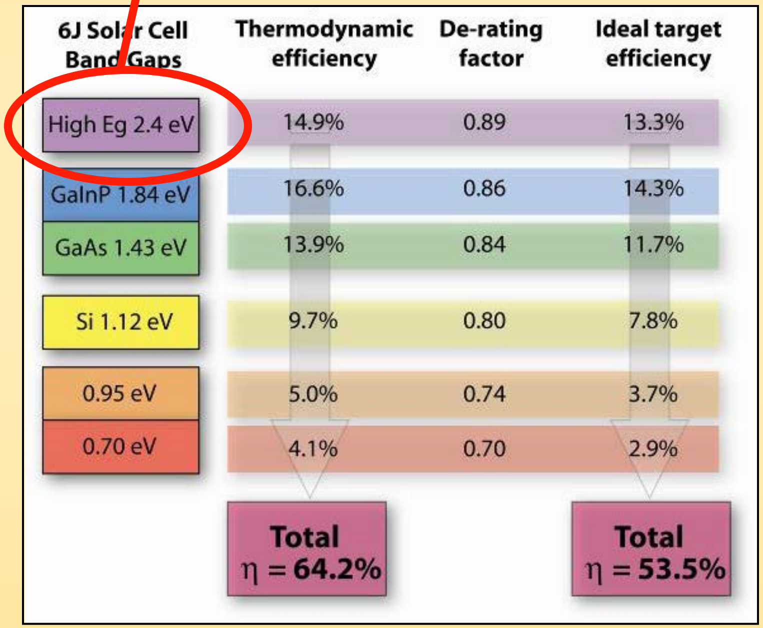

6J Solar Cell Band Gaps	Thermodynamic efficiency	De-rating factor	Ideal target efficiency
High Eg 2.4 eV	14.9%	0.89	13.3%
GaInP 1.84 eV	16.6%	0.86	14.3%
GaAs 1.43 eV	13.9%	0.84	11.7%
Si 1.12 eV	9.7%	0.80	7.8%
0.95 eV	5.0%	0.74	3.7%
0.70 eV	4.1%	0.70	2.9%
	Total $\eta = 64.2\%$		Total $\eta = 53.5\%$

Predicted efficiency contribution of each junction .

Research approach

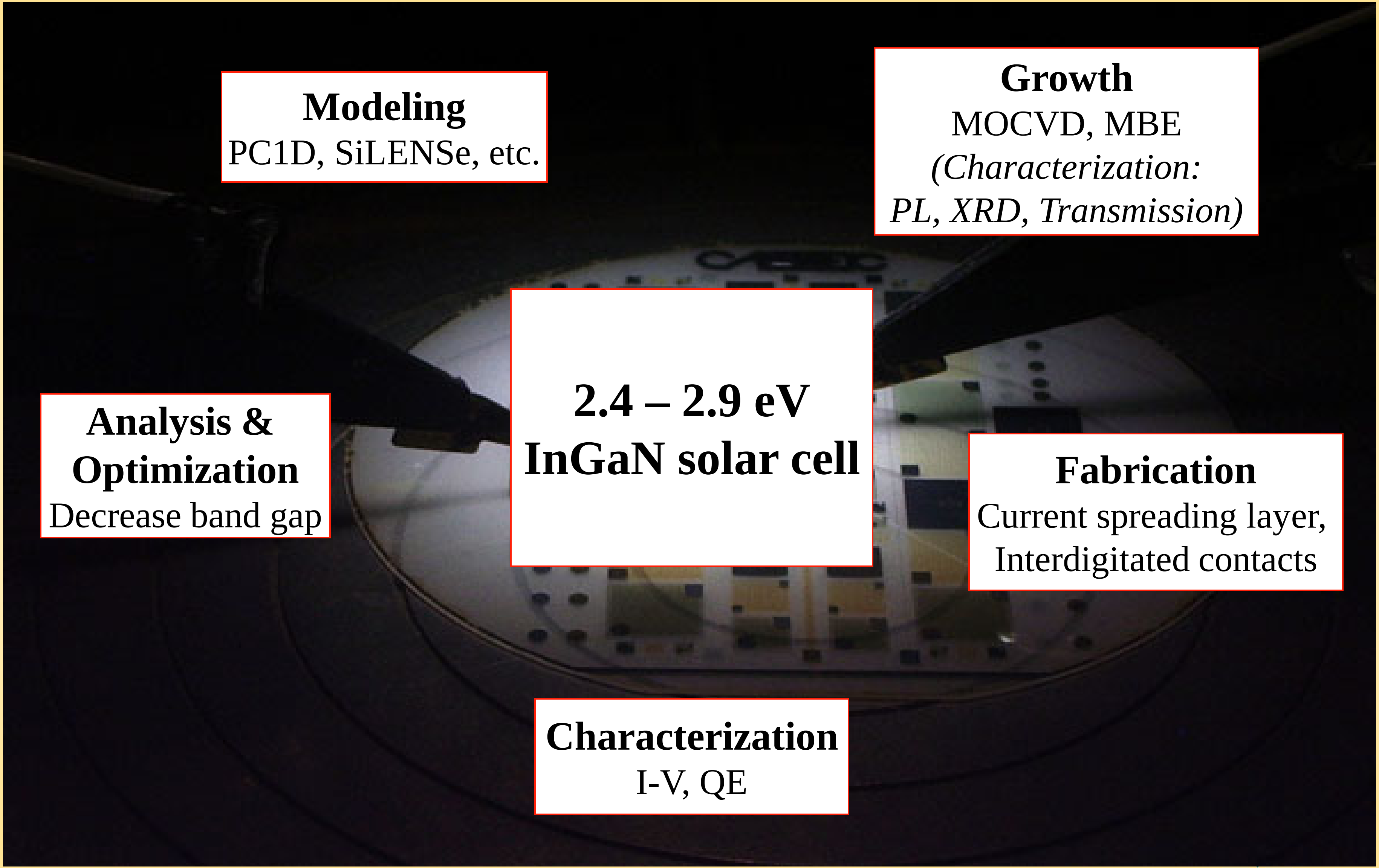

Modeling
PC1D, SiLENSe, etc.

Growth
MOCVD, MBE
(Characterization:
PL, XRD, Transmission)

2.4 – 2.9 eV
InGaN solar cell

Analysis & Optimization
Decrease band gap

Fabrication
Current spreading layer,
Interdigitated contacts

Characterization
I-V, QE

Design principles

FIRST ATTEMPT @ InGaN solar cells

- III-V solar cell technology
- III-nitride LED, photodetector, laser technology

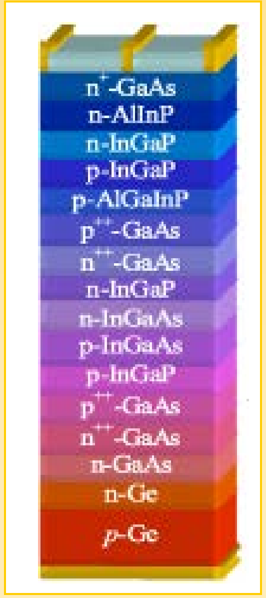

DESIGN PRINCIPLES

- Maximize light absorption
  - Thickness, light trapping, ARC, surface texturing, shadowing.
- Maximize collection
  - Surface passivation, electric fields, band engineering, gettering.
- Minimize dark current
  - Recombination, passivation, doping.
- Minimize resistive losses
  - Ohmic contacts, doping, spreading resistance, tunneling.

Preliminary design: p-i-n solar cell

- p-region ~ 100 nm
  - Maximize absorption in i-region.
  - Provide charge to junction.
- n-region ~ 200 nm (effective)
  - Hole diffusion length ~ 200 nm.
- **Test material → i-region.**

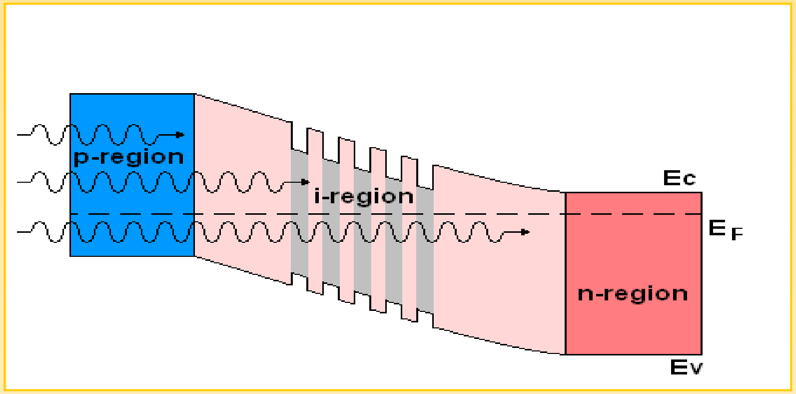

GaN/InGaN QW solar cell.

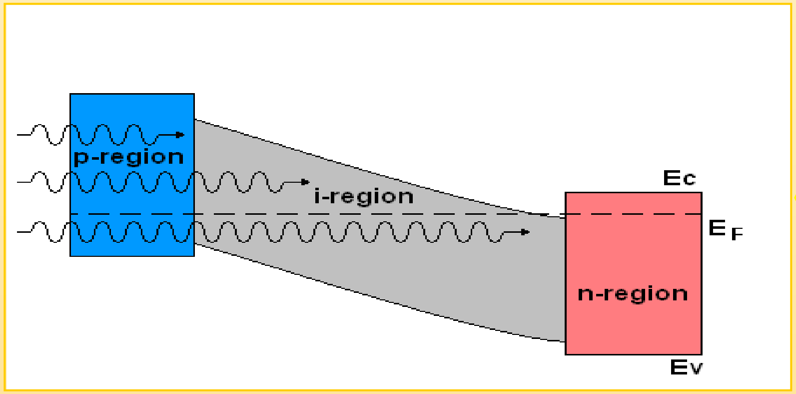

GaN/InGaN p-i-n solar cell.

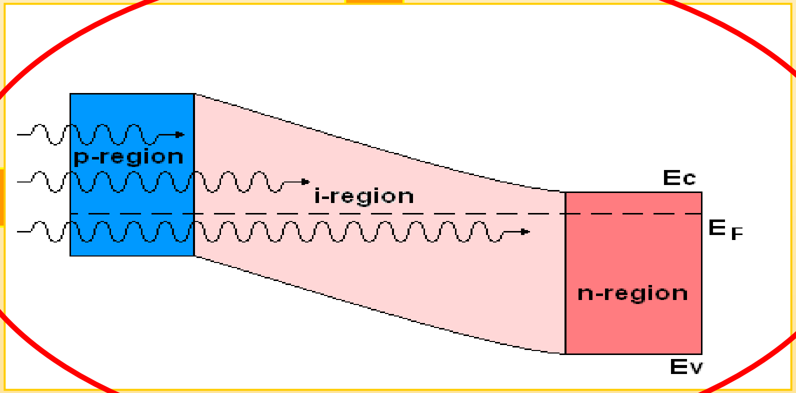

GaN p-i-n solar cell.

Modeling of solar cells: PC1D

Device parameter files

Device design, structure,
lifetime and recombination,
doping profiles, etc.

Material files

Band structure, recombination

Optical:

Absorption, refractive index

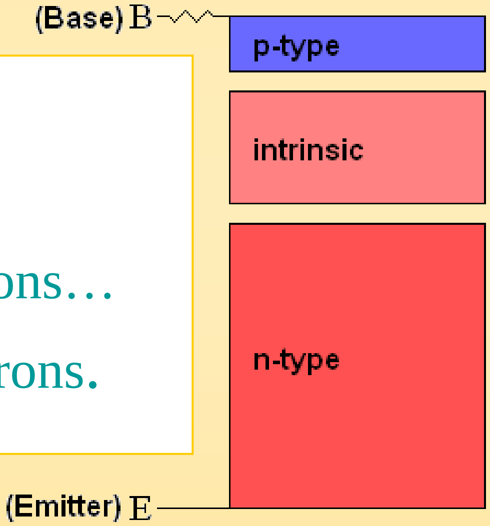

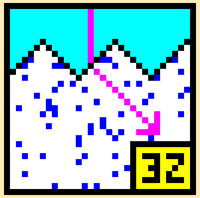

PC1D core

Solar cell simulation program

Solves fully coupled 1-D nonlinear equations…

for quasi-1-D transport of holes and electrons.

Result

- Graphical/numerical
- I-V, QE, band diagram, electric fields, generation/recombination

Modification of PC1D for III-nitrides

Step 1: Preliminary modification

Step 2: Advance modification

- Polarization, convergence, etc.

Material files

Band structure, recombination

Optical:

Absorption, refractive index

PC1D core

Solar cell simulation program

Solves fully coupled 1-D nonlinear equations…

for quasi-1-D transport of holes and electrons.

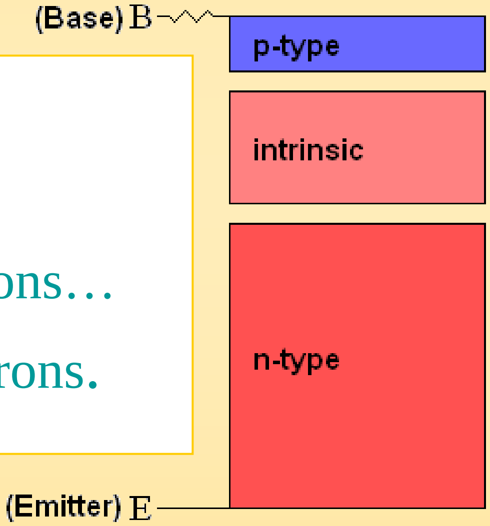

Preliminary design: i-region thickness

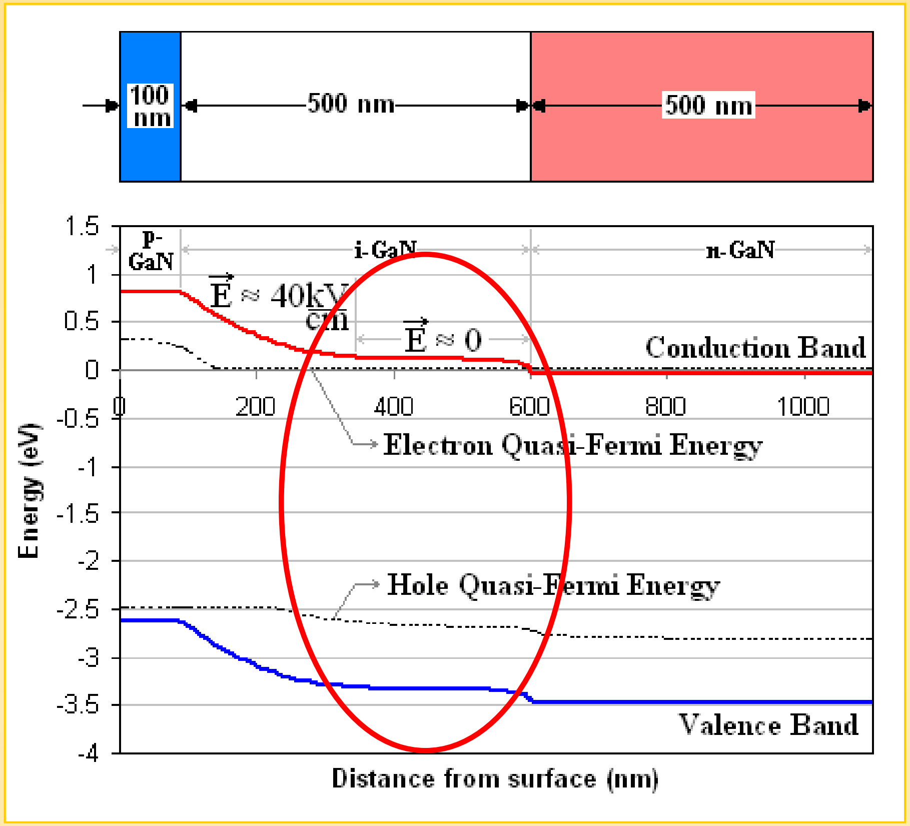

Band diagram of GaN p-i-n solar cell with 500 nm thick i-region.

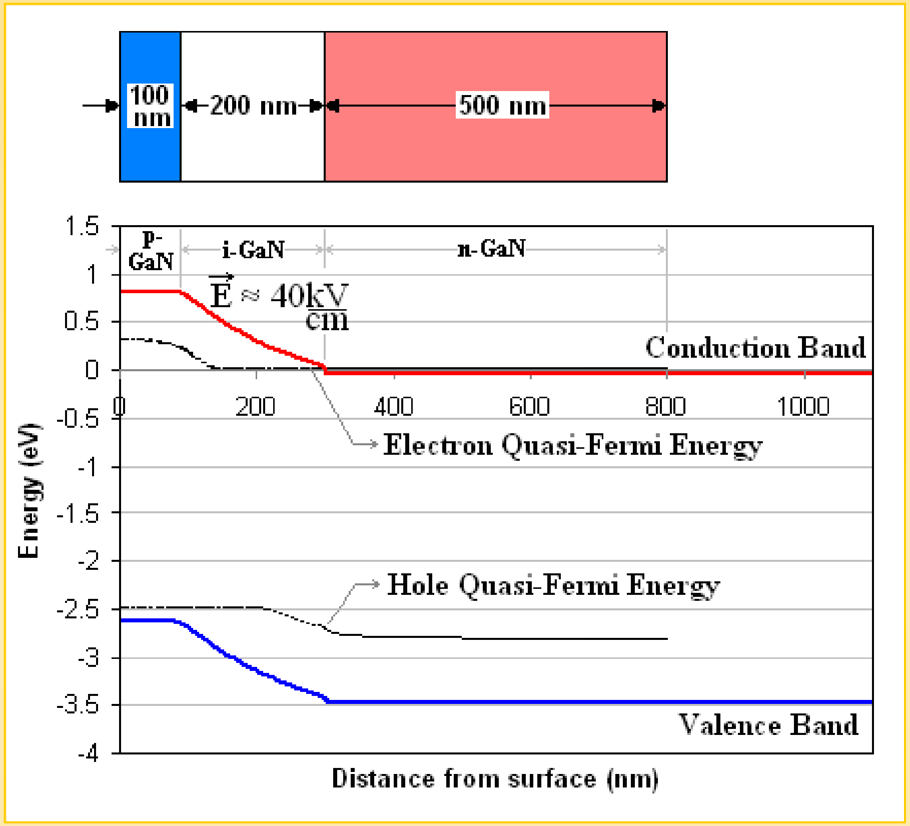

Band diagram of GaN p-i-n solar cell with 200 nm thick i-region.

- Background n-type concentration: 10^{16} cm^3.
- **Result:** i-region thickness limited to 200 nm.

Polarization parameter input in PC1D

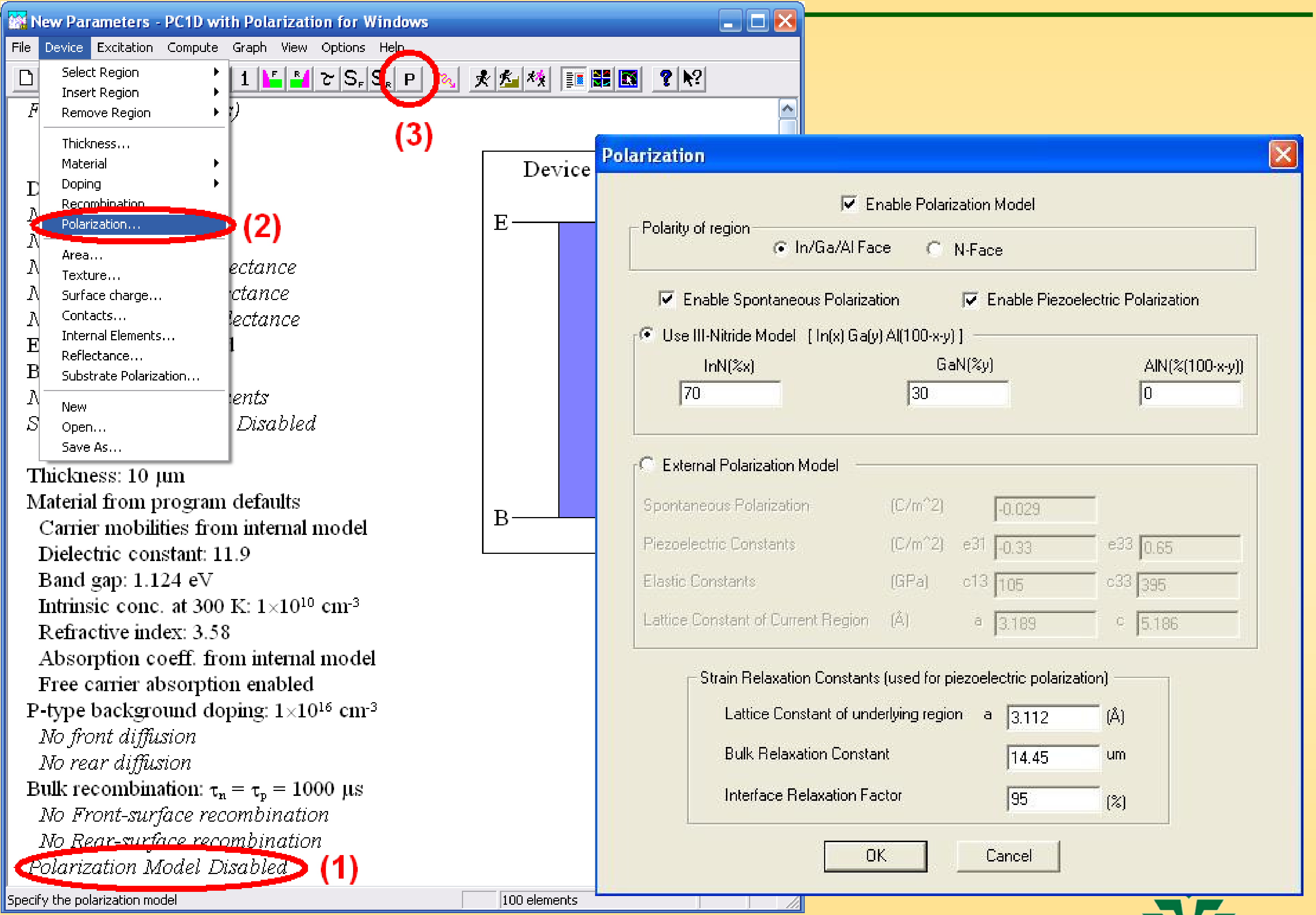

Thickness: 10 μm

Material from program defaults

Carrier mobilities from internal model

Dielectric constant: 11.9

Band gap: 1.124 eV

Intrinsic conc. at 300 K: 1×10^{10} cm^{-3}

Refractive index: 3.58

Absorption coeff. from internal model

Free carrier absorption enabled

P-type background doping: 1×10^{16} cm^{-3}

No front diffusion

No rear diffusion

Bulk recombination: $\tau_n = \tau_p = 1000$ μs

No Front-surface recombination

No Rear-surface recombination

Polarization Model Disabled

Specify the polarization model

100 elements

☑ Enable Polarization Model

Polarity of region: ● In/Ga/Al Face ○ N-Face

☑ Enable Spontaneous Polarization ☑ Enable Piezoelectric Polarization

● Use III-Nitride Model [In(x) Ga(y) Al(100-x-y)]

InN(%x)	GaN(%y)	AlN(%(100-x-y))
70	30	0

○ External Polarization Model

Spontaneous Polarization	(C/m^2)		-0.029		
Piezoelectric Constants	(C/m^2)	e31	-0.33	e33	0.65
Elastic Constants	(GPa)	c13	105	c33	395
Lattice Constant of Current Region	(Å)	a	3.189	c	5.186

Strain Relaxation Constants (used for piezoelectric polarization)

Lattice Constant of underlying region	a	3.112	(Å)
Bulk Relaxation Constant		14.45	um
Interface Relaxation Factor		95	(%)

Ian Ferguson
(ianf@uncc.edu)

UNC CHARLOTTE
Electrical and Computer Engineering

Test runs for polarization model

1. Spontaneous polarization in p-i-n GaN/InGaN structure

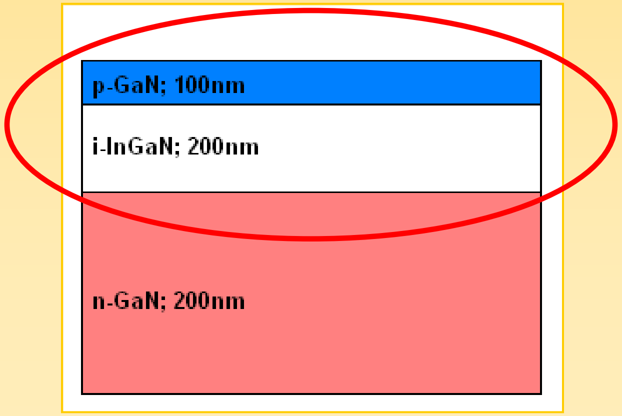

Without polarization.

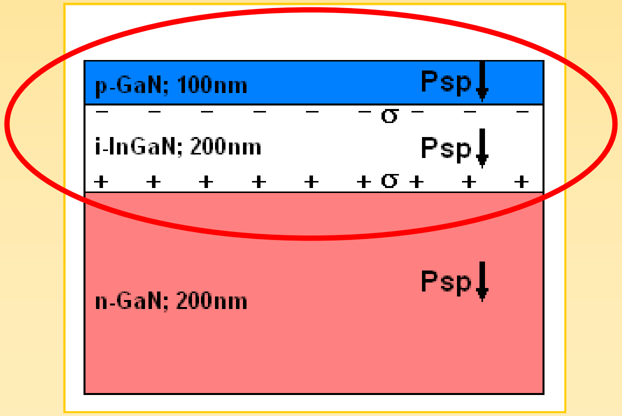

With spontaneous polarization.

2. Piezoelectric polarization in p-GaN window layer

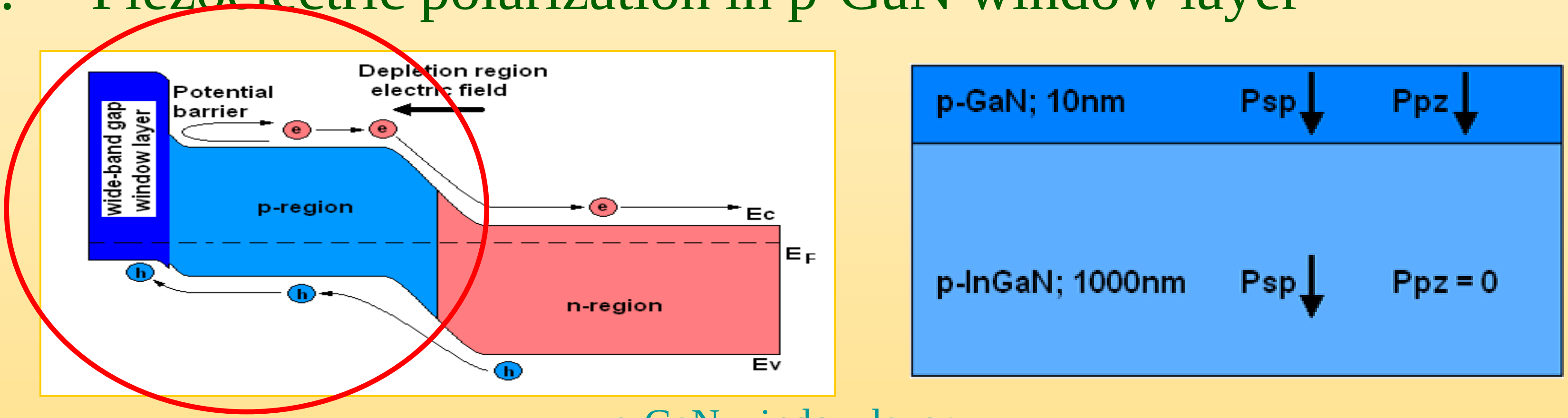

p-GaN window layer.

Sample polarization results: Spontaneous polarization

Test 1: p-GaN/u-InGaN interface of a p-i-n GaN/InGaN solar cell.

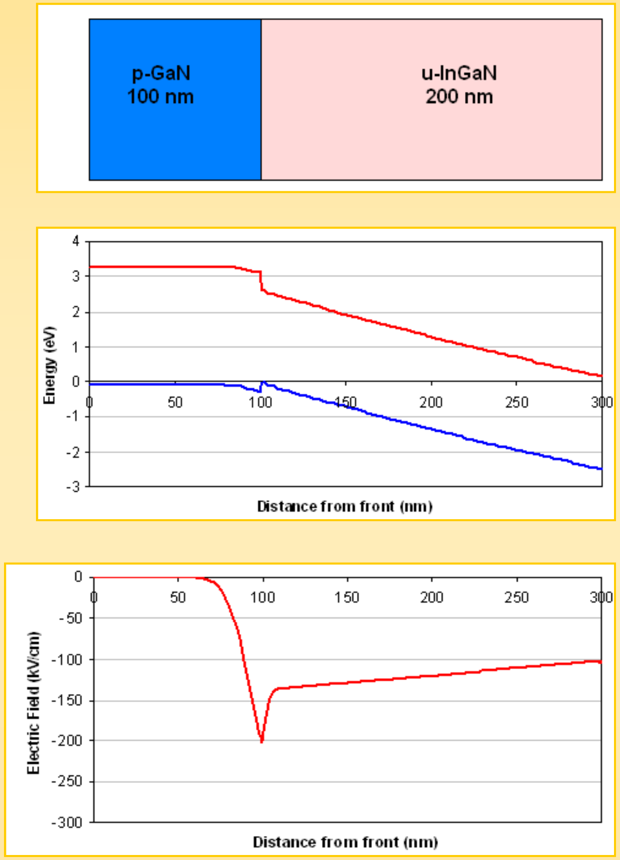

Without spontaneous polarization.

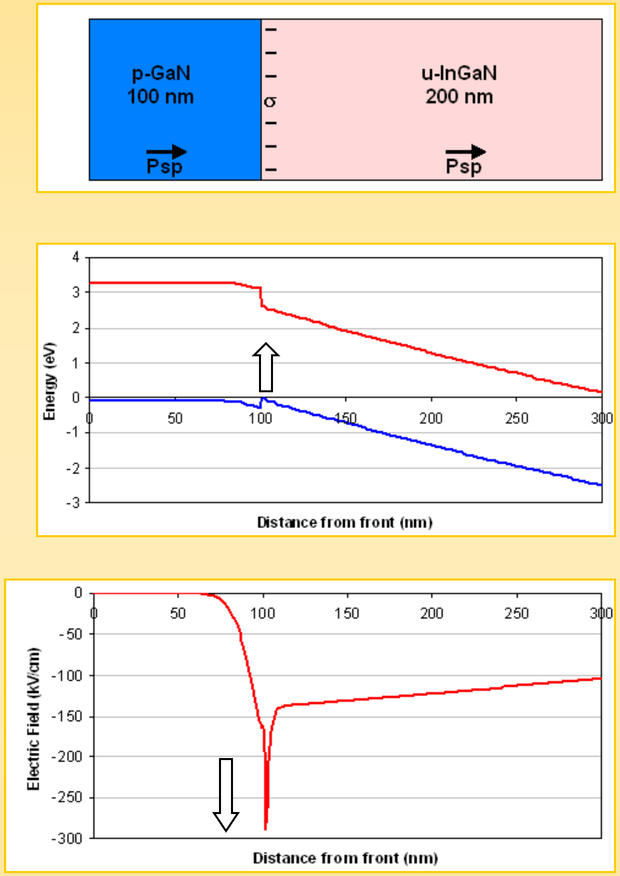

With spontaneous polarization.

- ➢ **Result:** Spontaneous polarization marginally enhances electric field.
- ➢ Reason: Marginal difference in P_{SP} between GaN and $In_{0.2}Ga_{0.8}N$.

Sample polarization results: Piezoelectric polarization

Test 2: Strained p-GaN window layer on p-InGaN junction.

- ➢ Conventional choice for window layer for InGaN.

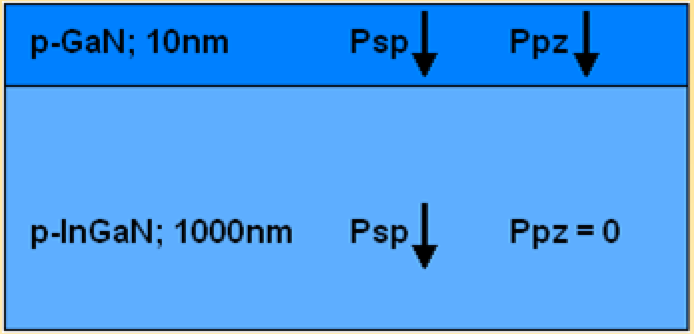

p-GaN; 10nm	Psp ↓	Ppz ↓
p-InGaN; 1000nm	Psp ↓	Ppz = 0

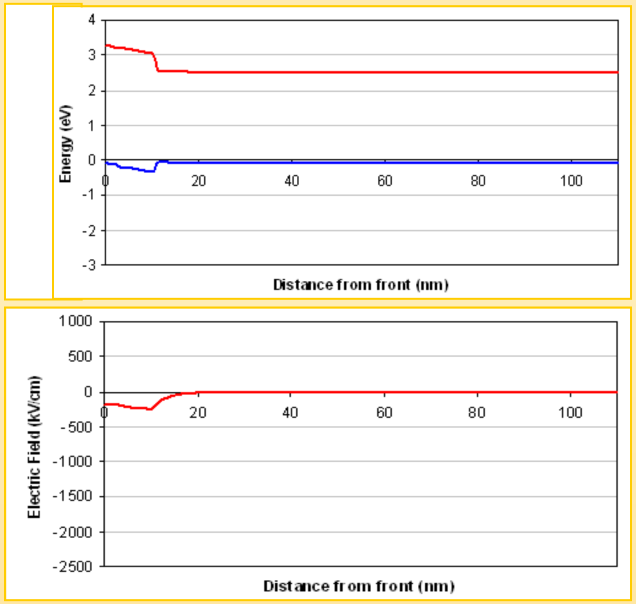

Completely relaxed window layer.
(Without piezoelectric polarization.)

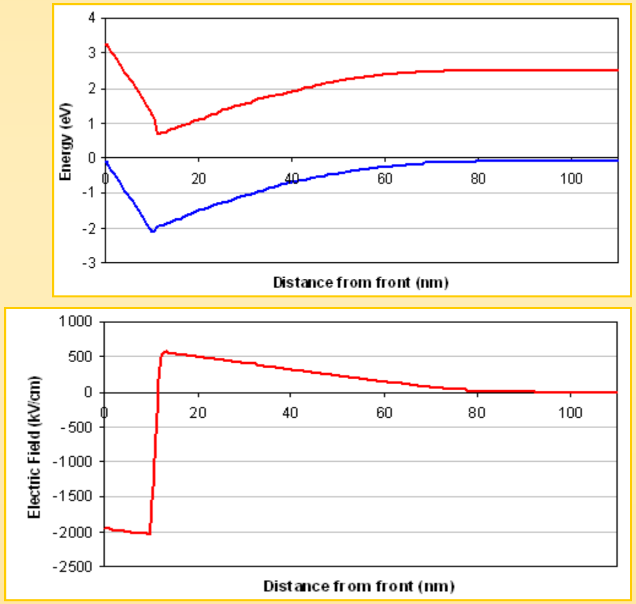

Completely strained window layer.
(With piezoelectric polarization.)

- ➢ **Result:** Strong detrimental band bending at GaN/InGaN interface.

InGaN material characterization

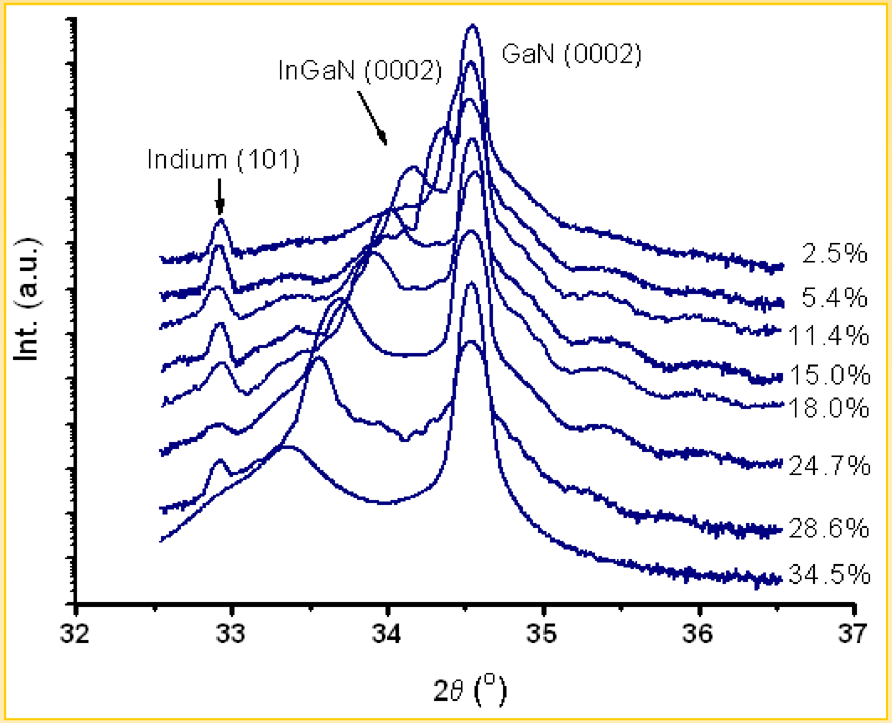

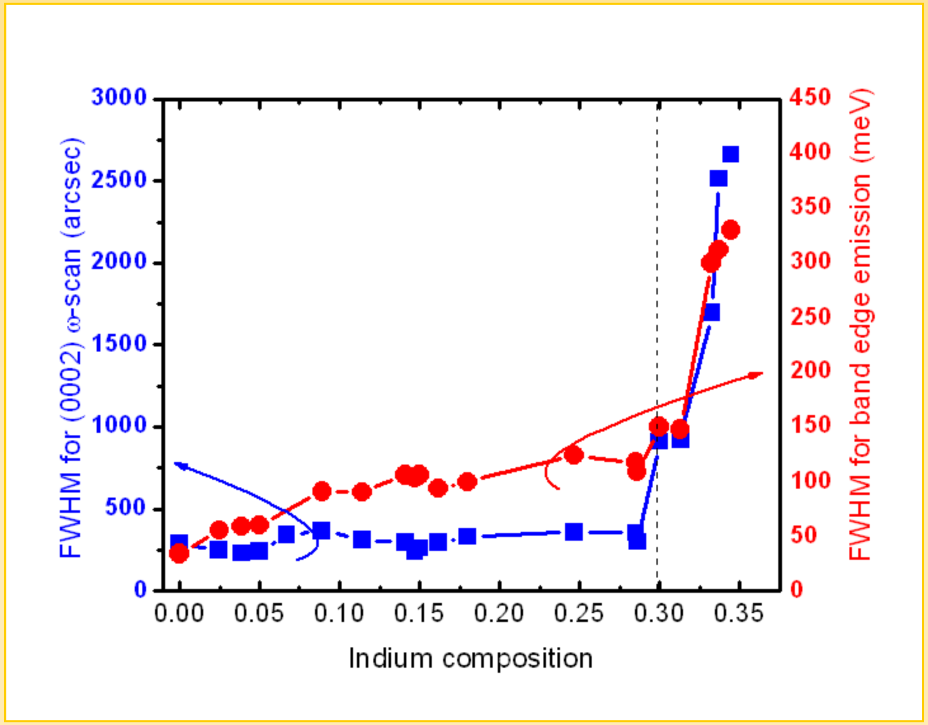

Summary of XRD & PL measurements of InGaN with variable [In] grown by MOCVD.

- ➢ Crystalline quality degrades for [In] > 30%
    - ➢ In segregation observed

InGaN material characterization - Photoluminescence

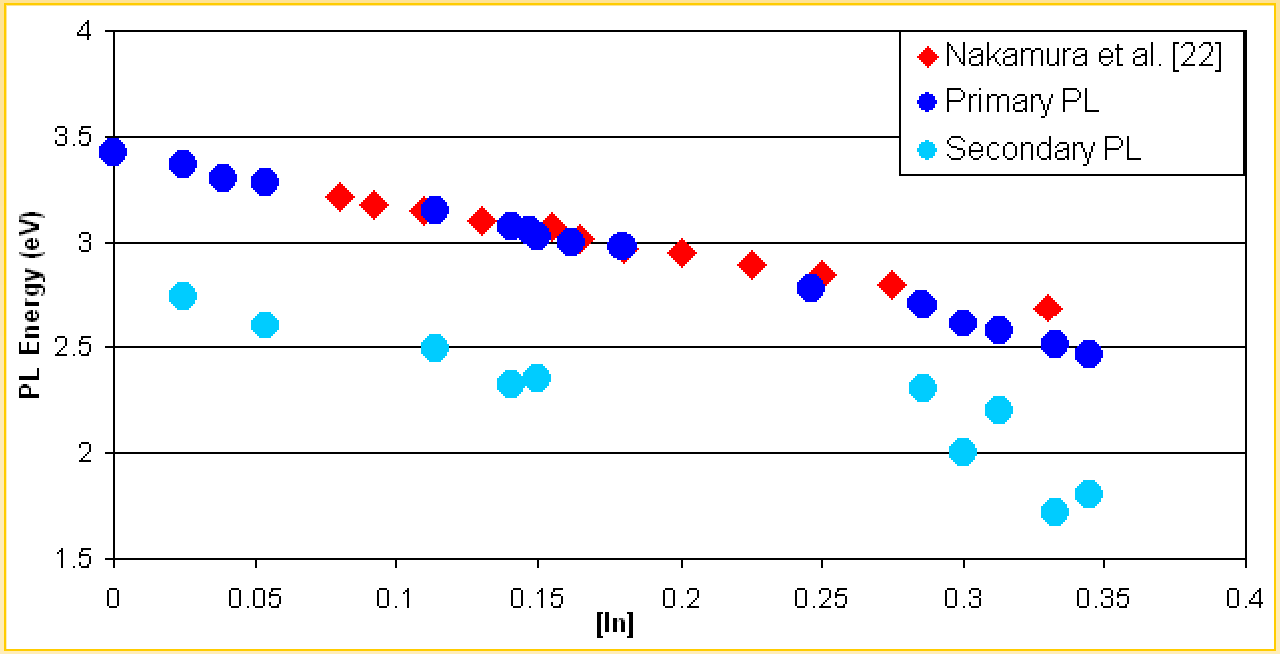

PL emission Vs. [In] from XRD

- InGaN growth consistent with literature
- Observation of secondary phase PL emission
  - → **Phase separation**
- Secondary phase emission intensity increases as [In] increases

Control of phase separation in MOCVD samples

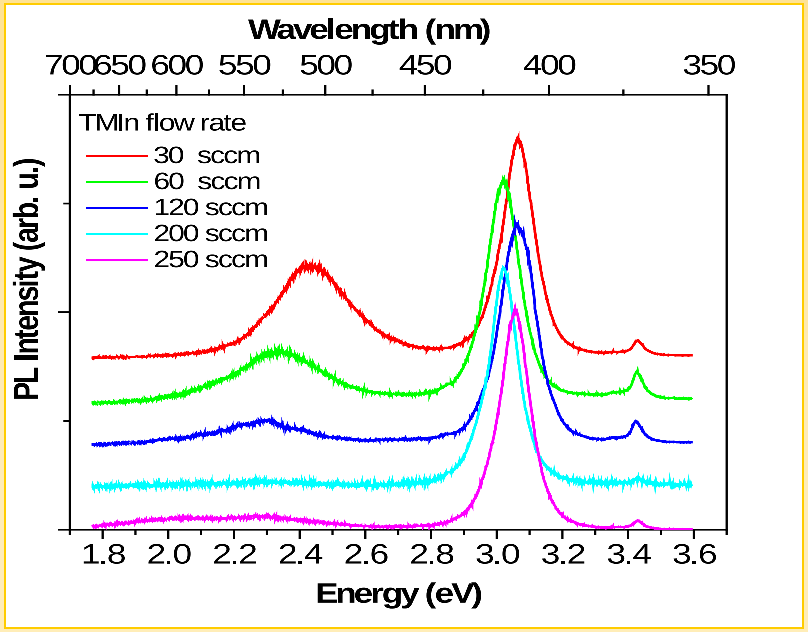

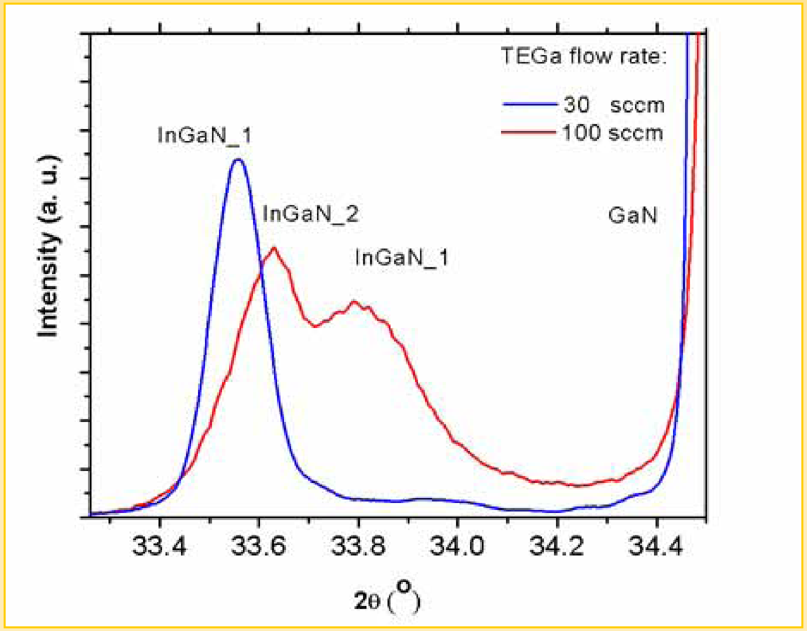

PL of InGaN grown at variable TMIn flow rate.

XRD of InGaN grown at variable TEGa flow rates.

- **Result:** Phase separation is controlled in MOCVD by:
  - Increasing TMIn flow rate → Growth rate
  - Moderating TEGa flow rate
  - Limiting thickness of epitaxy.

InGaN optical absorption: Implications

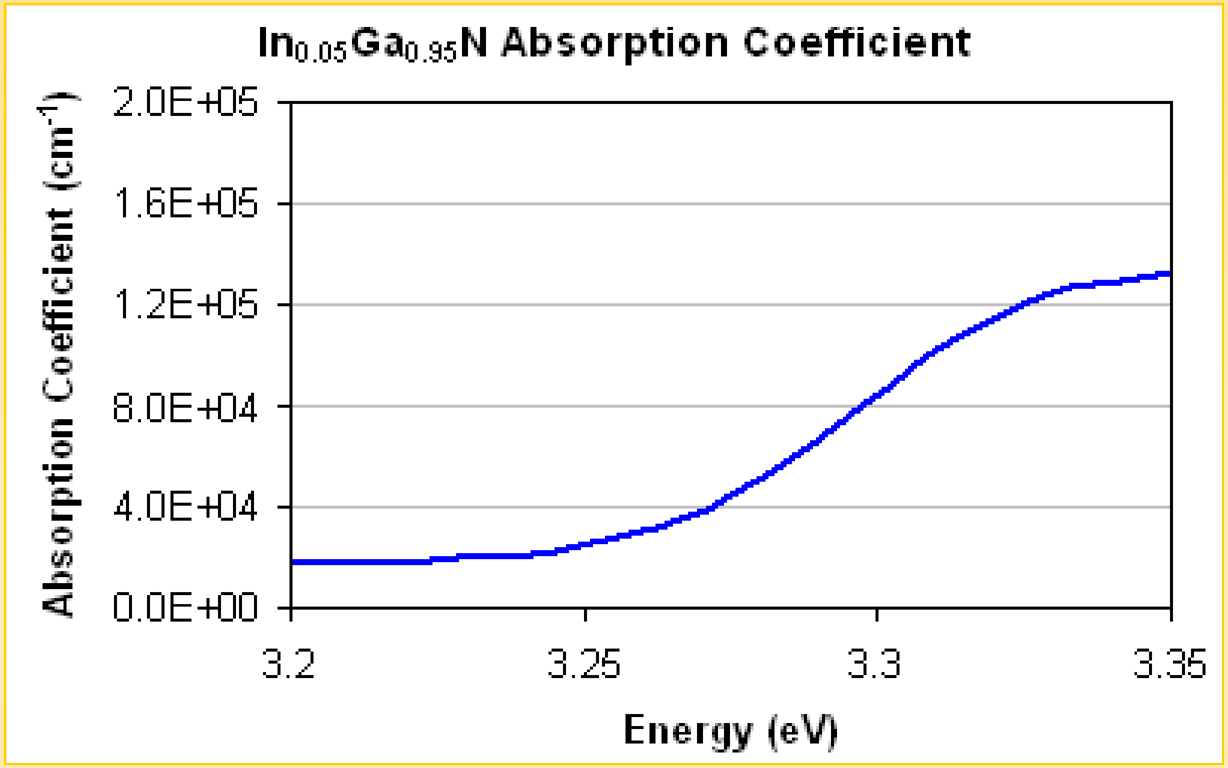

Thickness	Absorption
100nm	63%
200nm	86%
300nm	95%
400nm	98%
500nm	**99%**

Measured absorption coefficient for $In_{0.05}Ga_{0.95}N$ sample (EG = 3.3eV)

- High Absorption Coefficient: >**10^5cm^{-1}** at band edge.
  - Absorption is ~ 10X greater than GaAs.
- Device thickness ~ 500nm.
  - Complements low diffusion lengths.

Lessons Learned – Flexibility in Optical Absorption

Device thickness can be tuned for optimal system performance

Blue is full spectrum on High E chip. Magenta is Spectrum expected to be passed by 25% In InGaN (2.5 eV)

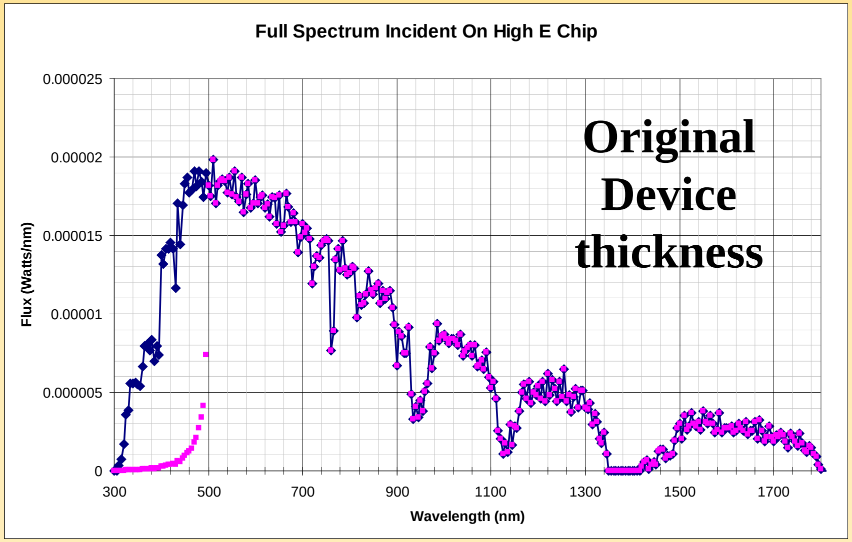

Original Device thickness

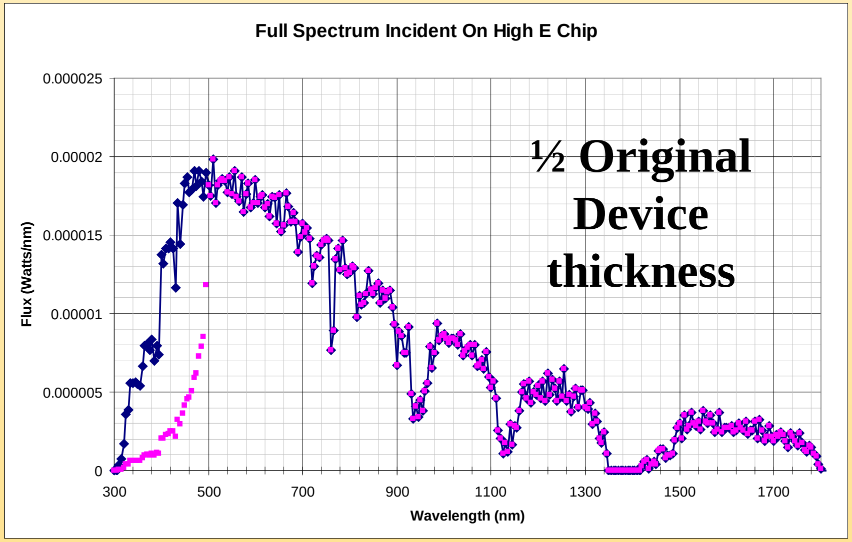

½ Original Device thickness

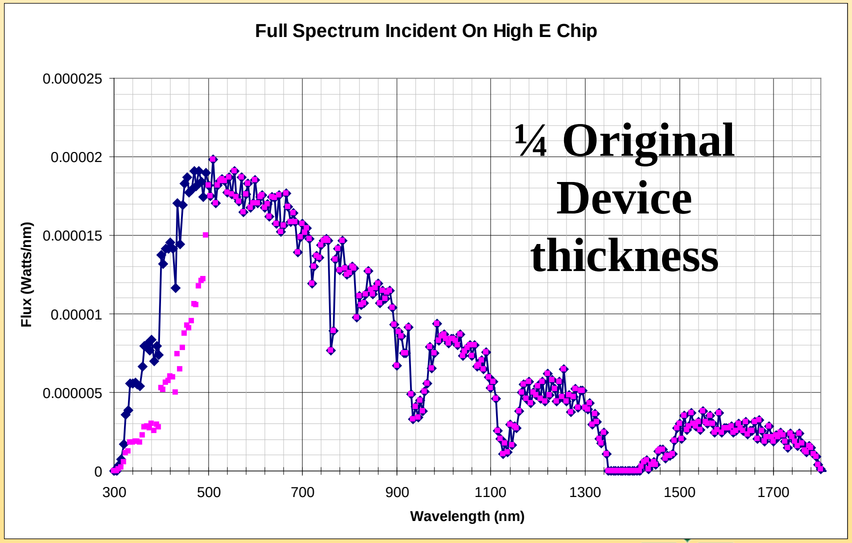

¼ Original Device thickness

P-type doping in InGaN

- Optimize:
  1. Material quality,
  2. Mg flow rate,
  3. Anneal conditions.

- **Material result:**
  - [In] = 15% → 10^{19} cm^{-3}
  - [In] = 28% → 10^{18} cm^{-3}

- High p-type doping also demonstrated in solar cell:

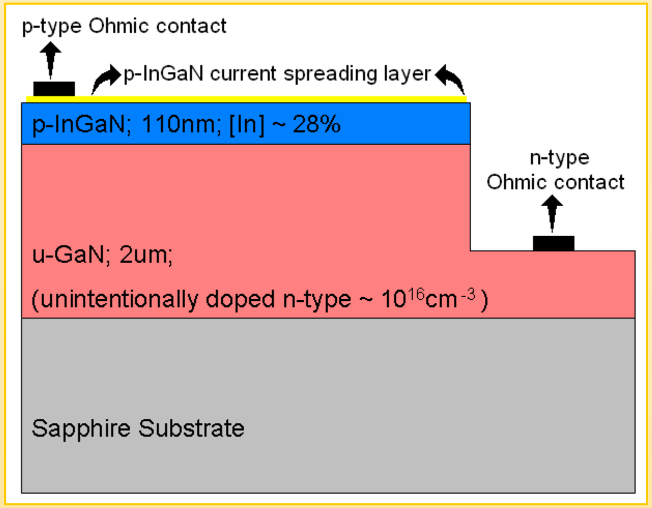

Test device for p-type $In_{0.28}Ga_{0.72}N$.

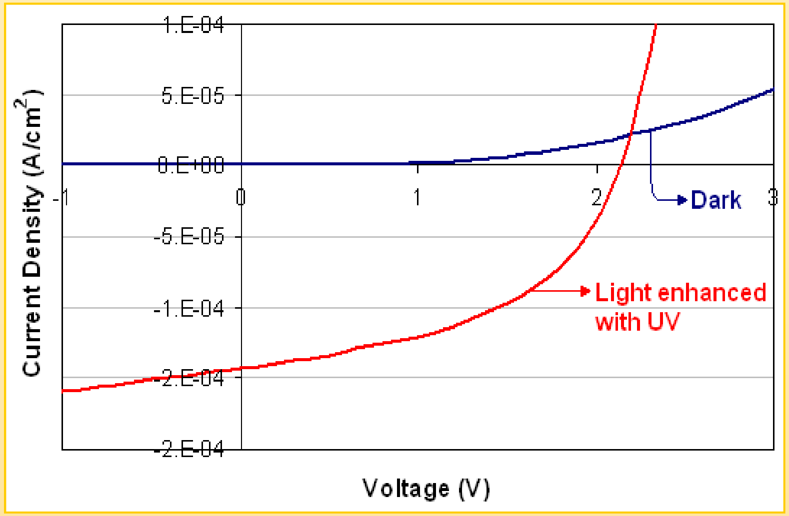

I-V curve for $In_{0.28}Ga_{0.72}N$ test device.

- **Device result:** Successful 2.1 V_{OC} for 2.5 eV device.

Test Validation Procedure

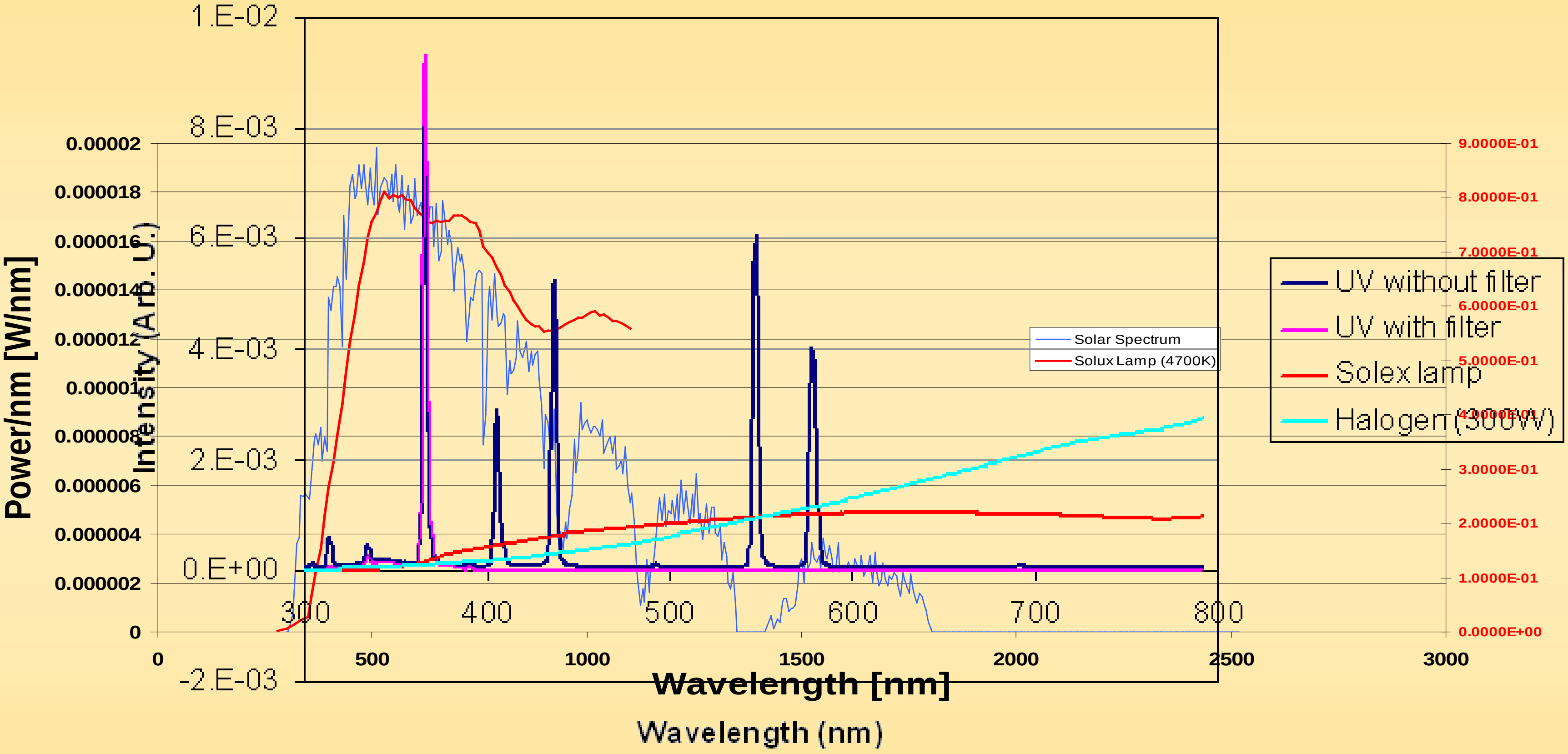

Baseline solar cell fabrication

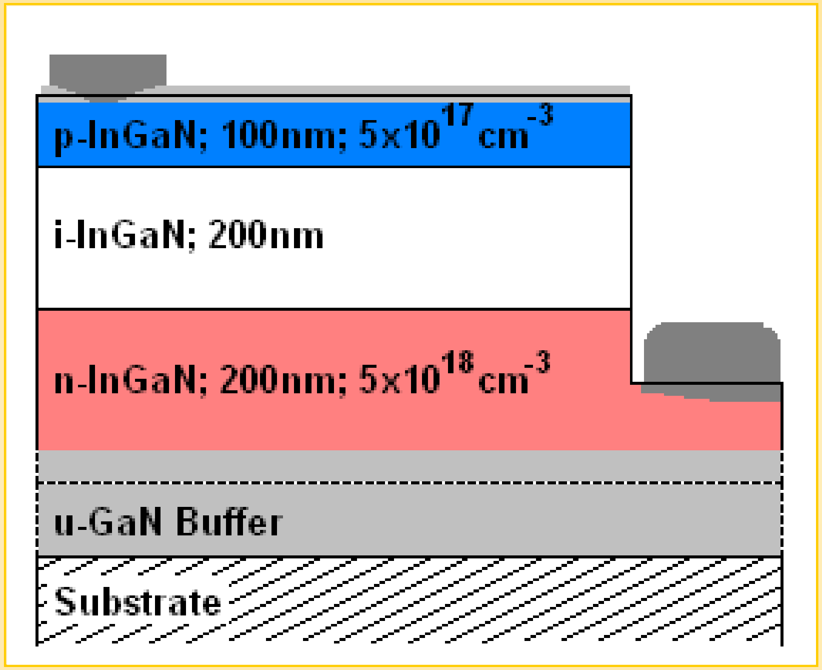

[illegible]

FINAL DEVICE

C O N T A C T I N G S C H E M E S

Solid contact device

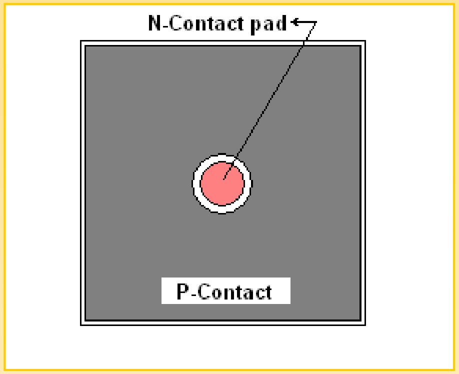

Transparent contact device

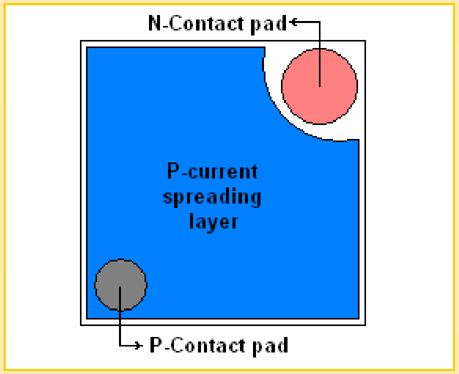

Interdigitated grid contact device

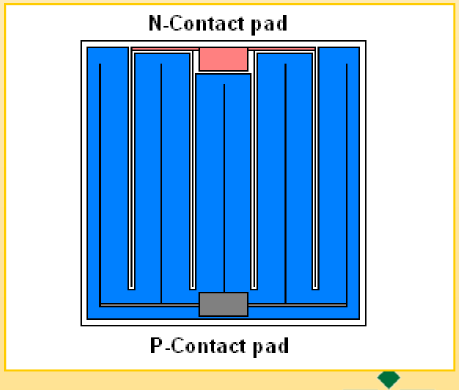

InGaN test solar cell fabrication

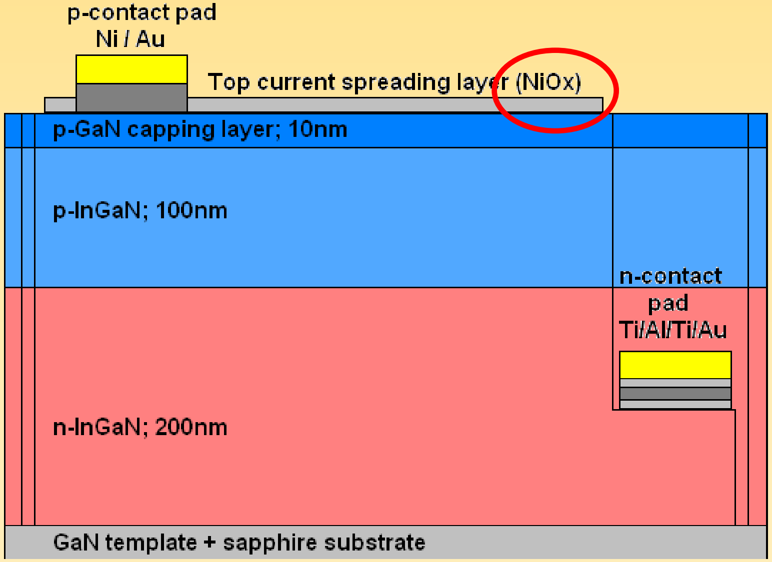

Fabricated solar cell with p-cap.

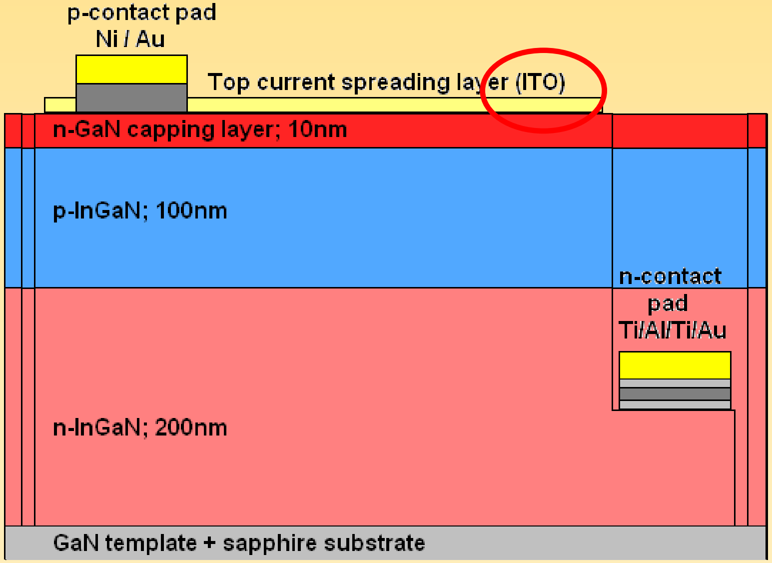

Fabricated solar cell with n-cap.

- NiO_x is used for Ohmic contact to p-GaN cap layer.
- ITO is used for Ohmic contact to n-GaN cap layer.

- Additional contacting schemes for n-GaN cap layer are investigated…

Contacting schemes for n-GaN cap layer

Current-spreading contact.

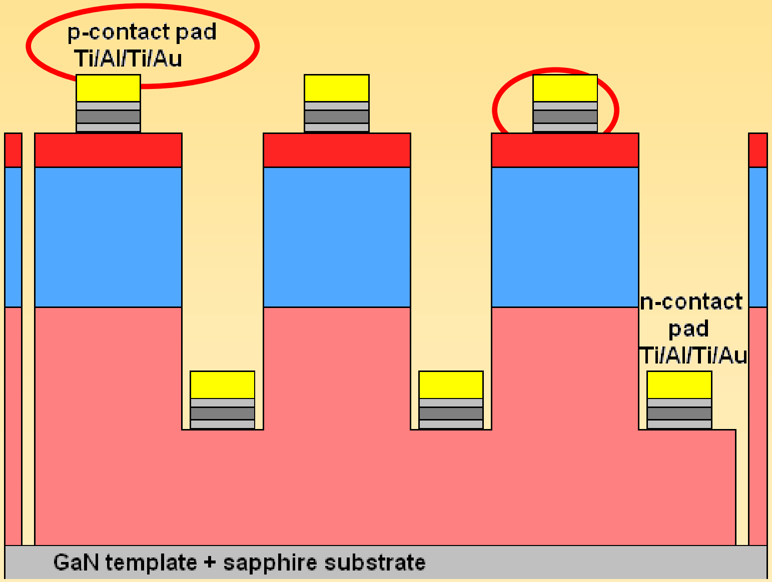

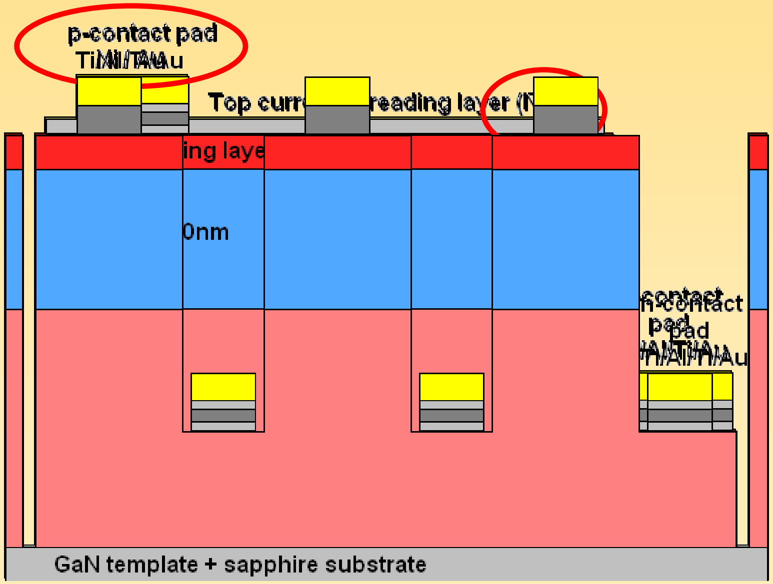

Grid contact.

Ian Ferguson
(ianf@uncc.edu)

Fabricated device structures

Current-spreading contact

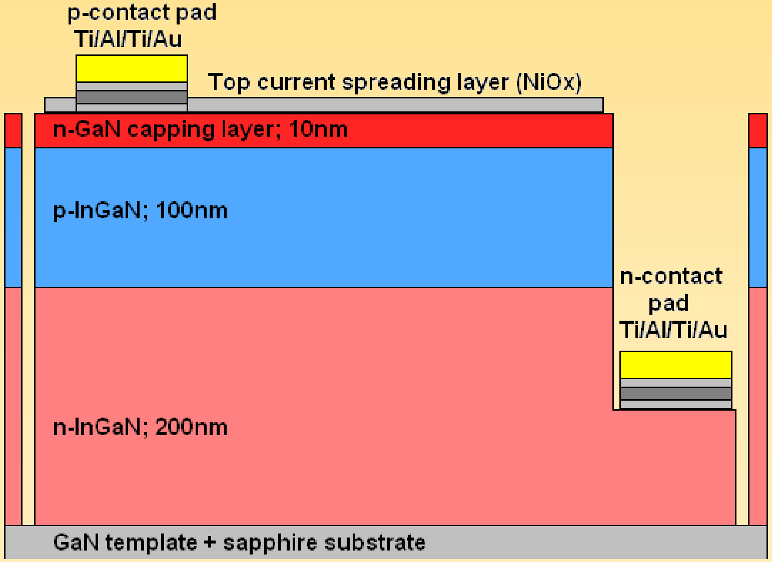

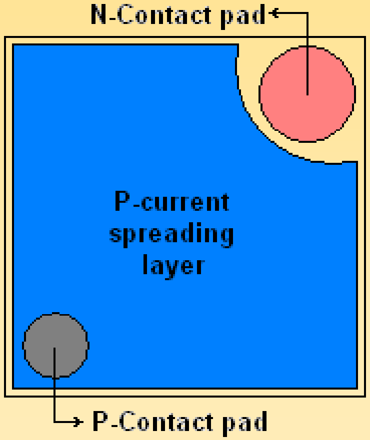

Device size: 1 mm^2, 9 mm^2, 25 mm^2

Grid contact

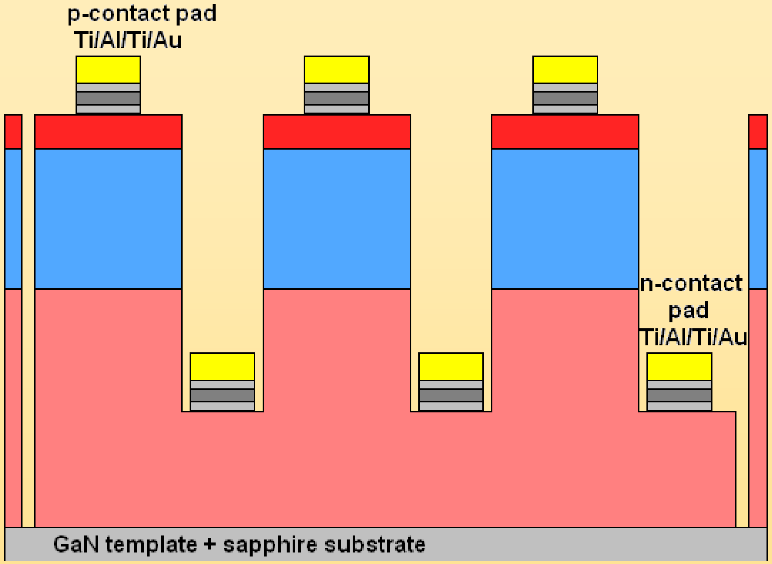

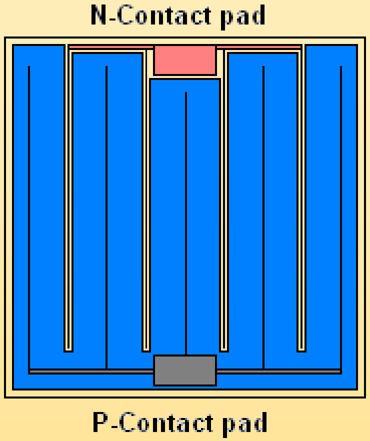

Device size: 1 mm^2, 9 mm^2, 25 mm^2

I-V characteristics: Best devices

Current-spreading contact

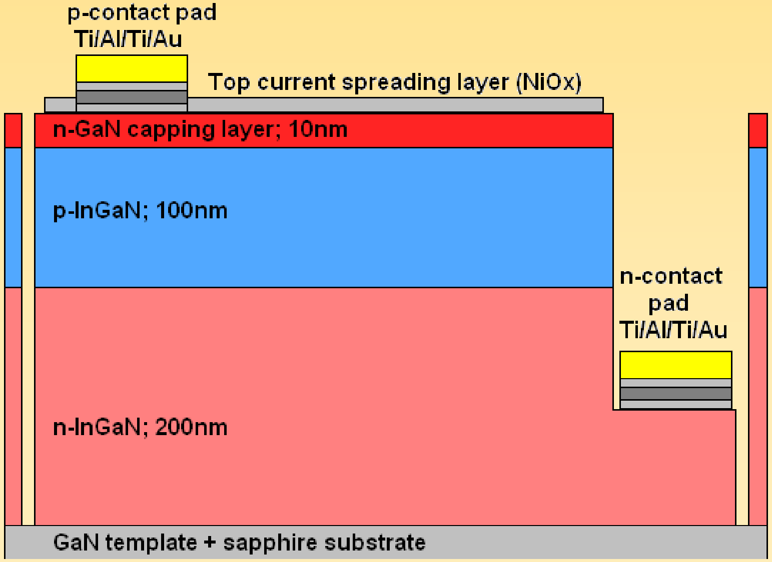

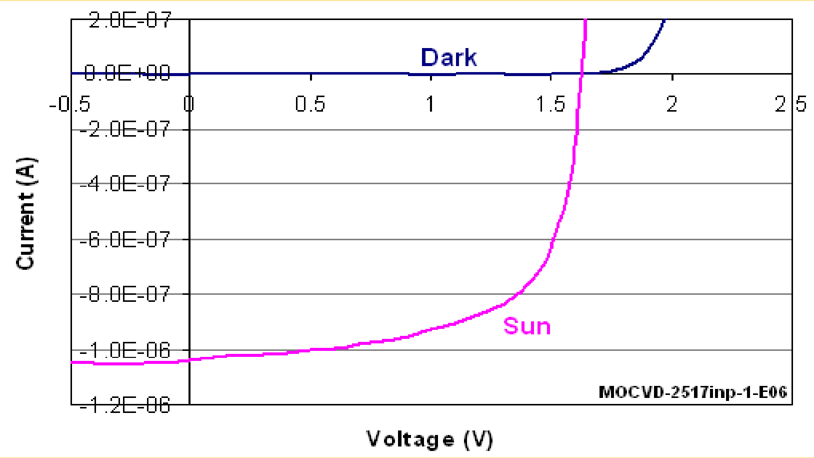

Voc = 1.7V; FF = 61.3%

Grid contact

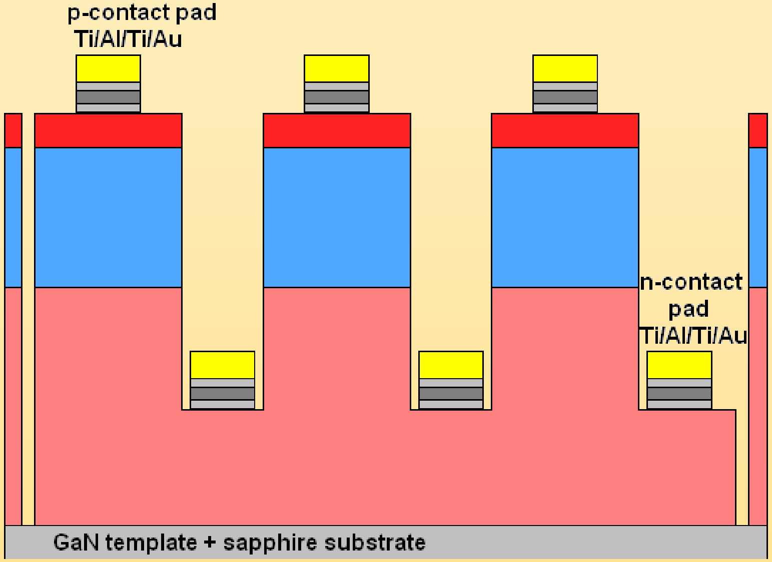

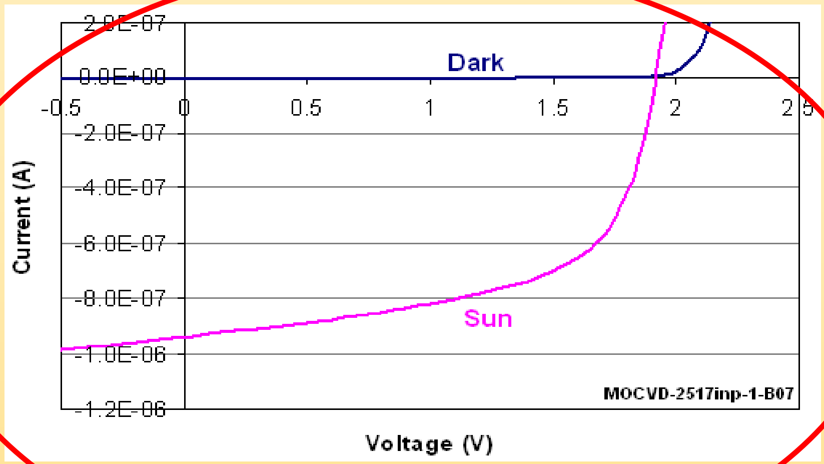

Voc = 1.95V; FF = 57.3%

Test I-V setup

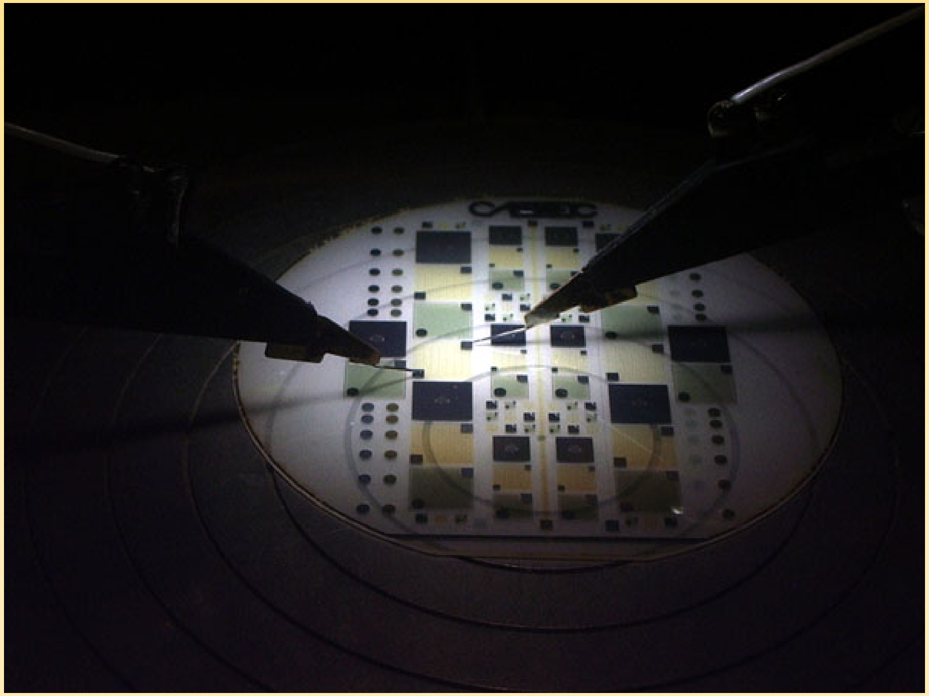

Fabricated InGaN solar cells under test.

I-V setup and test InGaN solar cell indicating a V_{OC} of 1.86V under 1 Sun.

III-Nitrides for Thermoelectric Applications

Thermoelectric (TE) Effect

- Temperature difference induces a voltage difference, the Seebeck voltage
- $S = -\Delta V/\Delta T$
- Seebeck coefficient $S < 0$ for n-type materials
- $S > 0$ for p-type materials

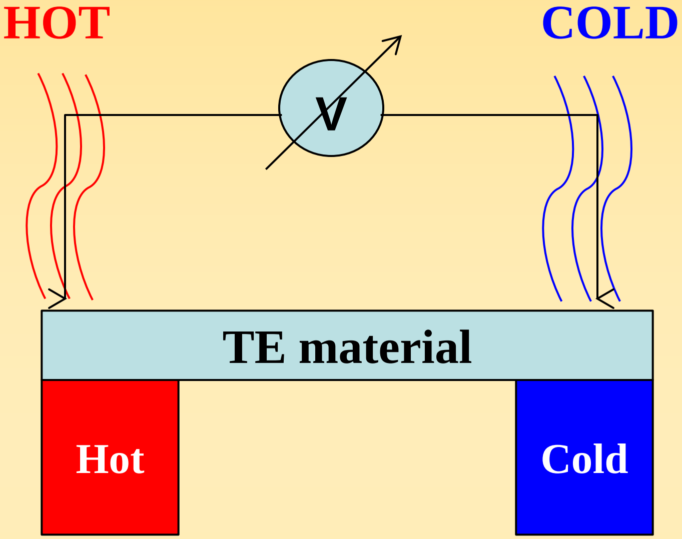

$ZT = (S^2\sigma/\kappa)T$ = "Thermoelectric Figure of Merit"

S = Seebeck coefficient
σ = Electrical conductivity
κ = Thermal conductivity = $\kappa_e + \kappa_{ph}$
T = *Delta* Temperature

TE Equations: A Function of Carrier Concentration

The Electrical Conductivity

$$1/\rho = \sigma = ne\mu$$

Electrical conductivity = σ
Carrier concentration = n
Electron charge = e
Mobility = μ

The Thermal Conductivity

$$\kappa = \kappa_e + \kappa_l$$

$$\kappa_e = L\sigma T = ne\mu LT$$

κ = thermal conductivity
κ_e = electronic thermal conductivity
κ_l = lattice thermal conductivity
L = Lorenz factor = $2.4 \times 10^{-8}\ J^2K^{-2}C^{-2}$

The Seebeck Coefficient

$$\alpha = \frac{8\pi^2 k_B^2}{3eh^2} m^* T \left(\frac{\pi}{3n}\right)^{2/3}$$

α = Seebeck coefficient
k_B = Boltzmann constant
h = Planck's constant
m* = effective electron mass
T = operating temperature

$ZT = (S^2\sigma/\kappa)T$ = "Thermoelectric Figure of Merit"

$S^2\sigma$ = "Power Factor"

J.G. Snyder and E. Toberer Nat. Mat. 7, 105 (2008)

State-of-the-Art Thermoelectric Materials

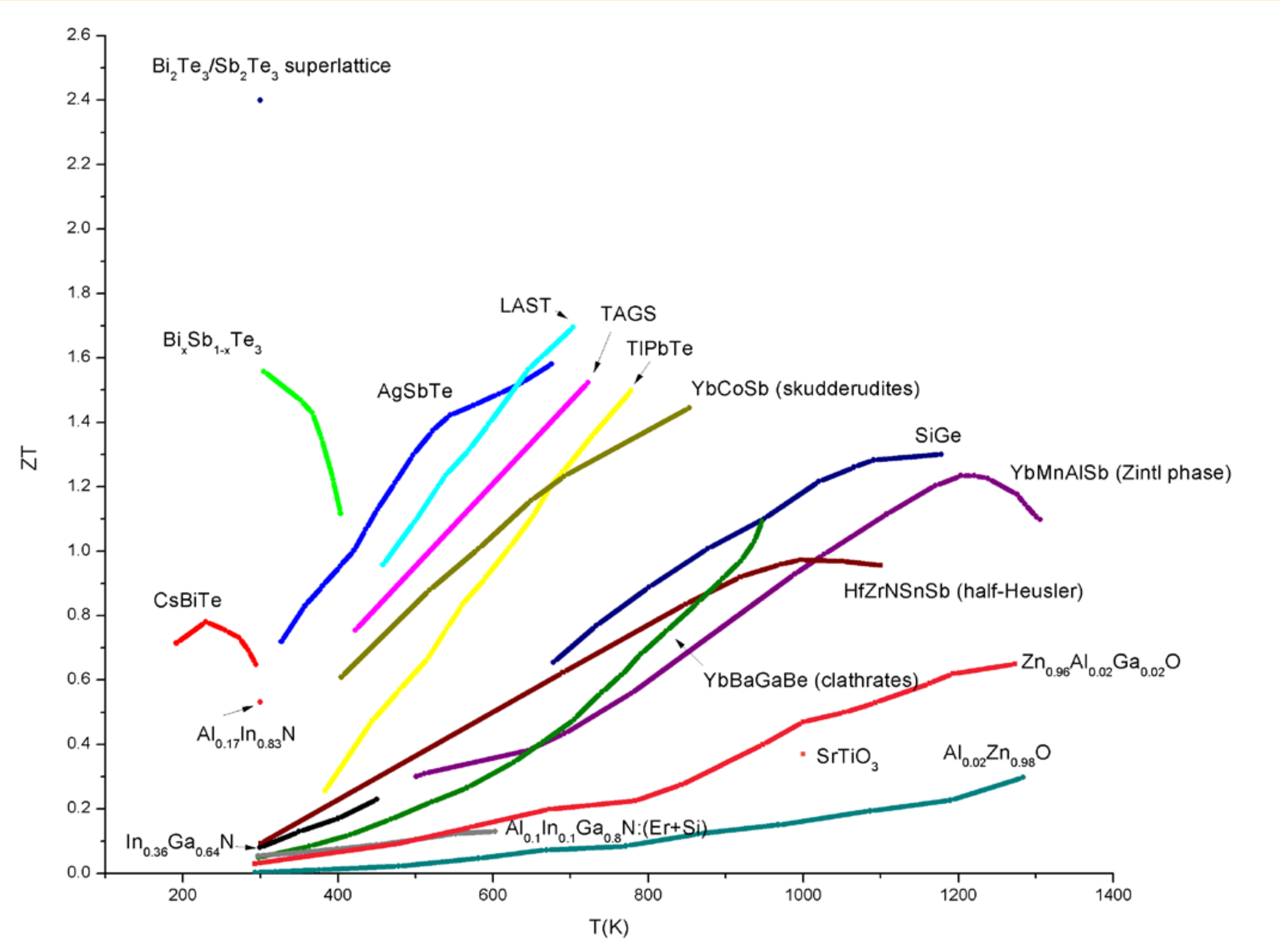

1. J.-F. Li et al. NPG Nature Mat. 2, 152 (2010)
2. M. Ohtaki et al. JAP 79, 1816 (1996)

Ian Ferguson
(ianf@uncc.edu)

GaN: Thermal properties

- Seebeck Coefficient is relatively constant up to 1000K
- Thermal Conductivity is decreased with T and doping concentration
- Piezoelectric acoustic phonons main contributor of thermal conductivity is at 3 orders of magnitude more than the electrical contribution in thermal conductivity

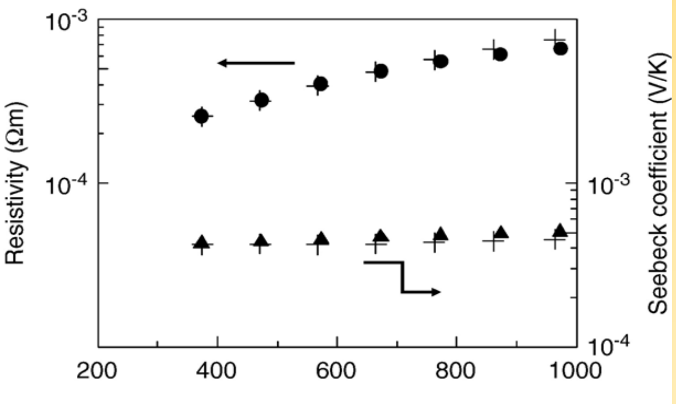

Temperature dependence of electrical resistivity (left ordinate) and Seebeck coefficient (right ordinate) of fr-GaN of experimental values (clo circles) and calculation values (crosses).

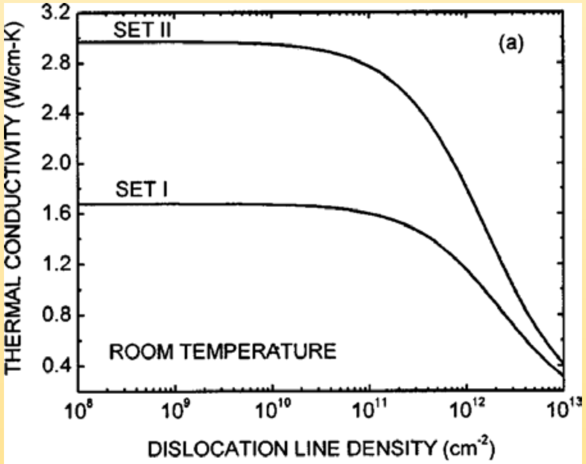

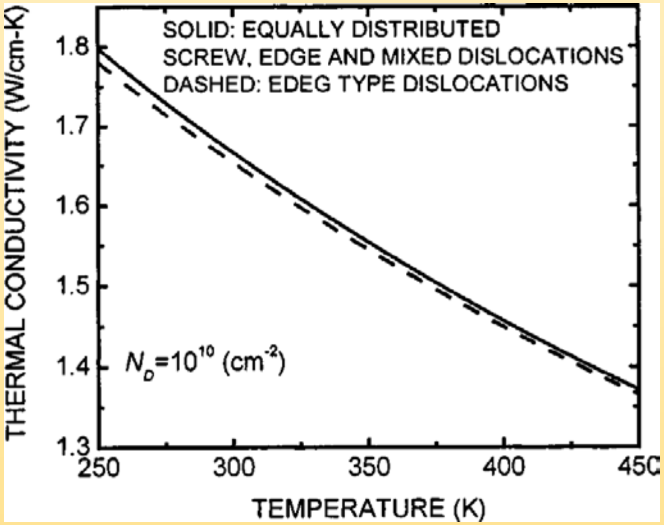

W. Liu & A. Balandin, JAP, 97, 123705 (2005)

TE Properties of III-Nitrides

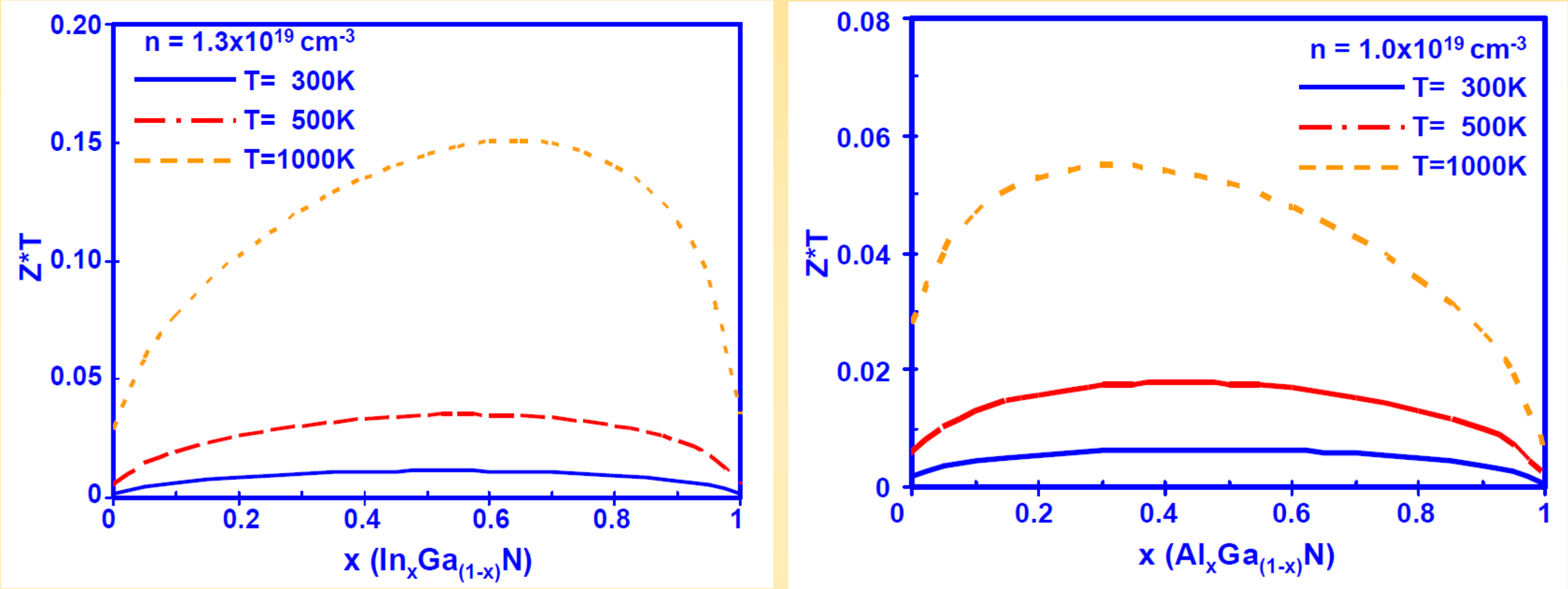

- **ZT of InGaN is at 3 times highers than AlGaN**
- **ZT of InGaN could reach at 0.15 at 1000K with 60% Indium concentration**

Tong et al., Proc. SPIE, vol. 7211, pg. 721103, 2009

GaN TE Generator

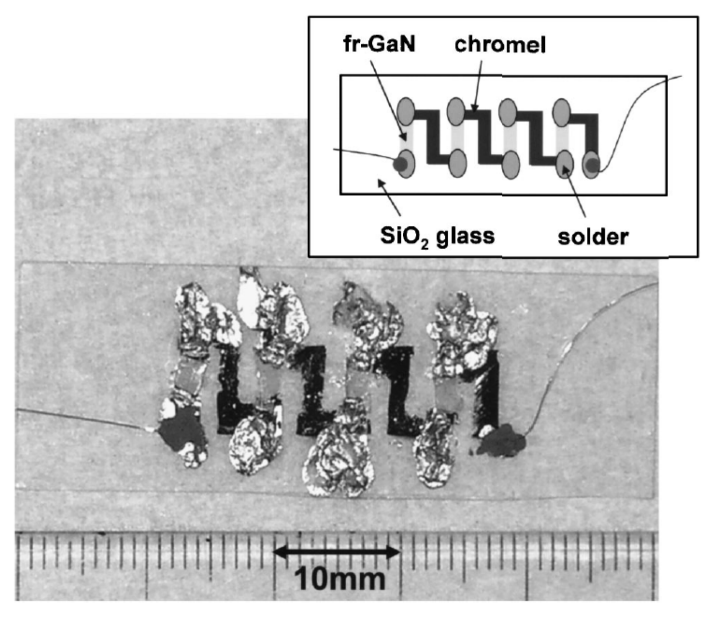

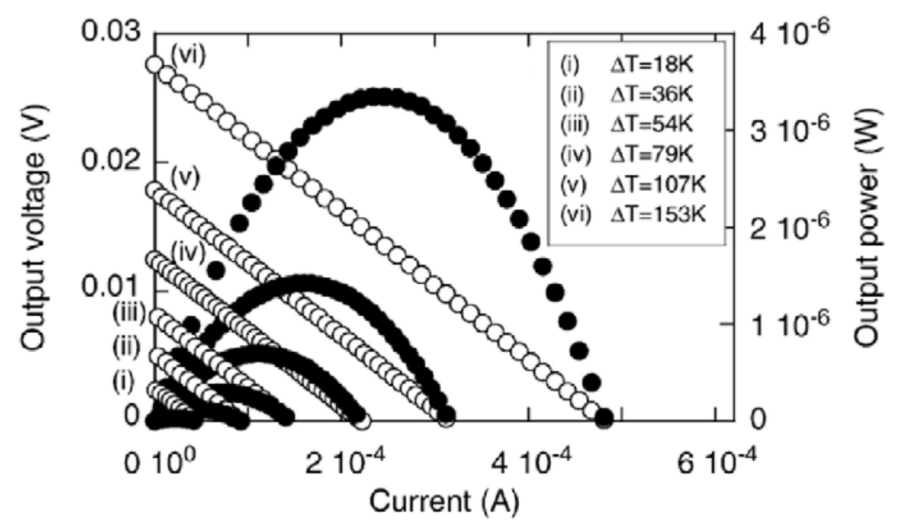

Crude TE generators made from free-standing GaN (HVPE)

Yamaguchi et al., APL, vol. 86, pg. 252102, 2005
Kaiwa et al., TSF, vol. 515, pg. 4501, 2007

Summary of GaN Data

Material	μ (cm²/(Vs))	n or p (cm^{-3})	σ (1/(Ωcm))	S (μV/K)	Power Factor (x10^{-4}W/m-K)
GaN	419	-5.91E+16	3.97	-304	0.37
GaN:Mg	10.43	1.55E+17	0.26	637	0.11
GaN:Si	344	-1.59E+18	87.87	-322	9.11
GaN:Si	245.3	-5.24E+18	205.90	-206	8.73
GaN:Si	254	-2.94E+18	119.50	-255	7.77
GaN:Si	190	-5.91E+18	180.00	-169	5.14

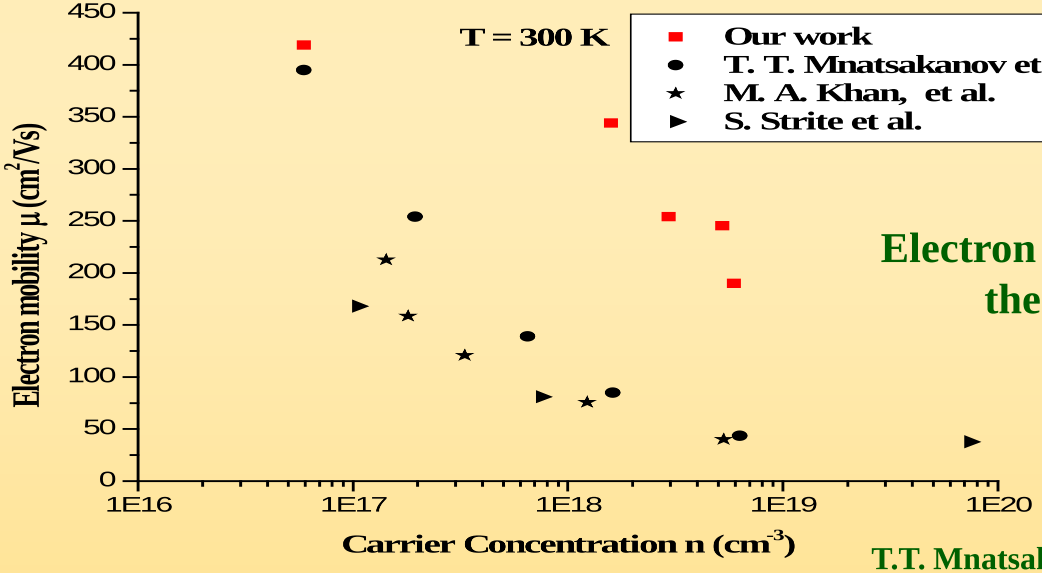

Electron mobility in n type GaN decreases with the increase in carrier concentration

T.T. Mnatsakanov *et al*. Solid. Stat. Elec., 47, 111 (2003)
M. A. Khan *et al*. Appl. Phys. Lett., 58, 526 (1991)
S. Strite *et al*. J. Vac. Sci. Tech. 10, 1237(1992)

Thermal Conductivity vs. Carrier Concentration

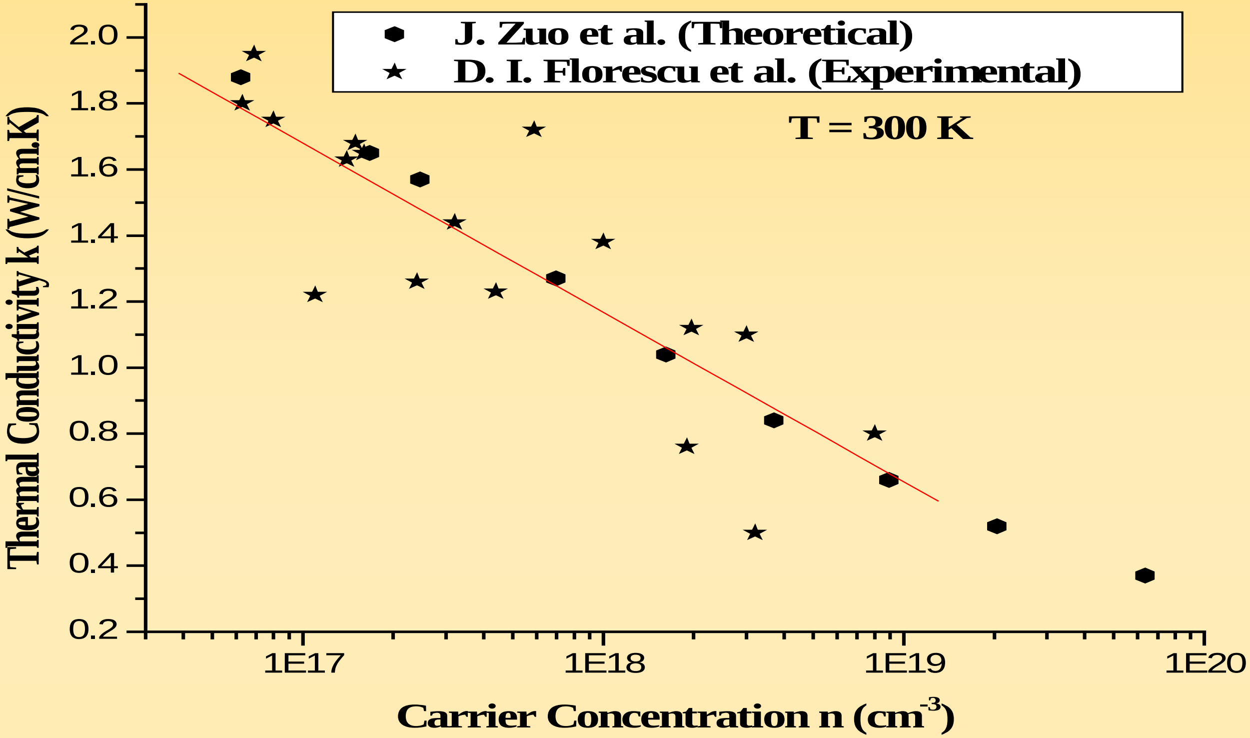

- Theoretical and experimental results follow the same trend
- Values of thermal conductivity were calculated by using first order exponential fit of experimental data. The equation used is $k = 1.24*\exp(-n/1.87\times10^{18}) + .533$

D.I. Florescu *et al.* J. Appl. Phys. 88, 3295 (2000)
J. Zuo *et al.* J. Appl. Phys. 92, 2534 (2002)

Seebeck Coefficient vs. Carrier Concentration

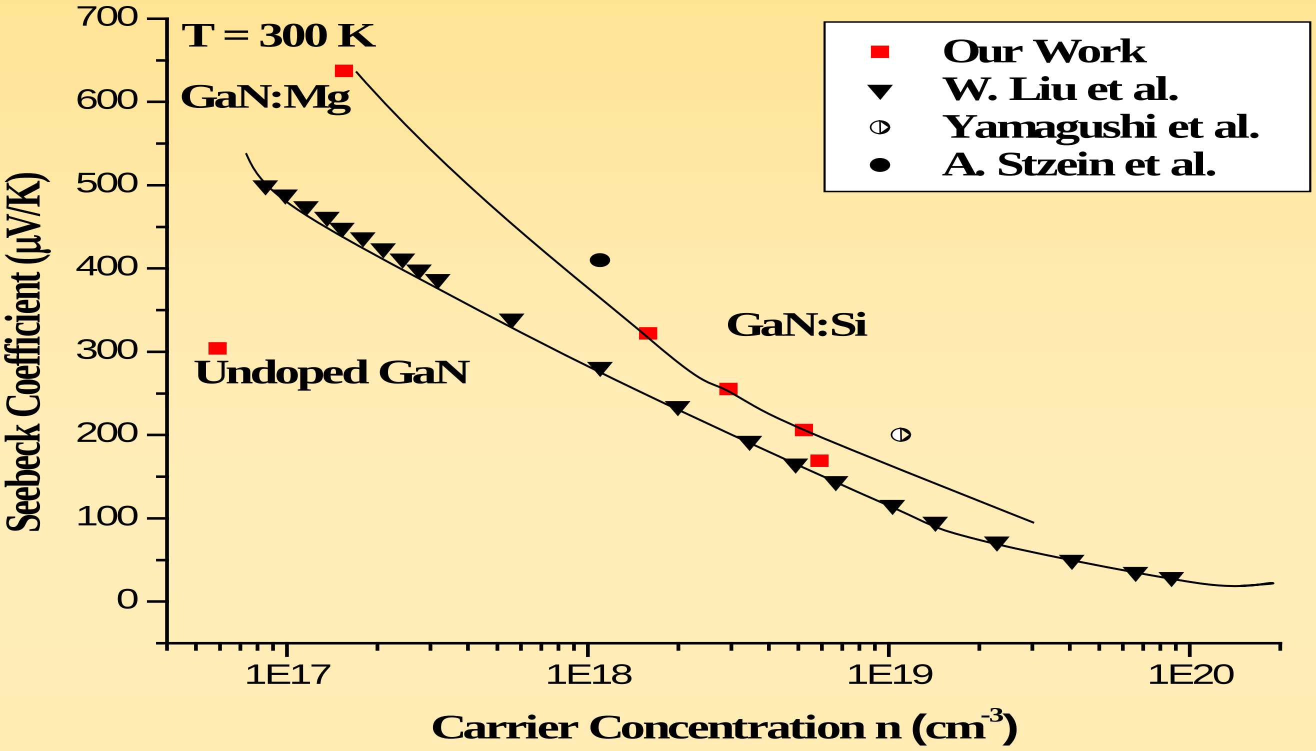

- Seebeck coefficient decreases with the increase of carrier concentration
- P-type doped GaN has higher Seebeck coefficient compared to N-type doped ones
- Seebeck coefficients for GaN:Si follow the trend reported in literature

A. Sztein *et al*. J. Appl. Phys., 110, 123709 (2011)
S. Yamagushi *et al*. Appl. Phys. Lett., 86, 252102 (2005)
W. Liu *et al*. J. Appl. Phys. 97, 123705 (2005)

Figure of Merit ZT vs. Carrier Concentration

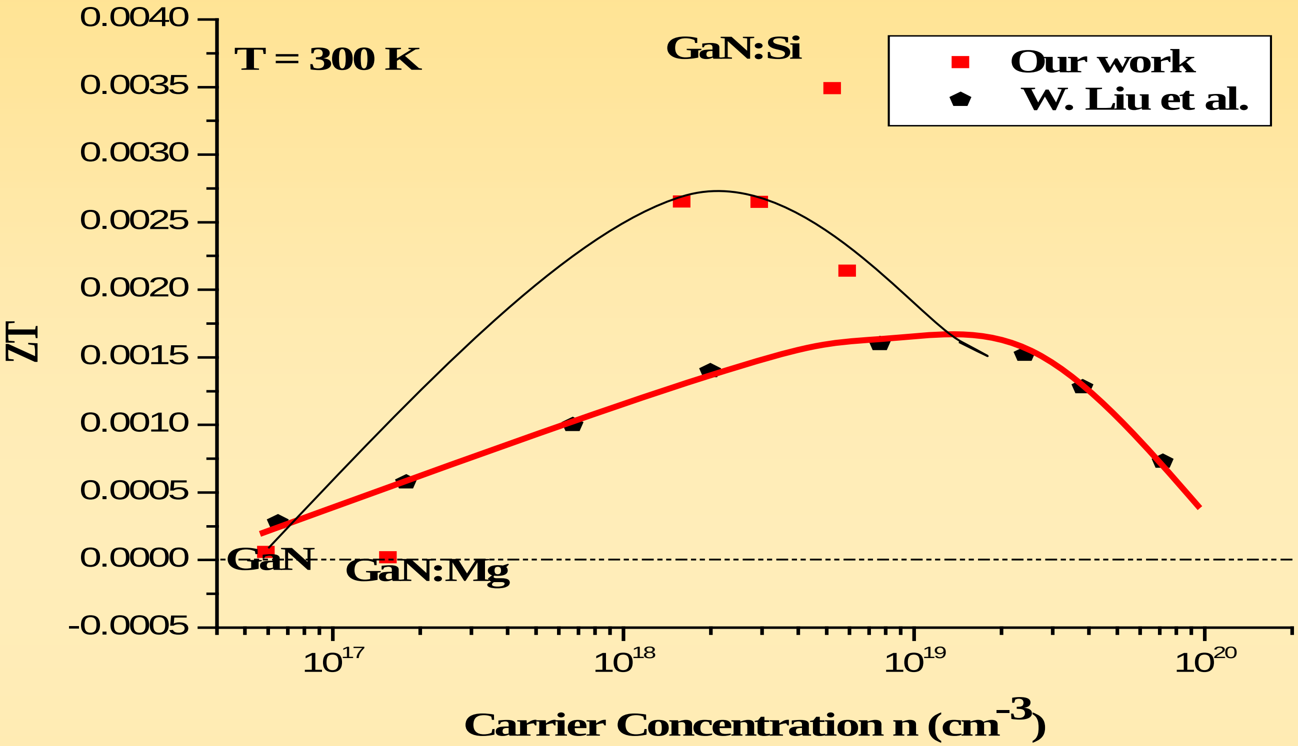

- **Our ZT values for GaN:Si are higher than reported in literature**
- **Higher Seebeck coefficient does not compensate for very low electrical conductivity of GaN:Mg**

D.I. Florescu *et al*. J. Appl. Phys. 88, 3295 (2000)

W. Liu *et al.* J. Appl. Phys. 97, 123705 (2005)

Comparison of GaN and ZnO results

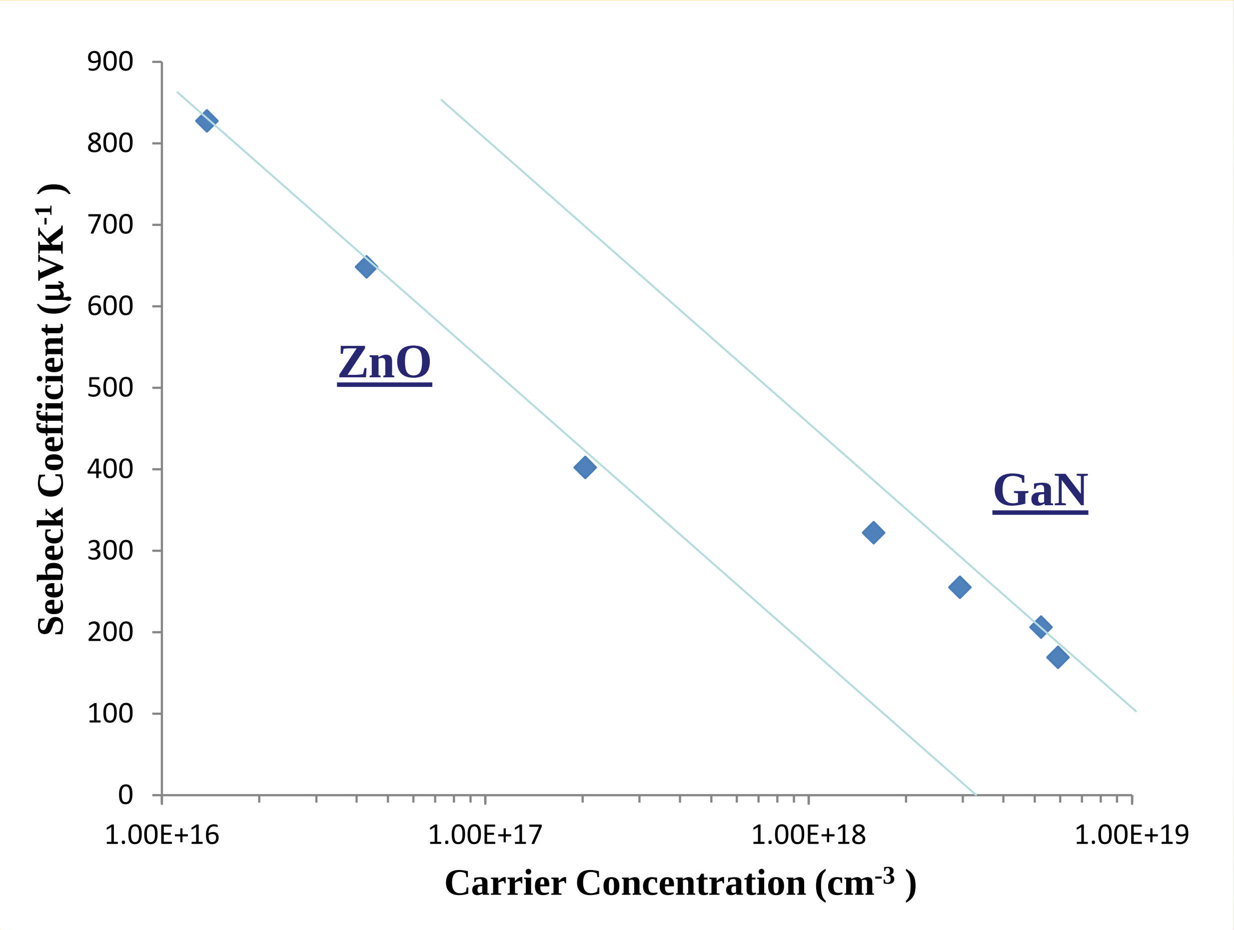

Summary of InGaN Data

Material	μ (cm^2/Vs)	n or p (cm^{-3})	σ (1/(Ωcm))	XRD peak (°)	XRD FWHM (arcsec)	S (μV/K)	Power Factor ($x10^{-4}$W/m-K)
$In_{0.07}Ga_{0.93}N$	15.55	1.53E+18	3.821	17.0876	233.64	4050	62.67
$In_{0.08}Ga_{0.92}N$:Mg	1.22	1.41E+18	0.2747	16.9697	240.84	1200	0.40
$In_{0.1}Ga_{0.9}N$	597.20	1.24E+18	118.8	16.8882	297.47	-960	109.49
$In_{0.16}Ga_{0.84}N$	110.40	1.82E+18	32.12	16.7296	467.17	-661	14.03
$In_{0.175}Ga_{0.835}N$	48.82	6.142E+17	4.80	16.7550	648.00	-209	1.57
$In_{0.21}Ga_{0.79}N$	200.90	2.063E+18	66.39	16.5050	536.40	-239	3.79

Correlation between crystal quality and Seebeck coefficient

Seebeck Coefficient vs. Indium Content

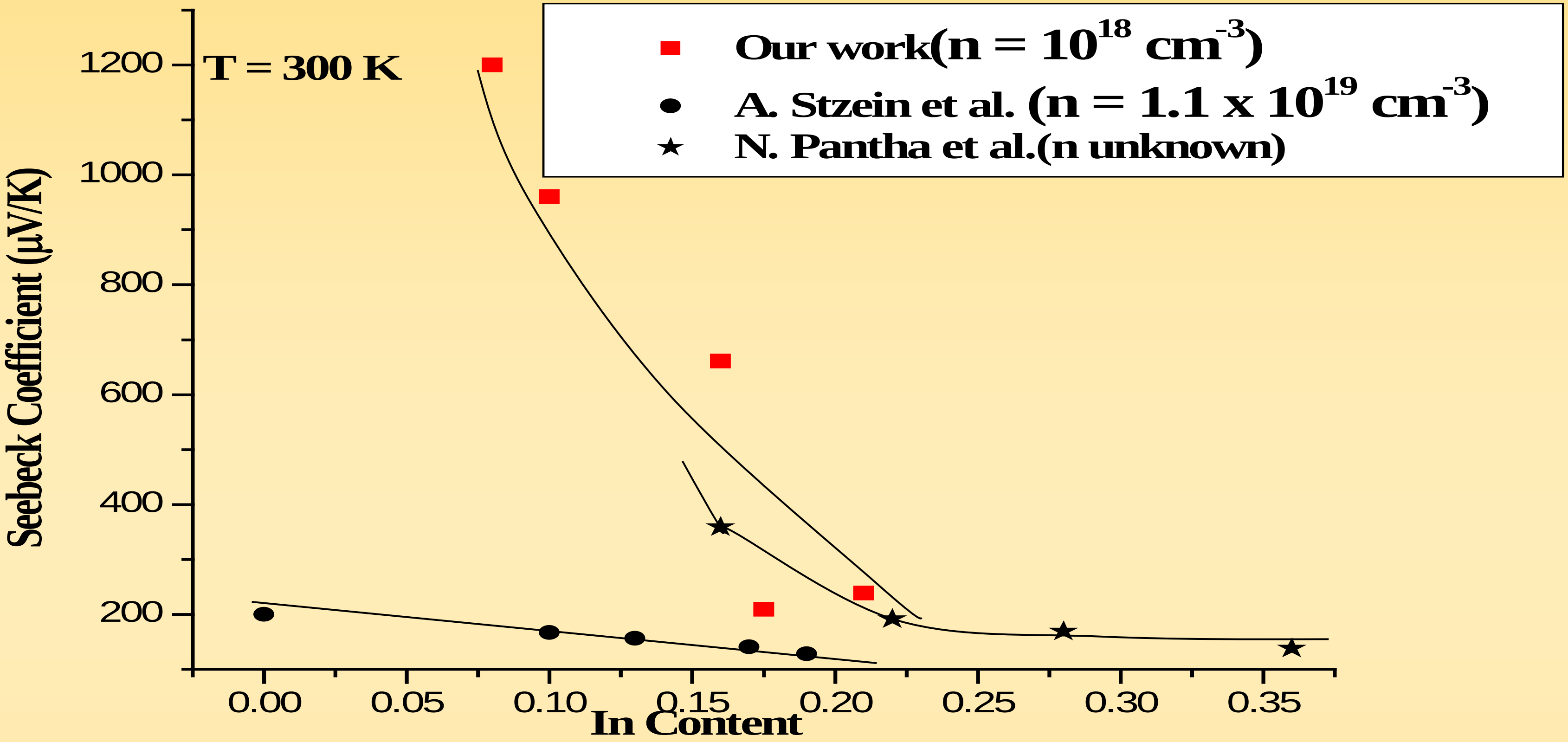

- Seebeck coefficient decreases with the increase in indium content
- Our Seebeck coefficients have higher values reported in literature

N. Pantha, *et al*. Appl. Phys. Lett. 92, 042112 (2008)

A. Sztein, *et al*. J. Appl. Phys. 110, 123709 (2011)

XRD patterns with different Indium concentration

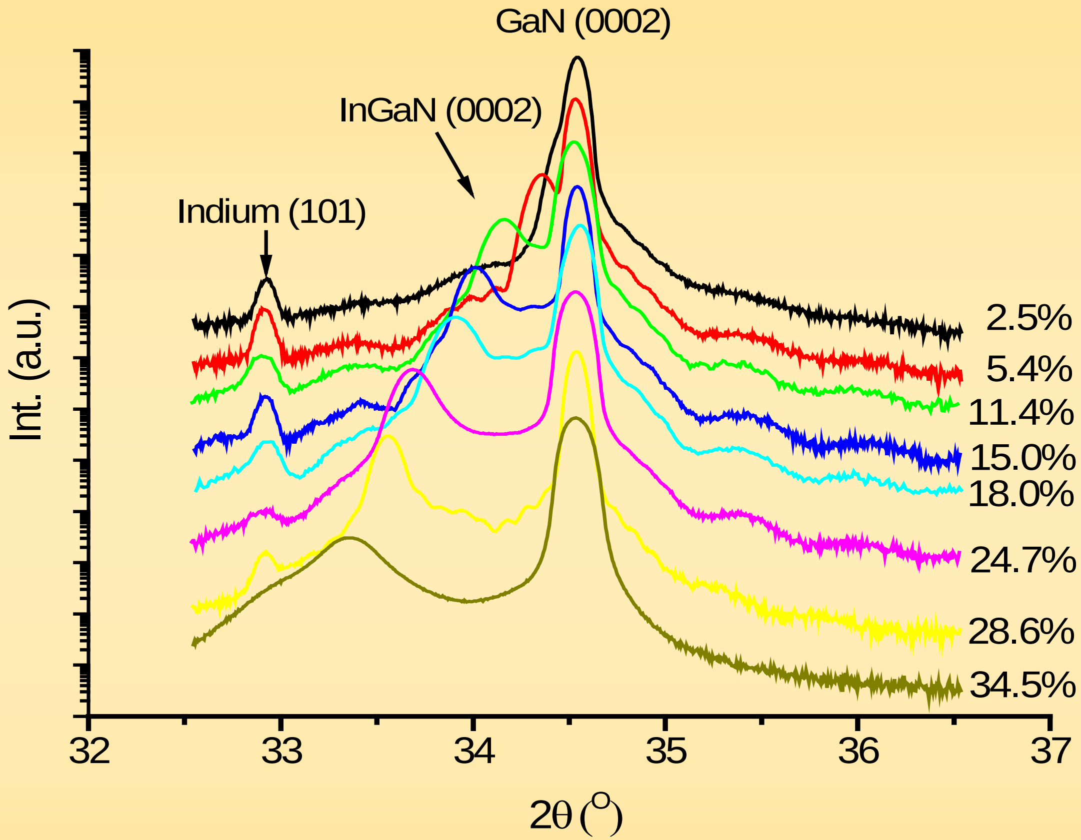

InGaN shows phase separation with increasing indium content even when attempts are made to minimize it

Phase separation in InGaN

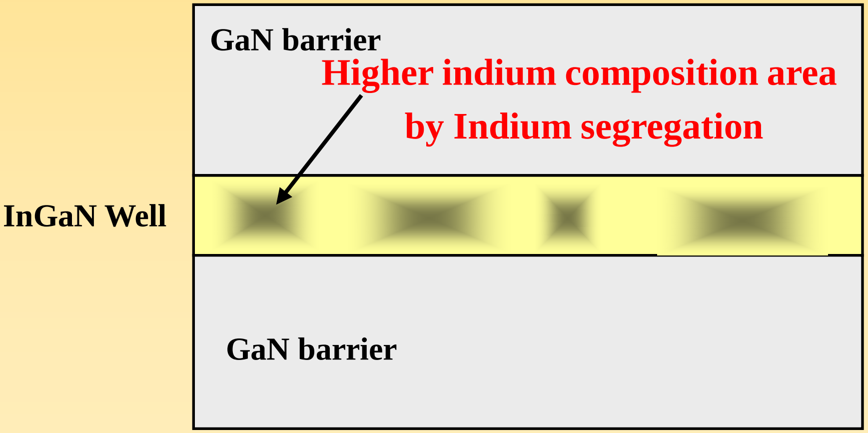

GaN barrier

Higher indium composition area by Indium segregation

InGaN Well

GaN barrier

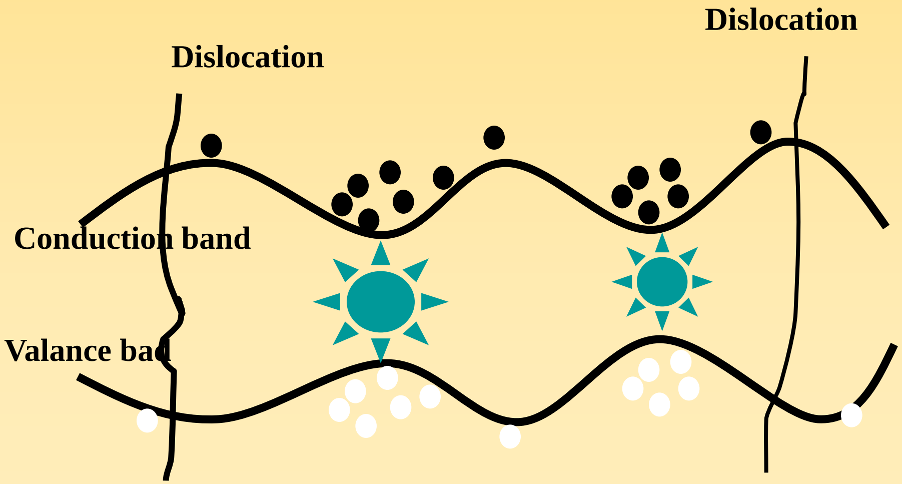

Dislocation

Dislocation

Conduction band

Valance bad

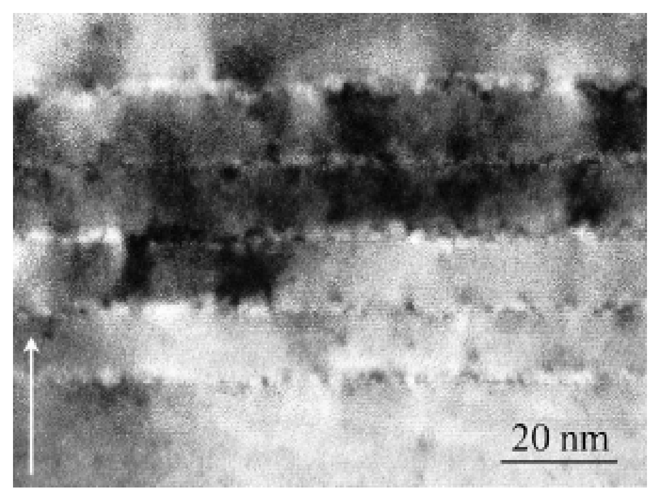

TEM image of indium segregated MQW

K.Jacobs et al, Journal of Crystal Growth 248(2003) 498

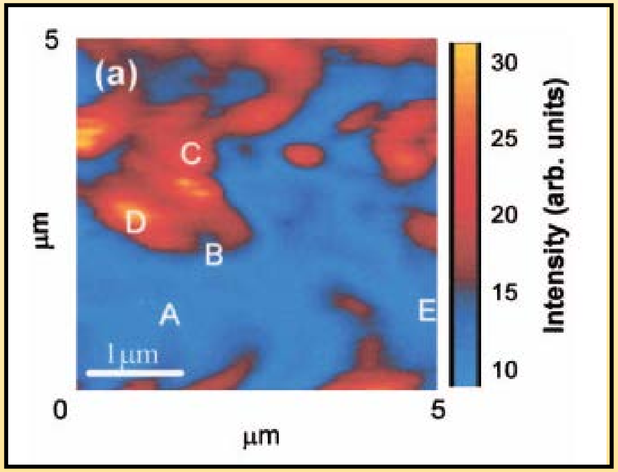

Micro-PL image of MQW

Koichi Okamoto et al. J. Appl.Phys. 98, 064503(2005)

Crystal quality at different indium composition

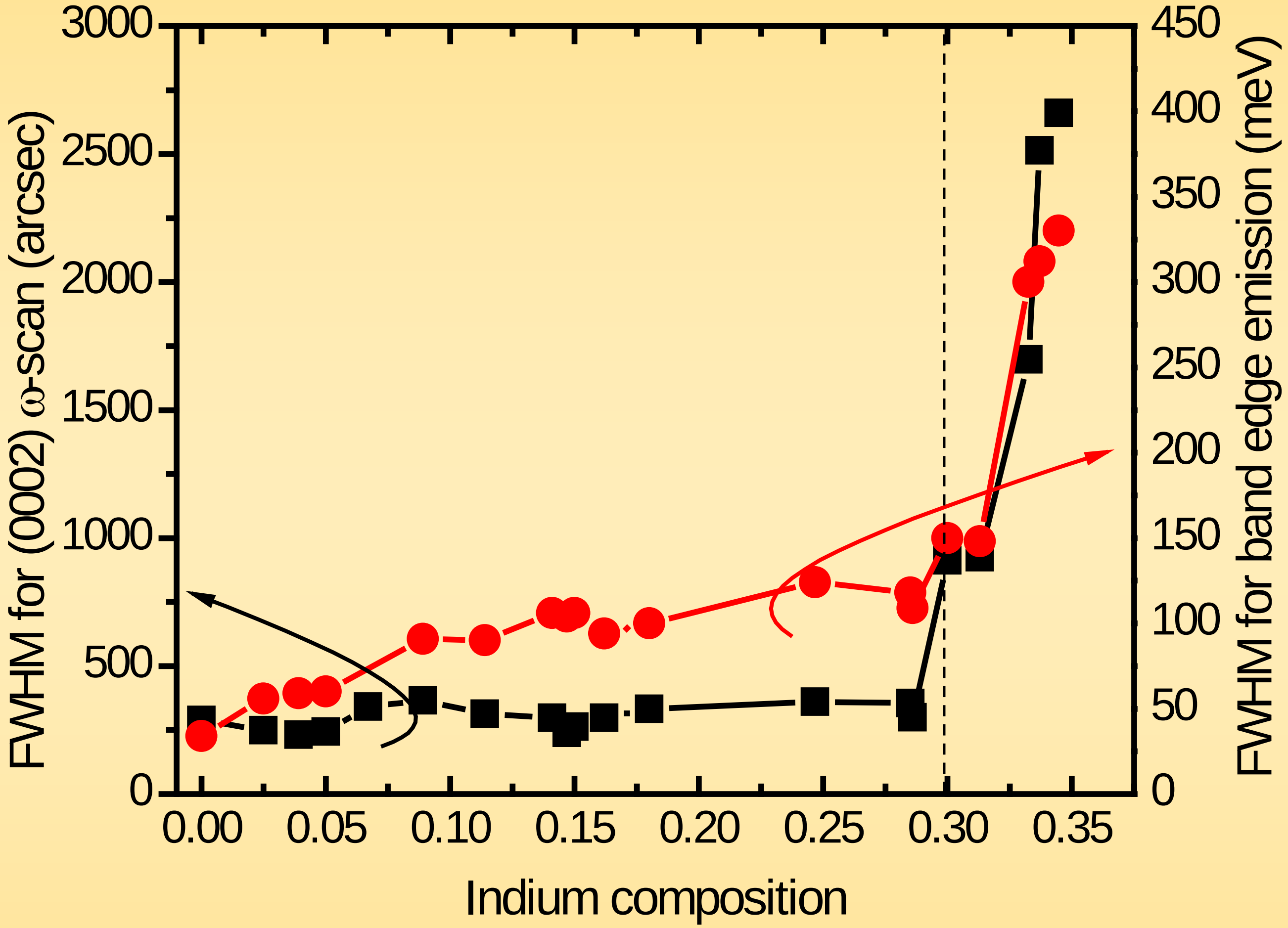

Sharp decrease of crystal quality when In% is > 25-30%

Figure of Merit ZT vs. Indium Content

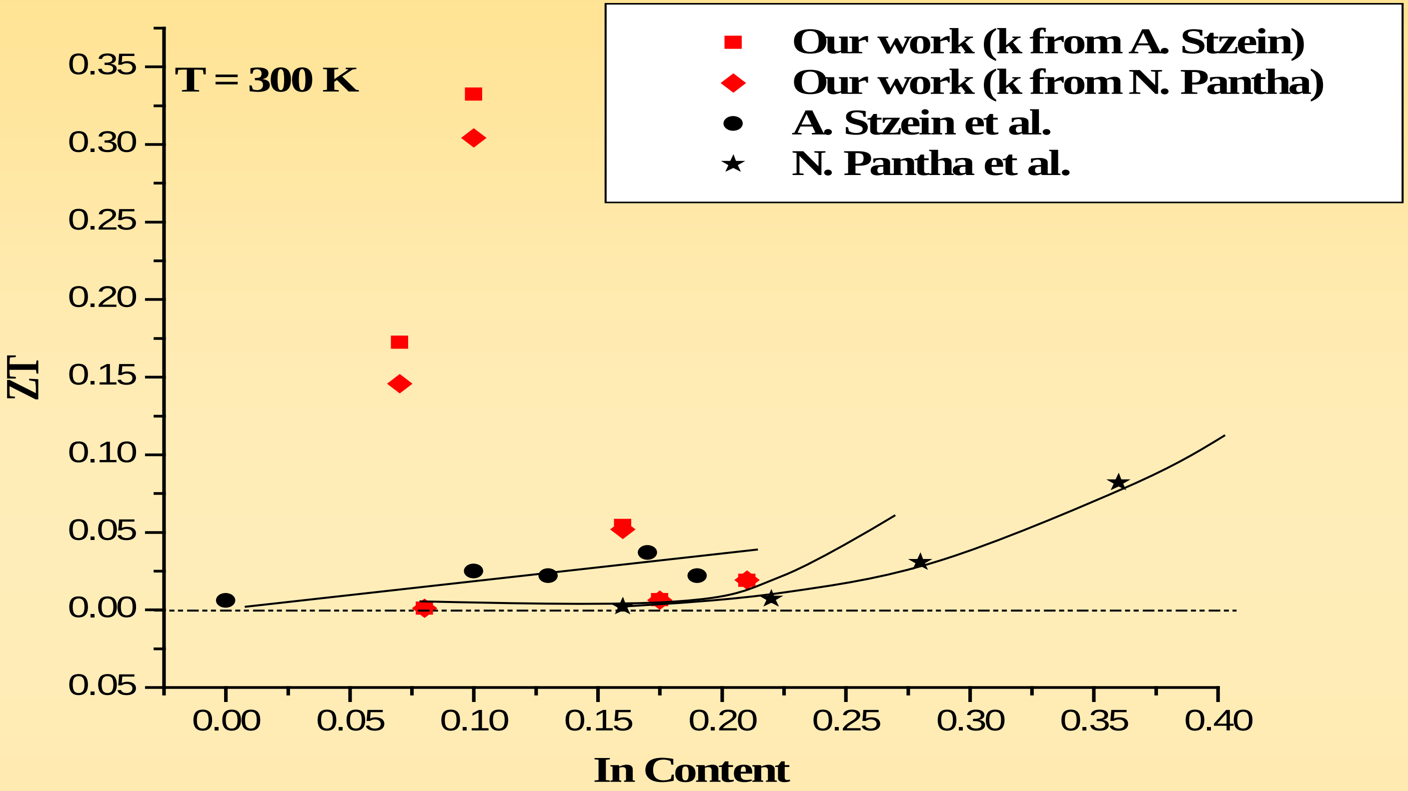

- ZT values are decreasing with the increase in indium content

N. Pantha *et al.* Appl. Phys. Lett. 92, 042112 (2008)
A. Sztein *et al.* J. Appl. Phys. 110, 123709 (2011)

UNC CHARLOTTE

Electrical and Computer Engineering

Wide Band Gap III-Nitride Compound Semiconductor Devices: The Universal Solution for Energy Applications

Ian Ferguson
University of North Carolina at Charlotte
Department of Electrical and Computer Engineering
Charlotte, NC 28223
Email: ianf@uncc.edu